AD

USAAVLABS TECHNICAL REPORT 64-68D

HEAVY-LIFT TIP TURBOJET ROTOR SYSTEM
VOLUME IV
STATIC AND DYNAMIC LOADS

October 1965

U. S. ARMY AVIATION MATERIEL LABORATORIES
FORT EUSTIS, VIRGINIA

CONTRACT DA 44-177-AMC-25(T)

HILLER AIRCRAFT COMPANY, INC.

DDC Availability Notices

Qualified requesters may obtain copies of this report from DDC.

This report has been furnished to the Department of Commerce for sale to the public.

Disclaimers

The findings in this report are not to be construed as an official Department of the Army position, unless so designated by other authorized documents.

When Government drawings, specifications, or other data are used for any purpose other than in connection with a definitely related Government procurement operation, the United States Government thereby incurs no responsibility nor any obligation whatsoever; and the fact that the Government may have formulated, furnished, or in any way supplied the said drawings, specifications, or other data is not to be regarded by implication or otherwise as in any manner licensing the holder or any other person or corporation, or conveying any rights or permission, to manufacture, use, or sell any patented invention that may in any way be related thereto.

Disposition Instructions

Destroy this report when it is no longer needed. Do not return it to the originator.

Task 1M121401D14412
Contract DA 44-177-AMC-25(T)
USAAVLABS Technical Report 64-68D
October 1965

HEAVY-LIFT TIP TURBOJET ROTOR SYSTEM

VOLUME IV

STATIC AND DYNAMIC LOADS

Hiller Engineering Report No. 64-44

Prepared by

Hiller Aircraft Company, Inc.
Subsidiary of Fairchild Hiller Corporation
Palo Alto, California

For

U. S. ARMY AVIATION MATERIEL LABORATORIES
FORT EUSTIS, VIRGINIA

(U. S. Army Transportation Research Command when report prepared)

CONTENTS

CONTENTS (CONTINUED)

ILLUSTRATIONS

ILLUSTRATIONS (CONTINUED)

ILLUSTRATIONS (CONTINUED)

ILLUSTRATIONS (CONTINUED)

ILLUSTRATIONS (CONTINUED)

TABLES

SYMBOLS

a	Airfoil lift curve slope, per radian
a_o	Rotor blade precone angle
b	Number of rotor blades
B	Tip loss factor
c	Blade chord
EI	Blade bending stiffness, lb-in^2
g	Gravitational units, 32.2 ft/sec^2
G	Damping factor
GJ	Blade torsional stiffness, lb-in^2
I_E	Mass moment of inertia of the engine rotating parts, lb-in-sec^2
n	Load factor, multiples of g
Q	Torque
r	Radial distance from the rotor centerline of rotation to a point on the blade
R	Rotor radius
T	Rotor thrust, lb.
T_E	Tip engine thrust, lb.
V	Forward velocity of helicopter, f.p.s.
V_T	Tip speed, f.p.s.
W	Weight, lb.
θ	Blade geometric pitch
θ_T	Blade twist, positive if the geometric angle at the tip is greater than at the root
λ	Rotor inflow parameter

SYMBOLS (CONTINUED)

ρ	Air mass density, slugs/ft^3
Ψ	Rotor blade azimuth angle, measured in direction of rotation from an aft position in the rotor disk
Ω	Rotor angular velocity, rad/sec.

1.0 SUMMARY

This volume presents the structural design criteria, static design loads, and dynamic design loads for the Model 1108 helicopter. This volume shall be the basis for the structural design and analysis of the tip turbojet main rotor system.

1.1 Structural Design Criteria

The structural design criteria for the tip turbojet main rotor system presents the following information:

a) A general description of all the components that are contained in the main rotor system.

b) Basic design data which includes weight data, main rotor data, engine data, rotor speeds, engine environmental requirements, blade movement, performance, and mechanical drive data.

c) Design requirements which include general requirements, flight and take-off loading conditions, ground loading conditions, control system loads, and mechanical instability, flutter, and vibration.

1.2 Steady-State Design Load Analysis

To determine the steady-state design loads, the following loading conditions were considered:

a) Centrifugal loads

b) Rotor blade torques which include gyroscopic torque, induced torque due to coning and collective pitch, aerodynamic torque, and torque due to one engine failure.

c) Aerodynamic loads were generated for ten flight conditions using the Cornell Aeronautical Laboratory (CAL) airload program which produced the steady and first through seventh harmonic airloads.

d) Rotor blade flapwise bending moments were generated using the uncoupled Mayo method (Reference 3) for the steady and first harmonics, and the analog computer rotor blade simulation method (Reference 4) which produced a coupled analysis for the second through seventh harmonics.

e) Rotor blade chordwise bending moments were derived in a similar manner as the flapwise moments, in which the steady and first

harmonics were considered in an uncoupled manner while the second through seventh harmonics were analyzed in a coupled manner using the same analysis that was used for the coupled flapwise moments.

1.3 Dynamic (Transient) Loads

The direct analog rotor simulation used in Reference 4 was used for studying dynamic loads and motions resulting from a sharp edge gust as well as cyclic and collective pitch inputs while hovering.

2.0 CONCLUSIONS

An investigation has been conducted to determine which loading conditions would produce the design loads for the tip turbojet rotor system. This volume includes all of the possible design loading conditions and presents either analytically or graphically the magnitude of these loads. The following paragraphs of this section summarize and conclude the importance of the different static and dynamic loading conditions.

2.1 Critical Static Design Loads

2.1.1 Centrifugal Load

The critical centrifugal loading for the rotor system is due to a rotor speed of 105 percent of the design maximum speed (650 feet per second). The critical centrifugal loading for the rotor system attachments is due to a rotor speed of 125 percent of the design maximum speed.

2.1.2 Rotor Blade Torque

Design torque for the rotor blade is a nose-down torque. This is due primarily to the gyroscopic moment caused by the tip engines. For the maximum design torque condition, three conditions are combined giving a conservative loading. These conditions are tip engine gyroscopic moment, rigid coning torque, and centrifugal centering torque.

2.1.3 Aerodynamic Loading

The rotor blade airloads were analyzed using Cornell Aeronautical Laboratory (CAL) airload program. This program produces the steady plus first through seventh harmonic alternating lift and drag airloads. An iterative procedure was necessary to obtain the proper steady airload, which corresponds with the proper thrust for different flight conditions. The inflow distribution and collective pitch were the two inputs changed for the iterative process.

2.1.4 Rotor Blade Bending Moments

2.1.4.1 Flapwise Bending Moments

Two methods were used to analyze flapwise bending moments, the Mayo method (Reference 3) and the direct analog computer simulation method (Reference 4). The Mayo method produced the steady, first, and second harmonic flapwise bending moments while the direct analog computer simulation method produced the second through seventh harmonic flapwise bending moments. The second harmonic flapwise bending moments were calculated by both methods, and a comparison shows that the second harmonic sine components have little correlation while the cosine components seem to correlate. However, the Mayo method has a 50- to 100-percent conserv-

ative margin. The second harmonic of the Mayo method should be used for comparison only and not for design purposes.

The 2.5g pullup is selected as being the condition which yields the largest steady bending moment in combination with its complement of harmonic moments. The 1g forward flight conditions are selected as yielding the harmonic bending moments of the longest duration (i.e., for fatigue considerations). The -0.5g hover condition produces the largest negative in-flight bending moment at the root of the blade while negative static droop moments are critical at blade sections outboard of the retention.

2.1.4.2 Chordwise Bending Moments

Chordwise bending moments were treated in a simple uncoupled manner for steady and first harmonic loadings while a coupled analysis was made for the second through seventh harmonic loadings using the direct analog computer simulation method (Reference 4). The largest steady chordwise bending moment is due to two engines inoperative. Only the conditions which produce the maximum harmonic chordwise coupled bending moments were plotted. Thus, combining these steady and harmonic chordwise loads for design purposes will produce a conservative design.

2.2 Dynamic (Transient) Design Loads

2.2.1 Gust

Gust load factors were derived by two separate methods: first, considering the rotor blades to be rigid and treating the hovering rotor as having undergone an instantaneous change in inflow equal to the gust velocity; and second, considering the rotor blade to be flexible and using the direct analog computer simulation method (Reference 4). Considering the blade as rigid gives a load factor greater than the design maximum of 2.5g while consideration of the flexible blade reduces the load factor to 2.25g. The rigid rotor analysis is considered to be too conservative and therefore the analog computer simulation of the flexible blade shall be used for design loading.

2.2.2 Cyclic Pitch Transient

The direct analog computer studies simulated a whirling of the cyclic stick at a critical frequency which is considered to be within the pilot's capability. This simulation produced a bending moment at the root only; therefore, a conservative chordwise bending moment distribution, based on the transient gust response mode shape, was utilized for this condition. This condition results in the maximum positive and negative chordwise bending moments. Because the structural damping factor used for this analysis was assumed, it is recommended that a simulation of

this condition be made on a test stand to verify the magnitude of the in-plane design bending moments.

2.2.3 Collective Pitch Transient

An exponential collective pitch input of 0.01 radian was used to determine the blade response using the direct analog computer. The transient collective pitch in-plane bending moment is less than that resulting from the transient cyclic pitch condition. The pitching (torsional) deflection at the tip is similar in character to the flapwise deflection curve insofar as there is no transient overshoot from the initial tip angle to the final steady-state value. Therefore, the transient torsional moments on the blade will be noncritical for the collective pitch input condition.

2.2.4 Dynamic Tip Environment

The maximum g loadings at the tip occur during a forward flight condition and a 40-foot-per-second gust during hover. This tip acceleration environment was determined by considering the second harmonic motion of the blade and the associated deflection at the tip, then differentiating the motion twice to produce acceleration.

3.0 RECOMMENDATIONS

The recommendations pertaining to the work contained in this volume are as follows.

a) Because of the relative importance of identifying the structural damping factor in determining the chordwise bending moments due to a cyclic whirling (Section 5.2.2.1), it is recommended that a simulation of this condition be made on a test stand.

b) In view of the poor correlation between the Mayo method and the direct analog computer method for determining the second harmonic blade moments (Section 5.1.4.1), it is recommended that the first harmonic airload be verified using the direct analog computer. This would eliminate performing harmonic bending moment analyses by the Mayo method (digital method).

4.0 STRUCTURAL DESIGN CRITERIA

4.1 General Information

4.1.1 Introduction

Printed herein are the structural design criteria for a tip turbojet main rotor system.

4.1.2 General Description

A tip turbojet rotor system is designed for a cargo helicopter having a payload of 12 tons and a gross weight of 72,000 pounds. The rotor system shall have four blades and two engines mounted in an over-under arrangement on the tip of each blade. Each blade shall have a radius of 56 feet to the centerline of the engines and a chord of 6.5 feet. The maximum tip speed shall be 650 feet per second. The mean blade lift coefficient shall be 0.328. The turbojet engines used for the rotor system shall be a modification of the J69-T-29 engine designed by Continental Aviation and Engineering Corporation.

4.1.3 Description of Components

4.1.3.1 Main Rotor System

The rotor system shall be defined as the components above the attachment of the rotor to the rotor shaft. The blades are hinged to the hub by a retention system which allows the blades to pitch while supporting the centrifugal load. A drag link is provided to support the load due to drag on the blade. The hub is supported by a gimbal which allows the blades to teeter freely in any direction. The engines are supported at the tips by a mounting system that is bolted to the blade structure. Nacelles are partially restrained by the engine-mounting structure and partially on the blade tip end.

4.1.3.2 Control System

Control arms connect the roots of the blades to a swash plate on the rotor shaft. Lateral and longitudinal control is obtained by tilting the swash plate which causes cyclic feathering of the rotor blades, tilting the tip path plane in the desired direction of flight. Vertical control is obtained by raising the swash plate vertically which causes direct collective feathering of each blade by an equal amount.

The cyclic and collective control systems have dual hydraulic power cylinders, which provide power boost to these control systems. A dual system is provided for fail-safe purposes, which allows the second cylinder to operate if the first cylinder fails.

4.1.3.3 Engine Section - Fuel and Oil Systems

There are eight engines for each rotor system. Each blade will have two engines mounted on the tip in an over-under arrangement. The engines are a modification of the J69-T-29 engine designed by Continental Aviation and Engineering Corporation and have been assigned Model No. 357-1 by that company. The fuel system consists of fuel lines, two rotary joints, and two fuel supply manifolds which separate the fuel into individual lines for each engine.

The airframe-mounted oil system consists of oil lines and an oil replenishing tank located in the airframe, together with a pump, pressure regulator, bypass and filter. The replenishing tank-mounted pump supplies oil under pressure to engines in static operation, and during rotation will raise oil to blade height.

4.1.3.4 Electrical Section

Electrical power will be required for engine control, fuel valves, oil valves, and a starting air valve.

4.1.3.5 Mechanical Drives

The main rotor pylon is driven by the tip turbojet rotor system. The main rotor pylon drives a hydraulic p[illegible] full-time governor, AC generator, tachometer, and tail rotor. The [illegible]l rotor is driven by the pylon only during an emergency operation, in which the auxiliary power unit is not operating. The tail rotor drive has an engage clutch.

4.2 Basic Design Data

4.2.1 Weight Data

Preliminary weight data which is to be the basis of initial structural analysis and testing is presented in this section. A weight breakdown of the rotor system is as follows:

a)	Rotor group (hub and blades)			16,398
b)	Rotor pylon			1,731
c)	Engines			2,920
d)	Engine components			1,599
e)	Oil system	20%	of	160*
f)	Fuel and fuel system	1%	of	14,216*
g)	Electrical system	20%	of	750*
h)	Instruments	25%	of	296*
i)	Flight controls	70%	of	1,434*

* Th[illegible]e are estimated percentages of the gross weight of the respective groups. (Reference Volume VII, Section 4.2.2.)

4.2.2 Main Rotor Data

Type	Teetering
Radius	56.0 ft.
Chord	6.5 ft.
Disk loading	7.3 lb/ft^2
No. of blades	4
Solidity	0.148
Design mean blade lift coefficient	.328
Blade aspect ratio	8.60
Twist	-10 deg.
Hover tip speed	650 f.p.s.
Cruise tip speed	592 f.p.s.

4.2.3 Engine Data

The engines used are a modification of the J69-T-29 engine designed by Continental Aviation and Engineering Corporation. Engine data pertinent to the structural analysis are:

Thrust of each engine (static) ..... 1,700 lb.

Mass moments of inertia of each engine:

$I_{(roll)}$	38 in-lb-sec^2
$I_{(yaw)}$	125 in-lb-sec^2
$I_{(pitch)}$	125 in-lb-sec^2

Speed of rotating parts (maximum) = 22,000 r.p.m.

Polar moment of inertia of rotating parts for each engine = 1.7 in-lb-sec^2.

4.2.4 Main Rotor Speeds

The rotor speeds for power on shall be as follows:

a)	Design maximum speed	V_T = 650 f.p.s.
b)	Design minimum speed	V_T = 562 f.p.s.
c)	Overspeed operation	V_T = 683 f.p.s.
d)	Limit speed	V_T = 813 f.p.s.

where: Design maximum speed is the rotor tip speed necessary during hover at 6,000 feet.
Design minimum speed is 95 percent of the rotor tip speed during sea level cruise.

It is more efficient to operate at a lower tip speed during sea level maneuvers; however, the higher tip speed is necessary for hovering at a 6,000-foot altitude.

Overspeed operation is 105 percent of design maximum speed for one minute with a total cumulative operation time of 30 minutes per 1,000 hours of operation.

Limit speed is 125 percent of design maximum speed and shall be used for structural design of attachments when combined with bending moments produced from a hover condition or a ground run-up condition.

4.2.5 Special Engine Environmental Requirements

Special engine environmental requirements shall be as follows:

a) Design maximum: - The engine shall be capable of operating in a continuous environment having a centrifugal load of 235g normal to the tip path plane axis.

b) Overspeed operation: - The engine shall be capable of operating in a continuous environment having a centrifugal load of 259g normal to tip path plane axis for one minute with a total cumulative operating time of 30 minutes per 1,000 hours of operation.

c) Limit: - The limit centrifugal load for structural design analysis is 367g normal to the tip path plane axis for nonrotating parts of the engine only.

d) The engine shall be capable of operating in a continuous environment having a vertical load normal to the blade axis due to an alternating or transient loading condition.

e) The engine shall be capable of operating in a continuous environment having an in-plane load normal to the blade axis due to an alternating or transient loading condition.

4.2.6 Rotor Blade Movement

Collective	0° to 15°
Cyclic pitch, longitudinal	$+12^{\circ}$, -8°
Cyclic pitch, lateral	$\pm 12^{\circ}$

4.2.7 Performance

A preliminary estimate of performance for the tip turbojet is as follows:

Maximum speed (V_H)	125 m.p.h.
Limit dive (V_D)	115% of 125 m.p.h.
Hovering ceiling O.G.E.	6,000 ft., 95° F.

4.2.8 Mechanical Drives

4.2.8.1 Main Rotor Pylon

The outputs to the main rotor pylon from the main rotor necessary to drive

the tail rotor and accessories during an emergency flight condition shall be as follows:

Design speed	111 r.p.m.
Design horsepower	300 hp

4.2.8.2 Tail Rotor Drive

In an emergency flight condition the tail rotor will be driven by the main rotor pylon. The outputs to the tail rotor drive from the main rotor pylon shall be as follows:

Design speed	2,700 r.p.m.
Design horsepower	220 hp

4.3 Design Requirements

4.3.1 General

4.3.1.1 Strength

The rotor system structure shall be capable of supporting without failure the ultimate loads resulting from the loading conditions, and repeated load and endurance tests of Specification MIL-T-8679. Allowable stress values to be used in the stress analyses shall be those taken from approved government publications, such as MIL-HDBK-5 or various NACA or Bureau of Standards reports, whenever possible.

4.3.1.2 Factor of Safety

The minimum yield factor of safety shall be 1.0 and the minimum ultimate factor of safety shall be 1.5.

4.3.1.3 Deformations

The magnitude and distributions of the limit, yield, and ultimate loads shall include in their determination the effects of deformation of the structure which results from the corresponding loads. The structure shall be capable of supporting the yield and limit loads without permanent deformation that would affect adversely the aerodynamic characteristics or the mechanical operation of any part of the helicopter, or that would be noticeable upon inspection. The magnitude and distributions of internal loads shall include in their determination the effects of thermal deformation. Deformations resulting from operation under all ambient temperatures in the range -65° F. to +160° F. shall be considered.

4.3.1.4 Fatigue

The magnitude of stress reversals shall be minimized, and materials and design details shall be used that minimize the possibility of fatigue failure. The following three basic factors must be known to give a rational determination of the fatigue life of a structure.

4.3.1.4.1 Flight Stress Measurements

Because of the approximations employed in rotor load and stress distribution analyses, the calculated rotor fatigue stress levels are not considered to be accurate enough for competent blade design. Rotor stress levels shall therefore be determined by means of carefully controlled, instrumented flight strain gage testing. These tests shall determine the magnitude of steady and oscillatory stresses associated with normal helicopter operation and the correlation of the occurrence of critical stresses with specific maneuvers or operating conditions. A rational evaluation of the critical stress areas shall be made in order to determine the proper distribution of gages.

Table 2, page 18, contains a list of maneuvers for investigation in a flight strain survey. These maneuvers shall be investigated over the complete r.p.m., speed, altitude, center of gravity, and weight ranges.

4.3.1.4.2 Frequency of Loading

Table 1, page 17, gives an estimation for the percentage of total operating time associated with each flight maneuver.

4.3.1.4.3 Fatigue Strength

The maximum acceptable stress levels are to be obtained by use of modified Goodman Diagrams. If the maximum fatigue stresses fall below the maximum acceptable stress level, the system can safely be assumed to have infinite life and no fatigue testing is necessary. If the operating stresses are above the acceptable stress level, fatigue tests of the actual component are required. Methods for determining the service life may be found in Appendix A of Civil Aeronautics Manual 6.

4.3.1.5 Load Factors

The vertical load factor at the center of gravity for a Class III helicopter shall be +2.5 or -0.5. Table 2, page 18, summarizes the load factors at the center of gravity for different flight maneuvers.

4.3.2 Flight and Take-Off Loading Condition

4.3.2.1 Flight Load Parameters

4.3.2.1.1 Airspeed

Table 2, page 18, summarizes the airspeeds for different flight maneuvers.

4.3.2.1.2 Altitudes

The altitudes shall be the altitude at which the equivalent airspeed corresponding to V_H (125 m.p.h.) is a maximum, the altitude at which the maximum Mach number at the rotor blade tip is attained, and any intermediate altitude that results in limitations (critical loads, excessive vibration, etc.) arising from variations of the aerodynamic characteristics of rotor blade stall.

4.3.2.1.3 Control Motions

For a Class III helicopter, a time interval of 0.4 second shall be used for control forces and displacements specified for different flight maneuvers shown in Table 2.

4.3.2.2 Symmetrical Flight

Table 2, page 18, summarizes the following flight maneuvers.

4.3.2.2.1 Maximum Speed

The airspeed shall be V_D (1.15 x 125 m.p.h.) in forward, rearward, and sideward flight. The normal load factor shall be unity. The rotor speed shall be as follows:

a) The overspeed operation, power on
b) The design minimum rotor speed, power on

4.3.2.2.2 Design Fatigue Loading

The design fatigue loading shall be in accordance with the fatigue design loading schedule, Table 1, page 17. The rotor system, except those items covered by applicable specifications, shall be designed for a minimum fatigue life of 1,000 hours.

4.3.2.2.3 Symmetrical Dive and Pullout

The forward airspeed shall be V_D (1.15 x 125 m.p.h.) and 0.6 V_H (0.6 x 125 m.p.h.). The normal load factor shall be -0.5 or +2.5 for each specified airspeed. The rotor speed shall be as follows:

a) The overspeed operation, power on
b) The design minimum rotor speed, power on

The pitching accelerations shall be those developed by a linear displacement of the controls in not more than 0.4 second, which results in the specified load factor, then returning the controls in not more than 0.4 second to that displacement required for level flight.

4.3.2.2.4 Vertical Take-Off

With the helicopter on the ground, the collective pitch control shall be displaced to change the main rotor blade pitch from the minimum to the maximum angle in not more than 0.4 second. The resultant normal load factor shall be +2.5, and the rotor speed shall be an overspeed operation, power on.

4.3.2.3 Unsymmetrical Flight

Table 2, page 18, summarizes the following flight maneuvers.

4.3.2.3.1 Rolling Pullout with Maximum Control Displacement

The forward airspeed shall be V_D (1.15 x 125 m.p.h.) and any lower speed that results in critical loads. The rotor speed shall be as follows:

a) The overspeed operation, power on
b) The design minimum rotor speed, power on

The rate of roll shall be the maximum attainable with a 100-pound lateral control force, or full lateral displacement, applied in not more than 0.4 second. The normal load factor shall be 0.8 times the positive load factor of +2.5 and also shall be zero. The maximum rate of roll and the load factor shall occur simultaneously.

4.3.2.3.2 Yawing

The airspeed shall be V_D (1.15 x 125 m.p.h.) and any lesser speed which produces critical side load in forward flight and sideward flight. The directional control shall be displaced to the maximum displacement in not more than 0.4 second. The control displacement shall be maintained until the maximum angle of sideslip is developed and shall then be returned to neutral position at the same rate of displacement. The rotor speed shall be the overspeed operation, power on.

4.3.2.4 Gust

The airspeed shall be V_H (125 m.p.h.) in forward flight. A gust of 40 feet per second shall be encountered. The rotor speeds shall be all speeds up to the overspeed operation, power on.

4.3.2.5 Preliminary Design Spectrum for Rotor Airload Analysis

Table 3, page 19, summarizes the flight maneuvers to be used as a preliminary design spectrum for rotor airload analysis. These conditions shall give maximum airloads on the blade and also airload trends due to flight speed and rotor tip speed.

4.3.3 Ground Loading Condition

4.3.3.1 Wind Loads

The helicopter shall be on level ground with rotor turning at the critical rotor speed for ground flapping. The aerodynamic loads shall be those resulting from a 40 knot wind from any horizontal direction. Inertia loads resulting from the flapping of the rotor blades shall be combined with the aerodynamic loads.

4.3.3.2 Crash Landing

Sufficient strength shall be provided in the attachment of the rotor system to prevent failure of such attachments which would result in injury to personnel. The ultimate inertia-load factors shall be -4.0g longitudinal and vertical, and ±2.0g side.

4.3.4 Control System Loads

The controls considered as part of the rotor system shall be those above the swash plate. The controls shall be designed to withstand the loads resulting from the pilot-applied loads, the power cylinder output load, or the loads imposed by the rotor blades, whichever is greater.

A loading distribution from the swash plate to the rotor blades shall have the following considerations:

a) 50 percent to two blades, 50 percent to the other two blades.
b) 50 percent to two blades, 0 percent to the other two blades.
c) 60 percent to two blades, 40 percent to the other two blades.

All control systems are to be designed for fatigue loads based on normal operating loads, and the fatigue loading spectrum presented in Table 1, page 17.

4.3.5 Mechanical Instability, Flutter, and Vibration

4.3.5.1 Vibration Comfort Levels

The helicopter shall be so designed that the main rotor-induced fuselage and control-stick vibration levels do not exceed the limits specified in specification MIL-H-8501.

4.3.5.2 Flutter

The rotor blades and attached control surfaces, if applicable, shall be free of flutter and divergence at rotor speeds up to 1.25 times the overspeed (1.05 x 650 f.p.s.) operation.

4.3.5.3 Mechanical Instability of Rigid Blades

The calculations of the mechanical instability analysis shall demonstrate that the lower limit of the instability speed range is above the maximum speed for the main rotor.

4.3.5.4 Rotor Blade Clearance

The design of the rotor system shall be such that, upon installation on the helicopter, there shall be sufficient clearance of the blades to the ground, to each other, and to other parts of the helicopter. During operation in all flight regimes, the clearance between main rotor blades and other parts of the helicopter shall be not less than nine inches, and preferably 12 inches. Sufficient clearance shall be provided, with the rotors in operation, in order that crew members will not be in the plane of rotation and can safely enter and leave the aircraft.

4.3.6 Dynamic (Transient) Conditions

The rotor system shall be capable of withstanding dynamic (transient) moments and torques due to a 40-foot-per-second gust, a transient cyclic pitch, and a collective pitch input.

TABLE 1
DESIGN FATIGUE LOADING SPECTRUM

Maneuver	Percent Occurrence
A. GROUND CONDITION	3
1. Rapid increase of r.p.m. on ground	1
2. Taxiing with full cyclic control	1
3. Jump take-off	1
B. HOVERING	4
1. Steady hovering	1
2. Lateral reversal	1
3. Longitudinal reversal	1
4. Rudder reversal	1
C. FORWARD FLIGHT - POWER ON	93
1. Level flight - 20 percent V_H	5
2. Level flight - 40 percent V_H	20
3. Level flight - 60 percent V_H	25
4. Level flight - 80 percent V_H	15
5. V_H	6
6. 115 percent V_H	1
7. Right turns	3
8. Left turns	3
9. Climb (take-off power)	2
10. Climb (maximum continuous power)	4
11. Partial power descent (including condition of zero flow through rotor)	3
12. Landing approach	4
13. Cyclic and collective pullups from level flight	1
14. Lateral reversals at V_H	1
15. Longitudinal reversals at V_H	1
16. Rudder reversals at V_H	1

TABLE 2
MAIN ROTOR SYSTEM FLIGHT CRITERIA

Cond.	Flight Maneuver	Limit Load Factor	Flight Speed (m.p.h.)	Rotor Tip Speed (f.p.s.)
1	Hover	1.0	0	683 618
2	Minimum r.p.m. hover	1.0	0	415
3	Symmetrical - maximum speed	1.0	144 41	622 562
4	Symmetrical - design fatigue loading (see schedule, Table 1)	Minimum fatigue life of 1,000 hours		
5	Symmetrical - pullout	2.5	144 41	622 562
6	Symmetrical - dive	-0.5	144 41	622 562
7	Symmetrical - vertical take-off	2.5	0	622
8	Unsymmetrical - rolling pullout	2.0	144 41	622 562
9	Unsymmetrical - yawing	1.0	144 41	622
10	Gust (40 f.p.s.)	to be determined	144 41	622 562
11	Stop-bang ground gust load	-	40 f.p.s. (gust)	critical rotor speed
12	Special condition for attachments	1.0	0	813

TABLE 3
PRELIMINARY DESIGN SPECTRUM
FOR ROTOR AIRLOAD ANALYSIS (CRITERIA)

Flight Conditions	Flight Maneuver*	Limit Load Factor (n_z)	Flight Speed (m.p.h.)	Rotor Tip Speed (f.p.s.)
1	Minimum r.p.m. hover	1.0	0	415
2	Hover	1.0	0	650
3	Forward flight	1.0	41	592
4	Cruise	1.0	70	592
5	Dive	-0.5	41 144	562
6	Pullout	2.5	41 144	562
7	Design maximum forward flight	1.0	41 144	562
8	Design maximum forward flight	1.0	41 144	592
9	Design maximum forward flignt	1.0	41 144	622
10	Gust 40 f.p.s.	to be determined	41 144	622

* Sea level and gross weight.

5.0 ROTOR DESIGN LOADS

All rotor blade loads which are discussed in this report are based on the preliminary blade weight and stiffness data which were used in the rotor blade flutter study. These data are plotted in Figures 6 and 7 and represent one blade of a four-bladed, universally teetering rotor system. Additional data which are needed in this report are documented in those sections in which the data are used.

5.1 Steady-State Design Load Analysis

5.1.1 Centrifugal Loads

The rotor blade weight distribution presented in Figure 7 in combination with a concentrated tip weight, W_T, of 1,200 pounds are used to obtain the rotor blade radial load curve due to centrifugal force which is presented in Figure 8. The following general formulas are used to compute centrifugal force.

$168 \leq r \leq 672$ in.:

$$C.F. = \left[4139 + \left(\frac{.000899r - 2.356632}{386}\right) r^2\right] \Omega^2 \qquad (1)$$

$84 \leq r \leq 168$ in.:

$$C.F. = \left[4383 + \left(\frac{.040635r - 12.370010}{386}\right) r^2\right] \Omega^2 \qquad (2)$$

$0 \leq r \leq 84$ in.:

$$C.F. = \left[4352 - \frac{7.25r^2}{386}\right] \Omega^2 \qquad (3)$$

where:

r = Radial distance from centerline of rotation, in.
Ω = Rotor angular velocity, rad/sec.
W_T = Tip weight, 1,200 lb.

5.1.2 Rotor Blade Torque

5.1.2.1 Gyroscopic Torque

The four-bladed rotor design has two Continental 357-1 turbojet engines mounted on each blade tip in an over-under configuration. The compressor turbine components of both engines rotate in a counterclockwise direction viewed from the rear, while the rotor blades rotate in counterclockwise direction viewed from above. The gyroscopic moment imposed by the engines on the rotor blade, then, is in a nose-down direction.

The engine parameters which influence gyroscopic moment are as follows:

I_E = Inertia of rotating items, 1.67 lb-in-sec^2/engine

ω_E = Angular velocity of rotating items, 2,304 rad/sec. maximum

The gyroscopic moment is:

$T_G = -2I_E\omega_E\Omega$ (Negative sign indicates nose-down torque)

For rotor blade design, the maximum rotor speed is defined in Section 4.0 as 1.05 times the nominal operating speed.

Therefore: $\Omega_{max} = 1.05\left(\frac{650}{56}\right) = 12.19$ rad/sec. for blade design

and $T_G = -2(1.67)2,304(12.19) = \underline{-93,800 \text{ in-lb.}}$

For engine attachment design, the maximum rotor speed is defined in Section 4.0 as 1.25 times the nominal operating speed.

Therefore: $\Omega_{max} = 1.25\left(\frac{650}{56}\right) = 14.51$ rad/sec. for engine attachment design

and $T_G = -2(1.67)2,304(14.51) = \underline{-111,700 \text{ in-lb.}}$

5.1.2.2 Induced Centrifugal Torque

There are two induced centrifugal torques of interest: that due to blade coning and that due to collective pitch.

5.1.2.2.1 Induced Torque Due to Coning

The so-called "rigid coning" torque is primarily a function of the blade and tip mass chordwise center-of-gravity locations in relation to the blade feathering axis (quarter chord). Consider the unit mass of Figure 1 displaced a distance x aft (+) of the feathering axis.

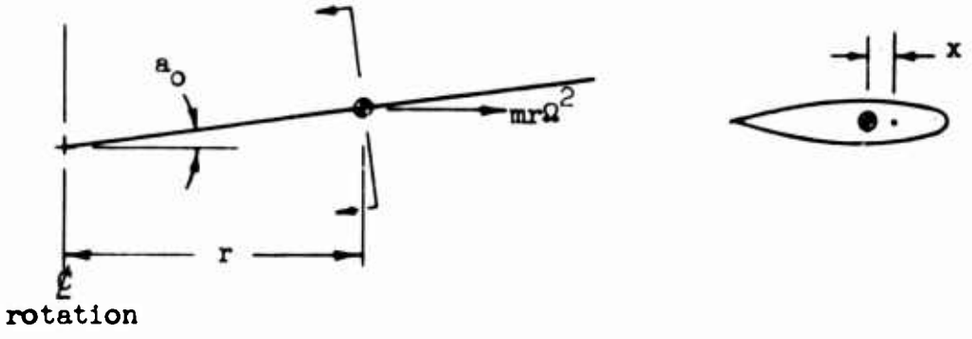

Figure 1. Induced Torque Due to Coning.

This unit mass causes a nose-up torque about the feathering axis of magnitude $mr\Omega^2 x \sin a_o$ which can be simplified to $mr\Omega^2 x a_o$ since the coning angle is small and $\sin a_o \approx a_o$.

For a blade with a tapered mass distribution and a concentrated tip weight, the formula for induced torque due to coning is as follows.

$$T_{a_o} = m_o R^2 \Omega^2 x_B a_o \left[\frac{1}{6} + \frac{\lambda}{3}\right] + \frac{W_T}{g} R\Omega^2 x_T a_o \qquad (4)$$

where

m_o = blade mass distribution at blade root, $\frac{\text{lb-sec}^2/\text{in.}}{\text{in.}}$

R = rotor radius, 672 in.

Ω = rotor angular velocity, rad/sec.

λ = ratio of blade mass distribution at the blade tip/mass distribution at the blade root

W_T = tip weight, 1,200 lb.

a_o = coning angle, rad.

x_B = distance of blade center of gravity from feathering axis, + aft, in.

x_T = distance of tip weight center of gravity from feathering axis, + aft, in.

Using Figure 7 and neglecting the root weight buildup, the mass parameters for Equation (4) are taken as

$$m_o = 4.7/386 \quad \text{lb-sec}^2/\text{in}^2$$

$$\lambda = 2.9/4.7$$

therefore

$$T_{a_o} = \Omega^2 a_o \left[2047 x_B + 2089 x_T\right] \qquad (5)$$

Present design specifies

$\Omega = 1.05(\frac{650}{56}) = 12.19$ rad/sec. (maximum)

$a_o \approx 2.25/57.3$ rad. (maximum 2.5g pullup)

$x_B = 0$ (quarter-chord balanced)

$x_T = -.03c = -2.34$ in.

Therefore

$$T_{a_o} = \underline{-\ 28{,}500 \text{ in-lb.}} \quad \text{(maximum)}$$

Since quarter-chord balancing the blade results in the use of non-structural material in the leading edge, it is possible that the center

of gravity of the distributed mass might be allowed to move aft (reducing T_{a_o}) but in no case will x_B become negative.

5.1.2.2.2 Induced Torque Due to Collective Pitch

The so-called "centrifugal centering" torque is primarily a function of the mass properties of the blades and tip weight.

A general definition for the centrifugal centering torque due to a unit length of rotor blade is

$$\frac{dT}{dr} = -\Omega^2(I_{zz} - I_{xx})\theta \quad \text{lb-in/in.} \tag{6}$$

where: Ω = Rotor angular velocity, rad/sec.

I_{zz} = "Yawing" mass moment of inertia of the unit section, lb-in-sec^2/in.

I_{xx} = "Rolling" mass moment of inertia of the unit section, lb-in-sec^2/in.

θ = Blade geometric pitch angle, rad.

I_{zz} is generally much larger than I_{xx} for a standard rotor blade section, and it is simplifying as well as conservative to neglect I_{xx}. If it is also assumed that I_{zz} is uniform for the entire blade, as the pitching inertia of Figure 7 suggests, the following formula can be written for root torque of a rotor blade with linear twist and a concentrated tip weight.

$$T_\theta = -\Omega^2 R I_{zz_B}\left(\theta_o + \frac{\theta_T}{2}\right) - \Omega^2(I_{zz} - I_{xx})_{tip}(\theta_o + \theta_T) \tag{7}$$

Present design indicates

$$\Omega = 1.05\left(\frac{650}{56}\right) = 12.19 \text{ rad/sec. (maximum)}$$
$$I_{zz_B} \approx 2 \text{ lb-in-sec}^2\text{/in.}$$
$$I_{zz_{tip}} \approx 305 \text{ lb-in-sec}^2$$
$$I_{xx_{tip}} \approx 518 \text{ lb-in-sec}^2$$
$$\theta_o \approx 22.5/57.3 \text{ rad. (maximum)}$$
$$\theta_T = -10/57.3 \text{ rad.}$$

Substituting these values into Equation (7) yields:

$$T_\theta = -(12.19)^2 672(2)\left(\frac{22.5 - 5}{57.3}\right) - (12.19)^2(305 - 515)\left(\frac{22.5 - 10}{57.3}\right)$$

$$T_\theta = -60{,}990 + 6{,}810 \approx \underline{-54{,}200 \text{ in-lb. (maximum)}}$$

5.1.2.3 Aerodynamic Torque

The torques created by airflow over the blade section and engine nacelle are not so precisely defined as are those previously discussed. Generalizations can be made, however, to assess their relative magnitudes.

5.1.2.3.1 Torque Due to Blade Airfoil Section

The pitching moment about the aerodynamic center (ac) of an NACA 0015 airfoil is taken as zero from several sources which need not be referenced. A torsional moment will result on the blade, however, due to the lift vector since the center of pressure of an NACA 0015 airfoil is usually taken near the 24 percent chord point or .01c forward of the feathering axis. The torsion thus created would be in the nose-up (+) direction and would subtract from the torques of Sections 5.1.2.1 and 5.1.2.2. It is conservative, then, to neglect the aerodynamic torque due to blade airfoil section.

5.1.2.3.2 Torque Due to Engine Nacelle

Numerous wind tunnel data were taken for several nacelle configurations, each of which was investigated aerodynamically through a pitching and yawing angle of attack range. Scaling these data for use on the tip turbine nacelle shows that the most severe pitching moment (torque) imposed at the blade quarter chord is insignificant (< 5%) when compared with the torques discussed in previous sections.

5.1.2.4 Torque Due to One Engine Failure

With an over-under engine configuration at each blade tip, there exists the possibility of losing thrust on one engine and imposing a torque on the blade due to the remaining engine's thrust vector being either 13.5 inches above or below the rotor blade chord line. It must be remembered, however, that total loss of thrust for one engine is accompanied by the loss of gyroscopic moment due to the same engine.

For one engine out, then,

$$T_{tip} = T_{\Delta thrust} + T_{gyro.}$$

$$T_{tip} = hT_E - I_E\omega_E\Omega \qquad (8)$$

where:

- h = Engine thrust distance from chord line, + downward 13.5 in.
- T_E = Engine thrust, lb.
- I_E, ω_E = Defined in Section 5.1.2.1
- Ω = Rotor angular velocity, rad/sec.

The largest positive (nose-up) torque would occur for a failure of the upper engine with $\Omega = 0$. For this condition

$$T_E = 1{,}700 \text{ lb.} \quad \text{(maximum static)}$$

and $$T_{tip} = +13.5(1{,}700) = \underline{+22{,}950 \text{ in-lb.}}$$

All of the additional torques which depend on Ω would be zero for this case and the total torsional loading on the blade would be low.

The largest negative (nose-down) torque would occur for a failure of the lower engine with

$$\Omega = 1.05 \left(\frac{650}{56}\right) = 12.19 \text{ rad/sec.}$$

$$\omega_E = 2{,}304 \text{ rad/sec.}$$

$$T_E = 1{,}550 \text{ lb. (compatible with } \omega_E)$$

For this condition

$$T_{tip} = -13.5(1{,}550) - 1.67(2{,}304)(12.19)$$

$$T_{tip} = \underline{-67{,}830 \text{ in-lb.}}$$

This torque is smaller than the combined gyroscopic torque of both engines, and so the torque due to a failure of one engine is not critical.

5.1.2.5 Total Torque Loading

A review of Section 5.1.2 indicates that the design torque for the rotor blades is nose-down primarily due to the gyroscopic moment caused by the tip engines. A general expression for blade torque as a function of radius can be written which contains only those terms which add to the nose-down moment. This approach is conservative for blade structural design.

$$T_{total} = T_G + T_{a_o} + T_\Omega$$

where: T_G = Tip engine gyroscopic moment

T_{a_o} = Rigid coning torque

T_Ω = Centrifugal centering torque

From Sections 5.1.2.1 and 5.1.2.2.1, it is conservative to write

$$T_G + T_{a_o} = -2I_E\omega_E\Omega + 2089\, x_T\Omega^2 a_o \qquad (9)$$

From Section 5.1.2.2.2, it is conservative to write

$$T_{\theta} = -\Omega^2 R I_{zz_B}\left[\theta_o\left(1 - \frac{r}{R}\right) + \frac{\theta_T}{2}\left(1 - \frac{r^2}{R^2}\right)\right] \qquad (10)$$

All of the variables in Equations (9) and (10) are defined in previous sections. The maximum rotor angular velocity for blade structural design and the maximum possible collective pitch setting are used for conservatism.

Combining Equations (9) and (10) gives the following expression for blade torque at any fraction of radius, r/R.

$$T_{total} = -2I_E\omega_E\Omega + 2089\, x_T\Omega^2 a_o - \Omega^2 R I_{zz_B}\left[\theta_o\left(1 - \frac{r}{R}\right) + \frac{\theta_T}{2}\left(1 - \frac{r^2}{R^2}\right)\right] \qquad (11)$$

Using Ω_{max} = 12.19 radians per second and θ_o = (22.5/57.3) radians, Equation (11) can be reduced to the following equation for design blade torque.

$$T_{total} = -122{,}330 - 3{,}485\left[22.5\left(1 - \frac{r}{R}\right) - 5\left(1 - \frac{r^2}{R^2}\right)\right] \text{ in-lb.} \qquad (12)$$

Equation (12) is plotted in Figure 9. This curve, once again, should be considered a conservative maximum, and such occurrences as engine failures would only tend to decrease this torsion.

5.1.3 Aerodynamic Loads

5.1.3.1 Discussion of Cornell Aeronautical Laboratory (CAL) Airload Program

With the use of CAL Airload Program (Reference 1) and Control Data Corporation's 1604A digital computer, airloads were generated for ten different flight conditions, shown in Table 5.

The airload program assumes the rotor is operating in steady-state flight. The generated wake and the airloads are, therefore, the same for each revolution of the blades. Each blade of the rotor is represented by a segmented lifting line (bound vortex) located along the steady deflected position of the quarter chord. The lifting line is considered to advance in a stepwise manner through equally spaced azimuth positions. In the wake, the shed and trailing vorticity distributions of each blade are represented by a mesh of segmented vortex filaments; each segment is straight and of constant vortex strength. The segmented trailing vortex filaments emanate from each of the end points of the lifting line segments. The segmented shed vortex filaments intersect the trailing filaments in a manner such that the end points of both are coincident. The strengths of the shed elements are equal to the change in strength of the bound vortex segments between successive azimuth stations and are deposited in the flow at each azimuth station of the bound vortex. The

strengths of the trailing vortex elements are equal to the differences in strengths of adjacent bound vortex segments and are deposited in the flow in a manner such that they connect the bound vortex end points to the shed vortex end points. The displacement time history of the wake is relatively unrestricted. Thus, any physically realistic distortion of the wake can be incorporated into the computation of the airloads. For each azimuth position, the airloads are computed at the mid-points of the lifting-line segments.

The airload program consists of five parts. Each parts accomplishes the following:

a) Part 1 computes the coordinates of the mid-points of the bound vortex segments and the coordinates of the vortex end points in the wake (end points assumed to move with constant velocity).

b) Part 2 generates the sigma matrix, where the sigma elements are the coefficients of the unknown bound vortex strengths.

c) Part 3 normalizes and rearranges the sigma matrix.

d) Part 4 solves the matrix equation by iteration and then computes the lift, induced velocity, induced drag, plunging drag, plunging velocity, geometric angle of attack, and bound vortex strengths.

e) Part 5 produces a harmonic analysis of those properties calculated in Part 4.

5.1.3.2 Input Data for Cornell Aeronautical Laboratory (CAL) Airload Program

5.1.3.2.1 Nomenclature of the Input Data

NC - Number of blades (must be a factor of IA)

N - Number of central points on the blade in which the load is computed

IA - Number of azimuth stations (must contain the factor of NC and ≤ 25)

IRR - Number of revolutions of wake used (maximum radii of 19)

VF - Forward velocity of rotor (f.p.s.)

OMEGA - Rotational speed (rad/sec.)

AT - Tip path plane angle, deg. (first harmonic cosine flapping plus forward inclination of the shaft)

HOFS - Flapping hinge offset (ft.)

RM1 and RM2 - Limits on distance from vortex filament to point where velocity is calculated (ft.)

AA - Lift curve slope

CWA - Control word for number of lift curve values to be read from cards

WZ(J) - Zero harmonic (steady) component of induced velocity normal to tip path plane at each bound vortex end point (f.p.s.) (J = 1, N + 1)

WC(L, J) - Lth harmonic Fourier cosine component of induced velocity normal to tip path plane at each bound vortex end point (f.p.s.) (L = 1, (IA - 1)/2; J = 1, N + 1)

WS(L, J) - Lth harmonic Fourier sine component of induced velocity normal to tip path plane at each bound vortex end point (f.p.s.) (L = 1, (IA -1)/2; J = 1, N + 1)

BZ(I) - Steady displacement due to steady bending plus coning at each blade segment mid-point (in.) (I = 1, N)

BZZ(J) - Steady displacement due to steady bending plus coning at each blade segment end point (in.) (J = 1, N + 1)

R(J) - Radial distance to end points of blade segments (ft.) (J = 1, N + 1)

A(K) - Lift curve slope (K = 1, N (IA))

B(I) - Blade semichord at mid-points of blade segment, ft. (I = 1, N)

AFMD - Maximum section stalling angle of attack (deg.)

KXX - Number of harmonics of the Fourier series input representation of the plunging and torsion motions at each blade station (KXX $\neq$ 0)

BTAIC - First harmonic Fourier cosine flapping coefficient (deg.)

BTAIS - First harmonic Fourier sine flapping coefficient (deg.)

ZCZSLO(I) - Zero harmonic (steady) slope of plunging displacement (I = 1, N)

ZC(L, I) - Lth harmonic Fourier cosine coefficient of plunging displacement at each station (in.) (L = 1, KXX; I = 1, N)

ZS(L, I) - Lth harmonic Fourier sine coefficient of plunging displacement at each station (in.) (L = 1, KXX; I = 1, N)

ZCPR(L, I) - Lth harmonic Fourier cosine coefficient of plunging displacement at each station (rad.) (L = 1, KXX; I = 1, N)

ZSPR(L, I) - Lth harmonic Fourier sine coefficient of plunging displacement at each station (rad.) (L = 1, KXX; I = 1, N)

TZER(I) - Zero harmonic (steady) blade torsional displacement (rad.) (I = 1, N)

THCO(L, I) - Lth harmonic Fourier cosine coefficient of torsional displacement (rad.) (L = 1, KXX; I = 1, N)

THSI(L, I) - Lth harmonic Fourier sine coefficient of torsional displacement (rad.) (L = 1, KXX; I = 1, N)

5.1.3.2.2 Input Data

Tables 6 and 7 present the input data for the five design conditions submitted in this report. The input data is explained as follows:

IRR - The number of wakes was determined by trial. Three were selected because greater than three changed the lower harmonics an insignificant amount. This was expected because the additional wake is relatively far from the rotor, and the induced velocities due to it are relatively uniform over the disk; whereas the induced velocities due to the nearer wake have a considerable variation over the rotor disk and is the primary source of the higher harmonics.

AT - Reference, Volume 10, Section 5.3.1

RM1 - Three revolutions of wake gives a wake termination approximately one-and-one-half rotor diameter away from the rotor disk (Reference 1)

RM2 - Maximum limit of RM1, approximately three percent greater than RM1

AA - Assumed constant at 5.73

CWA - Zero if AA is to be a variable and greater than zero if assumed constant

WZ(J) - Assumed equal to second order curve distribution. WZ = $\sqrt{g}\left[101.6(r/R) - 68.8(r/R)^2\right]$. This second degree curve is similar in shape to the program output of induced velocity.

WC(L, J) - First harmonic cosine coefficient is equal to $u_1/u_o\left[WZ(J)_{hover}\right]$ where u_1/u_o is based on Reference 2, Figure 4. The remaining harmonic cosine coefficients are assumed zero.

WS(L, J) - The harmonic sine coefficients are assumed zero.

BZ(I) - Preliminary deflection analysis

BZZ(J) - Preliminary deflection analysis

A(K) - Assumed constant

BTAIC - Reference, Volume 10, Section 5.3.1

BTAIS - Assumed zero

ZCZSLO(I) - Assumed zero

ZC(L, J) - Assumed zero

ZS(L, J) - Assumed zero

ZCPR(L, J) - Assumed zero

ZSPR(L, J) - Assumed zero

TZER(I) - Reference, Volume 10, Section 5.3.1

THCO(L, J) - Assumed zero

THSI(L, J) - Reference, Volume 10, Section 5.3.1

5.1.3.3 Results of the Cornell Aeronautical Laboratory (CAL) Airload Program

Airloads for ten different flight conditions were generated using Control Data Corporation's 1604A digital computer. Five of these ten conditions (Table 5) are presented in this report. These five conditions represent the maximum steady loads (positive and negative), the maximum alternating loads, and those alternating loads which may be used with the design fatigue loading spectrum. The results of these five conditions are plotted on Figures 10 to 61.

5.1.3.3.1 Steady and Alternating Lift Loads

The steady and alternating lift loads are obtained using CAL airload program. The results are plotted on Figures 10 through 35.

5.1.3.3.2 Steady and Alternating Drag Loads

The steady and alternating drag loads on the blade are determined by the following analysis.

$$\text{Drag} = (\text{Drag})_{\text{induced}} + \left[(\text{Drag})_{\text{blade}} + (\text{Drag})_{\text{nacelle}}\right]_{\text{profile}}$$

$(\text{Drag})_{\text{induced}}$ = Drag due to lift is analyzed in CAL airload program

$$[D]_{\text{profile}} = \int_o^R \left[\frac{1}{2}\rho\delta_b c(\Omega r + V_F \sin\psi)^2 dr\right]_{\text{blade}} + \left[\frac{1}{2}\rho\delta_n A(\Omega R + V_F \sin\psi)^2\right]_{\text{nacelle}}$$

$$[D]_{\text{profile}} = \int_o^R \left[\frac{1}{2}\rho\delta_b c(\Omega^2 r^2 + 2\Omega r V_F \sin\psi + V_F^2 \sin^2\psi)\,dr\right]_{\text{blade}} + \left[\frac{1}{2}\rho\delta_n A(\Omega^2 R^2 + 2\Omega R V_F \sin\psi + V_F^2 \sin^2\psi)\right]_{\text{nacelle}}$$

$$[D]_{\text{profile}} = \int_o^R \left[\frac{1}{2}\rho\delta_b V_T^2\left(\frac{r^2}{R^2} + \frac{1}{2}\mu^2 + 2\frac{r}{R}\mu\sin\psi - \frac{1}{2}\mu^2\cos 2\psi\right)dr\right]_{\text{blade}} + \left[\frac{1}{2}\rho\delta_n A V_T^2\left(1 + \frac{1}{2}\mu^2 + 2\mu\sin\psi - \frac{1}{2}\mu^2\cos 2\psi\right)\right]_{\text{nacelle}}$$

where:

ρ = mass density of air (.002378 lb-sec^2/ft^4)
δ_b = blade drag coefficient
δ_n = nacelle drag coefficient
c = chord (ft.)
Ω = blade angular velocity (rad/sec.)
r = radius (ft.)
V_F = velocity forward flight (f.p.s.)
ψ = azimuth angle (deg.)
A = area, nacelle (ft^2)
R = radius to tip (ft.)
V_T = tip speed (f.p.s.)
μ = V_F/V_T
T = required thrust per blade (lb.)

The input data necessary to obtain the profile drag for the five design conditions are as follows:

δ_b = .01
δ_n = .282
c = 6.5 ft.
R = 56.0 ft.
A = 2.08 ft.

TABLE 4
INPUT DATA TO DETERMINE PROFILE DRAG

Data	Condition				
	2	3	5	6	8
V_F	0	41	0	41	144
V_T	650	592	562	562	562
μ	0	.10	0	.11	.38
Ω	11.6	10.6	10.1	10.1	10.1
T	2,100	1,835	1,000	3,100	2,930

The results of the total drag are shown on Figures 36 through 61.

5.1.4 Rotor Blade Bending Moments

There are several reliable methods for calculating the steady flapwise and chordwise bending moments for rotor blades. One such method is a matrix approach developed in Reference 3 which shall be called the Mayo method. The Mayo method is a rational approach to blade bending moments using blade element theory wherein centrifugal force, inertia loads, and aerodynamic damping are taken into consideration. The method is limited, however, since it does not consider the effects of coupled bending and torsion nor does it include the dynamic response of the blade for airload harmonics which are nearly coincident with rotor blade natural frequencies.

A method has been evolved which makes use of the airloads presented in Section 5.1.3 and unit harmonic load investigations described and tabulated in Reference 4. The unit harmonic load studies include the coupled dynamic response of the blades since these studies were accomplished using the same direct analog computer simulation as was used for the rotor blade flutter study. The mechanics of using these unit load results are described in Section 5.1.4.1.2.

Four flight conditions are considered to be critical for blade design. These conditions along with pertinent speed data are as follows:

	V	Ω
1.0g forward flight	41 mph	10.57 rad/sec.
1.0g forward flight	144 mph	10.04 rad/sec.
2.5g pullup	41 mph	10.04 rad/sec.
-0.5g hover	0 mph	10.04 rad/sec.

The 2.5g pullup is selected as being the condition which yields the largest steady bending moment in combination with its complement of harmonic moments. The 1.0g forward flight conditions are selected as yielding the harmonic bending moments of longest duration (highest percent of occurrence). The -0.5g hover condition gives the largest negative in-flight bending moments at the root while static droop moment may be critical along the blade (Figure 63).

5.1.4.1 Flapwise Bending Moments

The Mayo method for calculating flapwise bending moments is used for the steady and first harmonic moments because the unit load method is applicable only for the second through the seventh harmonics. The second harmonic moments can also be calculated using Mayo's method and will be compared with the unit load method for compatibility. Since the Mayo method is completely uncoupled from chordwise and torsional modes while the unit load method yields completely coupled bending moments, it is expected that comparison of the second harmonic moments will show major differences. The steady and first harmonic airloads for use in the Mayo method are taken from Section 5.1.3 and should yield adequately accurate bending moments for blade design.

5.1.4.1.1 Uncoupled Bending Moments Using the Mayo Method

The mechanics of the Mayo method for calculating bending moments are not discussed in this report but may be found in Reference 3. The physical properties of the rotor blade used in this analysis are those plotted in Figures 6 and 7 with the addition of a 1,200-pound concentrated tip weight. The moment stations and mass stations which are used are tabulated in Figure 2.

The bending moments which result for the four design conditions are plotted in Figures 63, 64, 71, and 78. The steady and first harmonic bending moments are to be used for rotor blade design while the second harmonic bending moments are superseded by those of Section 5.1.4.1.2 which follows.

MOMENT STATIONS		MASS STATIONS	
r/R	Flapwise EI	r/R	Lumped Mass
0.85	5.3×10^9 lb-in^2	0.95	3.63 lb-sec^2/in.
.75	5.7×10^9 lb-in^2	.85	.55 lb-sec^2/in.
.65	6.1×10^9 lb-in^2	.75	.59 lb-sec^2/in.
.55	6.4×10^9 lb-in^2	.65	.62 lb-sec^2/in.
.45	6.8×10^9 lb-in^2	.55	.65 lb-sec^2/in.
.35	7.2×10^9 lb-in^2	.45	.68 lb-sec^2/in.
.275	7.4×10^9 lb-in^2	.35	.71 lb-sec^2/in.
.225	9.4×10^9 lb-in^2	.25	.92 lb-sec^2/in.
.15	14.7×10^9 lb-in^2	.15	2.13 lb-sec^2/in.
.05	21.7×10^9 lb-in^2	.05	2.52 lb-sec^2/in.

Figure 2. Moment and Mass Stations.

5.1.4.1.2 Coupled Bending Moments Using Unit Harmonic Loads

The rotor blade simulation used in Reference 4 uses the blade physical parameters of Figures 6 and 7 and represents a completely coupled model of the presently proposed tip turbojet rotor blade. Flapwise and in-plane unit harmonic loads (one pound) were simulated, independently, at five aerodynamic cells located radially at 0.25R, 0.41R, 0.57R, 0.73R, and 0.89R. These unit loads were applied at harmonics of rotor speed in a frequency range from two to eight cycles per revolution. The bending moments resulting from the harmonic loadings were measured at rotor blade stations 0.025R, 0.09R, 0.19R, 0.33R, 0.49R, 0.65R, 0.81R, and 0.945R. Both the moment magnitude and phase angle (in time) with respect to the applied load were tabulated at each moment station. Figure 62 presents a sketch of the rotor blade to aid the reader in visualizing the spanwise placement of the unit loads and bending moment stations.

The flapwise bending moment at any station can be obtained by resolving the actual flight airloads into five concentrated loads at the loading stations of Figure 62 and then multiplying these loads by the five respective unit bending moments for that station. Before doing this, however, the unit bending moments must be resolved into sine and cosine components of rotor azimuth angle (ψ) because the phase angles reported in Reference 4 are not always identical for all five applied loads. Reference 4 tabulates the maximum amplitude of each bending moment and the phase angle (in time) by which it leads the applied load as shown in Figure 3.

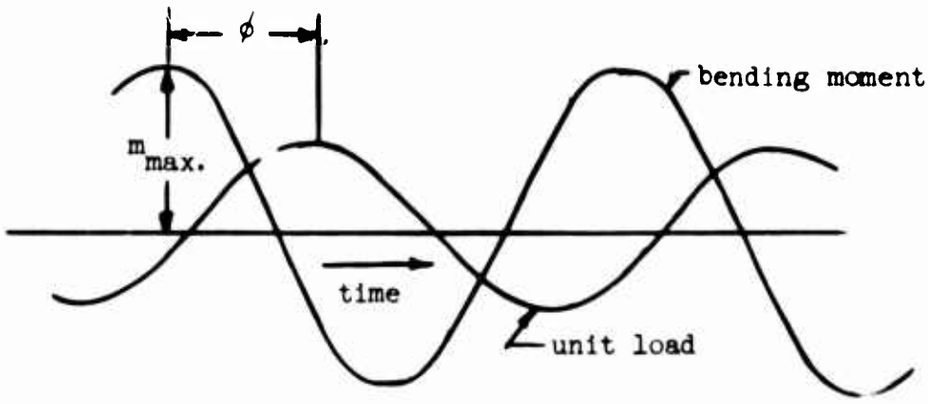

Figure 3. Unit Load and Bending Moment Phasing

Knowing the maximum unit moment and its phase angle with time, the following identities can be used for unit bending moments as they apply for cosine applied airloads (maximum amplitude at $\psi = 0^\circ$) or sine applied airloads (maximum amplitude at $\psi = 90^\circ$).

Cosine Applied Airloads

In general, for the n^{th} harmonic:

$$m = m_c \cos n\psi + m_s \sin n\psi$$

Specifically,

$$m_{max.}^2 = m_c^2 + m_s^2 \tag{13}$$

$$\tan n\psi = m_s/m_c \tag{14}$$

$$n\psi = 360^\circ - \phi \quad \text{at} + m_{max.} \tag{15}$$

Combining Equations (13), (14) and (15) gives

$$m_c = \pm \frac{m_{max.}}{\sqrt{1 + \tan^2(360^\circ - \phi)}} \begin{cases} + \text{ if } 270^\circ \leq (360^\circ - \phi) \leq 90^\circ \\ - \text{ if } 90^\circ \leq (360^\circ - \phi) \leq 270^\circ \end{cases} \tag{16}$$

$$m_s = m_c \tan(360 - \phi) \tag{17}$$

Sine Applied Airloads

In general, for the n^{th} harmonic:

$$m = m_c \cos n\psi + m_s \sin n\psi$$

Specifically,

$$m_{max.}^2 = m_c^2 + m_s^2 \tag{18}$$

$$\tan n\psi = m_s/m_c \tag{19}$$

$$n\psi = (360^\circ - \phi) + 90^\circ n \text{ at } m_{max.} \tag{20}$$

Combining Equations (18), (19), and (20), gives

$$m_c = \pm \frac{m_{max.}}{\sqrt{1 + \tan^2[(360^\circ - \phi) + 90^\circ n]}} \quad \begin{cases} + \text{ if } 270^\circ \leq (360^\circ - \phi) + 90^\circ n \leq 90^\circ \\ - \text{ if } 90^\circ < (360^\circ - \phi) + 90^\circ n \leq 270^\circ \end{cases} \tag{21}$$

$$m_s = m_c \tan\left[(360^\circ - \phi) + 90^\circ n\right] \tag{22}$$

The flapwise (or in-plane) coupled bending moments can now be calculated for any set of harmonic airloads plotted in Section 4.1.3.3. using the following matrix equation:

$$\{M\} = [m]_{c,z}\{L_c\} + [m]_{s,z}\{L_s\} + [m]_{c,x}\{D_c\} + [m]_{s,x}\{D_s\} \tag{23}$$

where

$\{M\}$ = column matrix (8 elements) of bending moments at stations shown in Figure 62.

$[m]_{c,z}$ = rectangular matrix (8 rows, 5 columns) of unit bending moments due to cosine applied airloads (c) in the vertical (z) direction.

$[m]_{s,z}$ = rectangular matrix of unit bending moments due to sine applied airloads (s) in the vertical (z) direction.

$[m]_{c,x}$ $[m]_{s,x}$ = unit bending moments due to airloads applied in the drag (x) direction (in-plane).

$\{L_c\}$, $\{L_s\}$ = column matrices (5 elements) of cosine and sine applied airloads in the flapwise direction.

$\{D_c\}$, $\{D_s\}$ = column matrices (5 elements) of cosine and sine applied airloads in the drag direction (in-plane).

Solving matrix Equation (23) using the airloads plotted in Section 4.1.3.3 yields the second through seventh harmonic bending moments shown in Figures 65 through 70, 72 through 77, and 79 through 84.

The second harmonic bending moments may be compared with the Mayo method, Section 5.1.4.1.1. The sine components show no correlation while the Mayo method seems to correlate but has between a 50- and 100-percent conservative margin for the cosine component. The second harmonic of the Mayo method should be used for comparison only and not for design purposes.

5.1.4.2 Chordwise Bending Moments

The chordwise (in-plane) bending moments can be treated in a simple, uncoupled manner or in a completely coupled manner as were the flapwise bending moments in the preceding section. In either case, it can be shown that the transient chordwise loads of Section 5.2 are much more severe than the steady-state loads of this section.

5.1.4.2.1 Uncoupled Chordwise Bending Moments

In order to visualize the magnitudes of steady bending moments which are likely to be encountered, consider the helicopter hovering at sea level at design gross weight. Two cases are discussed in which (a) all engines are operating and (b) both engines on one blade are inoperative but normal rotor speed is maintained.

a) All Engines Operating

Equilibrium engine thrust is 2,020 pounds per blade tip for hover at sea level. The equivalent flat plate drag area ($C_D = 1.0$) for each nacelle

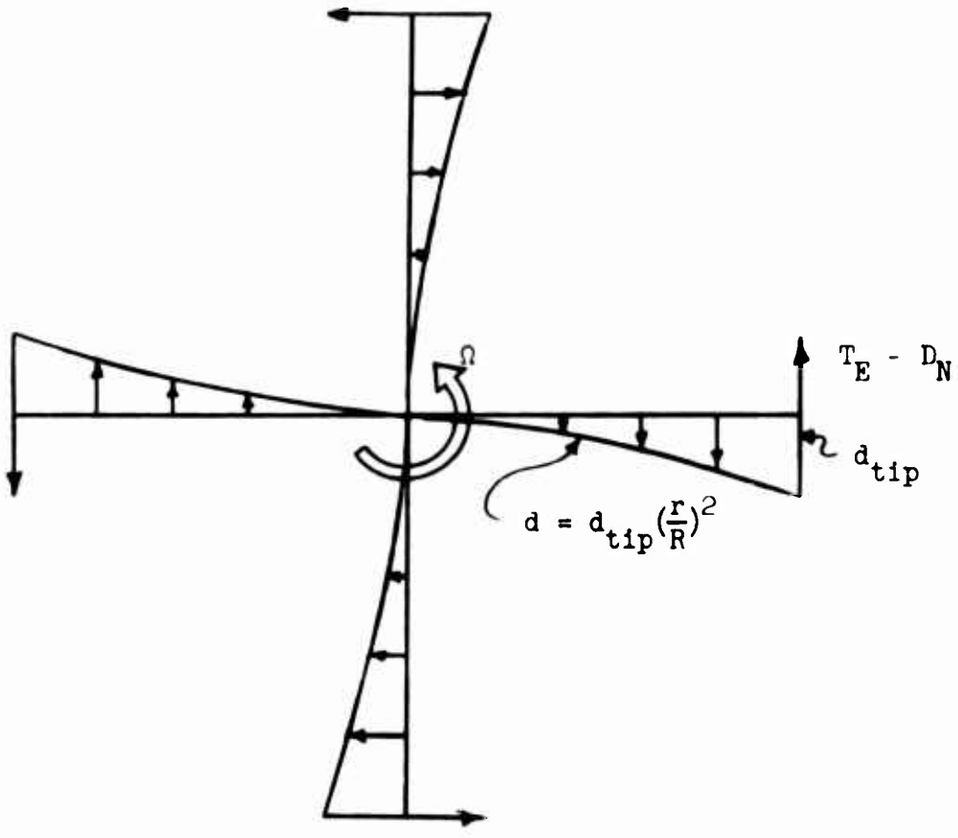

Figure 4. Rotor Drag and Thrust - All Engines Operating.

is taken as 0.63 feet^2 and the in-plane drag of each rotor blade is assumed to vary as the square of distance from the centerline of rotation.

For equilibrium rotor speed with all engines operating, the drag moment about the centerline of rotation must equal the moment due to engine thrust. Figure 4 shows the rotor in equilibrium.

For $V_T = R\Omega = 650$ f.p.s., $R = 672$ in.:

$$T_E = 2{,}020 \text{ lb.}$$

$$D_N = 0.63\left(\frac{\rho V^2}{2}\right) = \frac{0.63(.002378)(650)^2}{2}$$

$$= 316 \text{ lb.}$$

$$\int_o^R d_{tip}\left(\frac{r}{R}\right)^2 r\,dr = R(T_E - D_N)$$

$$d_{tip} = 4(T_E - D_N)/R$$

The rigid-blade bending moments are:

$$M = \int_x^R (r - x)d_{tip}\left(\frac{r}{R}\right)^2 dr - (R - x)(T_E - D_N)$$

$$M = x\left(T_E - D_N - \frac{d_{tip}R}{3}\right) + \frac{d_{tip}x^4}{12R^2} = -\frac{x}{3}(T_E - D_N) + \frac{x^4(T_E - D_N)}{3R^3}$$

$$M = -568x + \frac{x^4}{534{,}270} \text{ lb-in.} \qquad (24)$$

where: x = distance from centerline of rotation, (in.)
M = in-plane bending moment, positive for tension in leading edge

The maximum rigid-blade moment is -180,340 lb-in. at $x = 423.3$ in. The maximum flexible-blade bending moment (including centrifugal force) would be slightly smaller than the maximum rigid-blade bending moment.

b) Two Engines Inoperative

In order to maintain normal rotor speed with two engines inoperative, the remaining six engines must increase their thrust to maintain a total tip thrust of 16,080 pounds, or 2,693 pounds per blade. Figure 5 shows the rotor in equilibrium.

The in-plane bending moments in blades 2, 3, and 4 are identical and loads the leading edge of the blade in compression while the bending moments for blade 1 load the trailing edge in compression. Since the centrifugal relief is small for chordwise bending, the rigid-blade moments are presented for design.

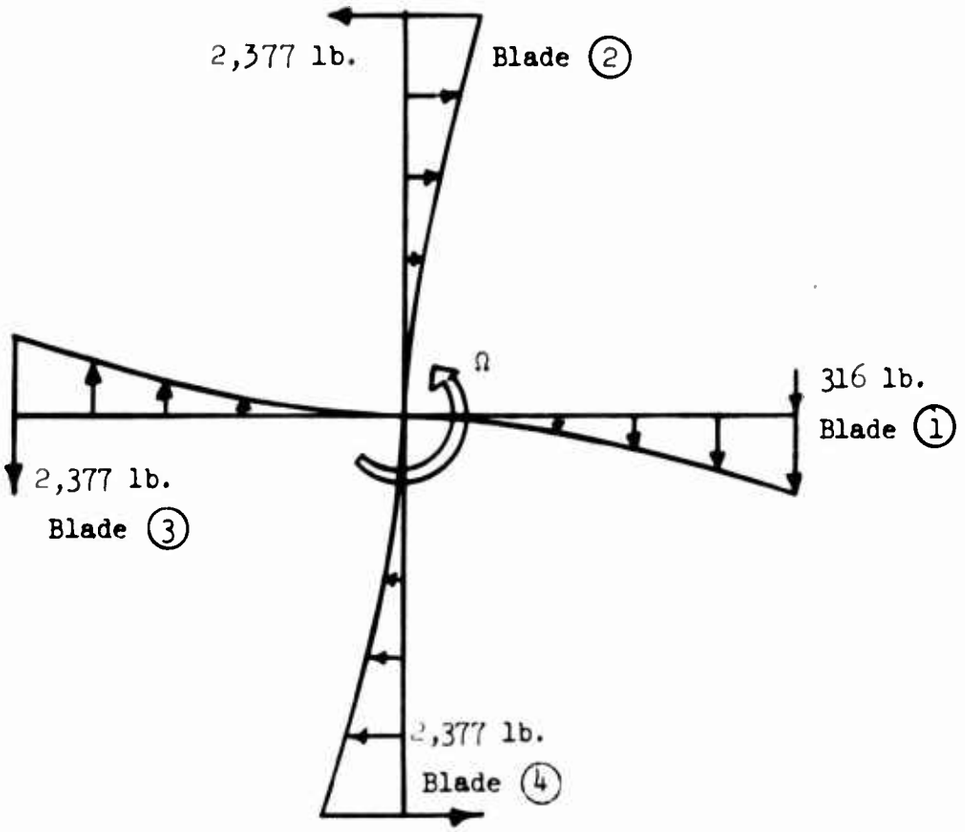

Figure 5. Rotor Drag and Thrust - Two Engines Inoperative.

The general equation for in-plane, rigid-blade bending moments is as follows.

$$M = -(R - x)(T_E - D_N) + \int_x^R (r - x)\, d_{tip}\left(\frac{r}{R}\right)^2 dr$$

$$M = -(R - x)(T_E - D_N) + d_{tip}\left(\frac{R^2}{4} - \frac{Rx}{3} + \frac{x^4}{12R^2}\right)$$

Blade 1: $R = 672$ in.

$T_E = 0$

$D_N = 316$ lb.

$d_{tip} = 4(2,020 - 316)/672 = 10.143$ lb/in.

$$M_1 = 1,357,455 - 2,588x + \frac{x^4}{534,270} \text{ in-lb.} \quad (25)$$

Blade 2: $R = 672$ in.

$T_E = 2,693.3$ lb.

$D_N = 316$ lb.

$d_{tip} = 10.143$ lb/in.

$$M_2 = -452{,}485 + 105.3x + \frac{x^4}{534{,}270} \text{ in-lb.} \qquad (26)$$

Equations (25) and (26) are plotted in Figure 85 and may be considered to be the largest steady in-plane bending moments likely to be encountered by the blades. It is not rational to consider the 5-percent rotor overspeed condition combined with an engine failure condition. Nor is it rational to consider military power for the engines since an overspeed would occur for design gross weight.

5.1.4.2.2 Coupled Chordwise Bending Moments

The coupled chordwise bending moments were analyzed in the same manner as the flapwise bending moments shown in Section 5.1.4.1.2. Figures 88 through 93 present the maximum coupled chordwise bending moments. Condition 6 (2.5g pullup, 41 mph) produces the maximum chordwise bending moments for even harmonics (second, fourth, and sixth) and condition 8 (1g, 144 mph) produces the maximum coupled chordwise bending moments for the odd harmonics (third, fifth, and seventh). Figure 86 presents the steady chordwise bending moment for condition 6 and Figure 87 presents the first harmonic uncoupled chordwise bending moment for condition 8. Reference 4 does not include a coupled unit response for the first harmonic; therefore, an uncoupled analysis was conducted using a magnification factor of 4.1. The magnification factor was derived using the natural frequency of 1.15 cycles per revolution in Reference 4.

5.2 Dynamic (Transient) Design Loads

The rotor simulation used in Reference 4 for the direct analog computer study of rotor blade flutter boundaries is useful for studying dynamic blade loads and motions resulting from a sharp edge gust as well as cyclic and collective pitch inputs while hovering.

5.2.1 Gust Response

Three conditions were investigated, all of which were subjected to a 40-foot-per-second gust imposed as a uniform inflow change on the blade. The three conditions considered were (1) an infinite fuselage mass, (2) a 52,000-pound fuselage, and (3) a 25,000-pound fuselage. The first condition is of academic interest only while the second and third conditions are intended to simulate design gross weight and minimum flying weight, respectively. Flapwise and in-plane blade bending moments are given for each of these conditions as well as the vertical force resulting at the hub.

5.2.1.1 Gust Load Factor

In the absence of data such as that in Reference 4, the load factor resulting from a vertical gust is customarily calculated by considering

the rotor blades to be rigid and treating the hovering rotor as having undergone an instantaneous change in inflow equal to the gust velocity. A thrust change, ΔT, is calculated and the resultant load factor taken as $(W + \Delta T)/W$.

For design gross weight, $\Delta T = \left(\frac{B^2}{4}\right) \rho abcRV_T U_g$

where

B = tip loss factor, 0.97

ρ = sea level air density, .002378 slugs/ft^3

a = lift curve slope, 5.73 per radian

b = number of blades, 4

c = blade chord, 6.5 ft.

R = rotor radius, 56 ft.

V_T = rotor tip speed, 650 f.p.s.

U_g = gust velocity, 40 f.p.s.

W = design gross weight, 71,680 lb.

Therefore, ΔT = 121,335 lb.

and $$n = \frac{W + \Delta T}{W} = \frac{71,680 + 121,335}{71,680} = \underline{2.69}$$

This method of calculating gust load factors leads to the belief that 40 feet per second would result in a load factor in excess of the design load factor of 2.5 specified in Section 4. The gust conditions presented in Reference 4 show that an alleviation of the gust load factor occurs due to the flexibility of the rotor blades. For the design gross weight condition, each blade is shown to exert a 29,200-pound vertical load on the hub. Since the blade inertias are already taken into account in arriving at this load, the load factor caused by the gust is calculated using only the fuselage mass as follows:

$$n = \frac{4(29,200)}{52,000} = \underline{2.25}$$

5.2.1.2 Blade Loads Due to Gust

The flapwise bending moments resulting from this gust condition are recorded in Reference 4 and are less than those shown in Figure 71 for the 2.5g pullup condition.

The in-plane bending moments resulting from the gust condition are recorded in Reference 4 and are plotted in Figure 94. It is of interest to note that the initial in-plane motion of the blades is in an aft direction but the peak bending moment occurs approximately half a revolution

after the gust is imposed and is in the negative direction (compression in the leading edge).

No directly pertinent data are given regarding blade torsion due to a gust condition but sufficiently accurate data are recorded in Reference 4 to estimate that the pitching (torsional) displacement at the blade tip does not exceed 0.004 radians. If the simplifying assumption is made that the blade torsional rigidity is constant along the span and that the torsional mode shape is a sinusoidal twist, the torque due to the gust condition would be as follows:

$$\theta = \theta_{tip} \sin \frac{\pi r}{2R} = .004 \sin \frac{\pi r}{2R}$$

$$T = GJ\left(\frac{\partial \theta}{\partial r}\right) = .004GJ\left(\frac{\pi}{2R}\right) \cos \frac{\pi r}{2R}$$

at the blade root

$$T_o = .004GJ_o\left(\frac{\pi}{2R}\right) = .004(8)10^9\left(\frac{\pi}{1,344}\right) = 75,000 \text{ in-lb.}$$

This value of root torque is less than half of that plotted in Figure 9 and, even though the torque due to the gust is an incremental value, the addition of blade torque due to normal hover operation would not constitute a significant design loading.

5.2.2 Control Response

The rotor blade simulation used in Reference 4 was used to study the response of the blade to cyclic and collective pitch inputs. The data taken were not as complete as were the gust condition data, but conclusions can be drawn from the blade tip deflection data presented therein.

5.2.2.1 Cyclic Pitch Transient

A 1.0-cycle-per-revolution sinusoidal cyclic pitch input was imposed on the blade which resulted in flapwise and in-plane transient motions, both occurring very close to the 1.0-cycle-per-revolution forcing frequency. The plot of flapwise tip motion of the blade in Reference 4 shows that for a 0.01 radian cyclic pitch input the tip path plane will rotate about 0.01 radian. The absence of any higher harmonic content, however, suggests that the transient flapwise bending moments are small and, indeed, would not equal the steady first harmonic moments of Section 5.1.4.1.

The plot of in-plane motion, however, suggests a transient in-plane bending moment of approximately 1.0-cycle-per-revolution frequency. During these cyclic control transient studies, the in-plane bending moment at the blade root (r/R = .025) was measured and tabulated. For a 1.0-cycle-per-revolution cyclic input (step input by the pilot), the transient in-

plane bending moment is 240,000 inch-pounds per degree of cyclic pitch. Since the mode shape for the first cyclic in-plane frequency approximates a quarter cosine curve, the in-plane bending moments decrease with increasing radial position. These in-plane moments will not design the blades for normal cyclic pitch inputs.

A review of the cyclic control study indicates that there is a possibility of inadvertent cycling of the control at 0.46 cycles per second (in the stationary system) which will result in very large alternating in-plane bending moments. Reference 4 points out that with normal structural damping (G = .03), it is possible, by cycling at 0.46 cycles per second, to create in-plane bending moments at r/R = .025 of 3,500,000 inch-pounds. This bending moment is inversely proportional to structural damping and could be much higher if the blade has less than a normal amount of damping. Since whirling the cyclic stick at this critical frequency is well within pilot capability, a conservative treatment for creating a moment curve versus radius is taken.

Assume that the first in-plane mode shape of this motion is the following quarter cosine curve.

$$x = x_{tip}\left(1 - \cos\frac{\pi r}{2R}\right)$$

Differentiation twice gives

$$\frac{d^2x}{dr^2} = \left(\frac{\pi}{2R}\right)^2 x_{tip} \cos\frac{\pi r}{2R}$$

By definition,

$$M = EI\left(\frac{d^2x}{dr^2}\right) = K \cos \pi r$$

Since it is known that at r/R = .025 the bending moment is 3,500,000 inch-pounds,

$$K \approx 3{,}500{,}000$$

therefore

$$M \approx 3{,}500{,}000 \cos\frac{\pi r}{2R} \qquad (27)$$

Equation (27) is plotted in Figure 95. This bending moment variation with radial position is assumed, not actual, and is considered to be conservative.

5.2.2.2 Collective Pitch Transient

An exponential collective pitch input of 0.01 radian was used in Reference 4 to determine blade response. A time delay of approximately 0.1 second (to 0.6 of maximum magnitude) was used to simulate more closely pilot action than would be the case for a step input. The plot of flapwise tip action shows a damped 1-cycle-per-revolution motion which has

negligible transient overshoot. This absence of overshoot suggests that the flapwise bending moments resulting from a normal collective pitch input are well damped and will closely approximate a smooth transition from one steady bending configuration to the final steady-state values. In no case would the transient moments approach those of Figure 67.

The plot of in-plane motion due to the collective pitch input does not include the effects of tip engine governing, which would be very important due to the low frequency response of the blade in the in-plane direction. One analytical approach toward estimation of a transient in-plane bending moment would be to increase the induced and profile drag on the blade due to the additional collective pitch while holding tip engine thrust and rotor speed constant. It can be safely assumed, however, that the transient in-plane bending moments would not exceed those of Figure 85 which are assumed for the cyclic stick whirl condition.

The plot of pitching (torsional) deflection at the blade tip is similar in character to the flapwise deflection curve insofar as there is no transient overshoot from the initial tip angle to the final steady-state value. The transient torsional moments on the blade, then, will be non-critical for the collective pitch input condition.

5.2.3 Dynamic Tip Environment

The engines shall be capable of operating in a continuous tip environment due to an alternating or transient loading condition.

5.2.3.1 Alternating Airload Excitation (1g and 2.5g)

To determine the maximum load at the tip an area moment analysis was conducted to determine the tip deflection. Using the resultant moment for the second harmonic 1g and 2.5g flight conditions (Figures 68 and 75) and the flapwise EI distribution (Figure 1), the tip deflection for 1g is 4 inches and 2.5g is 2.2 inches. With these deflections, the following analysis can be made to give the tip acceleration.

1g Condition	2.5g Condition
$z_o = 4.0$ in.	$z_o = 2.2$ in.
$z = z_o \sin 2\Omega t$	$z = z_o \sin 2\Omega t$
$\dot{z} = 2z_o\Omega \cos 2\Omega t$	$\dot{z} = 2z_o\Omega \cos 2\Omega t$
$\ddot{z} = -4z_o\Omega^2 \sin 2\Omega t$	$\ddot{z} = -4z_o\Omega^2 \sin 2\Omega t$
$n_z = 16(12.17)^2/386 = \pm 6.1$	$n_z = 8.8(12.17)^2/386 = \pm 3.4$

The in-plane acceleration is analyzed in the same manner as flapwise acceleration. The deflection is 0.8 inches for a 2.5g flight condition. With this deflection, the acceleration is analyzed as follows.

2.5g Condition

x_o = 0.8 in.

$x = x_o \sin 2\Omega t$

$\dot{x} = 2x_o\Omega \cos 2\Omega t$

$\ddot{x} = -4x_o\Omega^2 \sin 2\Omega t$

$n_x = 3.2(12.17)^2/386 = \pm 1.2$

5.2.3.2 Gust

The flapwise and in-plane acceleration for a gust condition was analyzed in Reference 4. Figure 2.28 of Reference 4 shows the following accelerations:

$n_z = \pm 8.15$

$n_x = \pm 1.91$

TABLE 5
PRELIMINARY DESIGN SPECTRUM FOR ROTOR AIRLOAD ANALYSIS

Cond.	Flight Maneuver*	Limit Load Factor (n_z)	Flight Speed (m.p.h.)	Rotor Tip Speed (f.p.s.)	μ**
1	Hover	1.0	0	415	0
2	Hover	1.0	0	650	0
3	Forward flight	1.0	41	592	0.1
4	Cruise	1.0	70	592	0.17
5	Dive	-0.5	0	562	0
6	Pullout at forward flight	2.5	41	562	0.11
7	Pullout at design maximum forward flight	2.5	144	562	0.38
8	Design maximum forward flight	1.0	144	562	0.38
9	Design maximum forward flight	1.0	144	592	0.36
10	Design maximum forward flight	1.0	144	622	0.34

* Gross weight at sea level.

**Flight speed divided by tip speed.

TABLE 6
INPUT DATA FOR CAL AIRLOAD PROGRAM - PART I

CONSTANTS

Maneuver	Cond.	NC	N	IA	IRR	VF	OMEGA	AT	HOFS
Hover	2	4	5	16	3	0	11.6	0	0
Fwd. flt.	3	4	5	16	3	60.1	10.6	1.7	0
Dive	5	4	5	16	3	0	10.06	0	0
Pullout - fwd. flt.	6	4	5	16	3	60.1	10.06	6.4	0
Maximum fwd. flt.	8	4	5	16	3	210.9	10.06	15.5	0

Maneuver	Cond.	RM1	RM2	AA	CWA	AMFD	KXX	BTAIC	BTAIS
Hover	2	168	173	5.73	11.1	12	1	0	0
Fwd. flt.	3	168	173	5.73	11.1	12	1	0	0
Dive	5	168	173	5.73	11.1	12	1	0	0
Pullout - fwd. flt.	6	168	173	5.73	11.1	12	1	0	0
Maximum fwd. flt.	8	168	173	5.73	11.1	12	1	3.94	0

VARIABLES

Maneuver	Cond.	r/R	WZ(J)	WC(L,J)	WS(L,J)	BZ(I)	BZZ(J)	R(J)	A(K)	B(I)
		0	0	0	0	-	0	0	-	-
		.1	-	-	-	1.2	-	-	0	3.25
		.2	-21.0	0	0	-	2.5	11.18	-	-
		.3	-	-	-	3.9	-	-	0	3.25
		.4	-35.4	0	0	-	5.2	22.36	-	-
Hover	2	.5	-	-	-	6.5	-	-	0	3.25
		.6	-43.2	0	0	-	7.7	33.54	-	-
		.7	-	-	-	8.8	-	-	0	3.25
		.8	-44.9	0	0	-	9.6	44.72	-	-
		.9	-	-	-	10.3	-	-	0	3.25
		1.0	-39.2	0	0	-	10.8	55.9	-	-
		0	0	0	0	-	0	0	-	-
		.1	-	-	-	1.2	-	-	0	3.25
		.2	-10.9	-6.2	0	-	2.6	11.18	-	-
		.3	-	-	-	4.1	-	-	0	3.25
		.4	-18.4	-10.4	0	-	5.5	22.36	-	-
Fwd. Flt.	3	.5	-	-	-	7.1	-	-	0	3.25
		.6	-22.5	-12.7	0	-	8.5	33.54	-	-
		.7	-	-	-	9.8	-	-	0	3.25
		.8	-23.1	-13.1	0	-	10.8	44.72	-	-
		.9	-	-	-	11.7	-	-	0	3.25
		1.0	-20.4	-11.5	0	-	12.4	55.90	-	-

All values of "L" greater than 1 are assumed zero. All values of "K" are assumed zero.

TABLE 6 (Continued)

VARIABLES (Continued)

Maneuver	Cond.	r/R	WZ(J)	WC(L,J)	WS(L,J)	BZ(I)	BZZ(J)	R(J)	A(K)	B(I)
Dive	5	0	0	0	0	-	0	0	-	-
		.1	-	-	-	1.25	-	-	0	3.25
		.2	-12.3	0	0	-	2.67	11.18	-	-
		.3	-	-	-	4.23	-	-	0	3.25
		.4	-20.6	0	0	-	5.89	22.36	-	-
		.5	-	-	-	7.55	-	-	0	3.25
		.6	-25.6	0	0	-	9.10	33.54	-	-
		.7	-	-	-	10.48	-	-	0	3.25
		.8	-26.5	0	0	-	11.69	44.72	-	-
		.9	-	-	-	12.71	-	-	0	3.25
		1.0	-23.3	0	0	-	13.53	55.9	-	-
Pullout Fwd. Flt.	6	0	0	0	-	-	0	0	-	-
		.1	-	-	0	1.6	-	-	0	3.25
		.2	-17.2	-9.7	-	-	4.0	11.18	-	-
		.3	-	-	0	7.2	-	-	0	3.25
		.4	-29.1	-16.4	-	-	10.9	22.36	-	-
		.5	-	-	0	14.9	-	-	0	3.25
		.6	-35.5	-20.1	-	-	18.8	33.54	-	-
		.7	-	-	0	22.3	-	-	0	3.25
		.8	-36.5	-20.6	-	-	25.5	44.72	-	-
		.9	-	-	0	28.1	-	-	0	3.25
		1.0	-32.2	-18.2	-	-	30.4	55.9	-	-
Maximum Fwd. Flt.	8	0	0	0	-	-	0	0	-	-
		.1	-	-	0	1.3	-	-	0	3.25
		.2	-3.3	-2.5	-	-	2.7	11.18	-	-
		.3	-	-	0	4.2	-	-	0	3.25
		.4	-5.6	-4.1	-	-	5.9	22.36	-	-
		.5	-	-	0	7.6	-	-	0	3.25
		.6	-6.9	-5.1	-	-	9.1	33.54	-	-
		.7	-	-	0	10.5	-	-	0	3.25
		.8	-7.1	-5.2	-	-	11.7	44.72	-	-
		.9	-	-	0	12.7	-	-	0	3.25
		1.0	-6.2	-4.6	-	-	13.5	55.9	-	-

TABLE 7

INPUT DATA FOR CAL AIRLOAD PROGRAM

Part II

			VARIABLES							
Maneuver	Condition	r/R	ZCZSLO(I)	ZC(L,I)	ZS(L,I)	ZCPR(L,J)	ZSPR(L,I)	TZER(I)	THCO(L,I)	THSI(L,I)
		0	-	-	-	-	-	-	-	-
		.1	0	0	0	0	0	.25	0	0
		.2	-	-	-	-	-	-	-	-
		.3	0	0	0	0	0	.22	0	0
		.4	-	-	-	-	-	-	-	-
Hover	2	.5	0	0	0	0	0	.18	0	0
		.6	-	-	-	-	-	-	-	-
		.7	0	0	0	0	0	.14	0	0
		.8	-	-	-	-	-	-	-	-
		.9	0	0	0	0	0	.11	0	0
		1.0	-	-	-	-	-	-	-	-
		0	-	-	-	-	-	-	-	-
		.1	0	0	0	0	0	.23	0	-.02
		.2	-	-	-	-	-	-	-	-
		.3	0	0	0	0	0	.20	0	-.02
		.4	-	-	-	-	-	-	-	-
Fwd. Flt.	3	.5	0	0	0	0	0	.16	0	-.02
		.6	-	-	-	-	-	-	-	-
		.7	0	0	0	0	0	.13	0	-.02
		.8	-	-	-	-	-	-	-	-
		.9	0	0	0	0	0	.09	0	-.02
		1.0	-	-	-	-	-	-	-	-
		0	-	-	-	-	-	-	-	-
Dive	5	.1	0	0	0	0	0	.21	0	0
		.2	-	-	-	-	-	-	-	-
		.3	0	0	0	0	0	.17	0	0
		.4	-	-	-	-	-	-	-	-

TABLE 7 (Continued)

			VARIABLES							
Maneuver	Condition	r/R	ZCZSLO(I)	ZC(L,I)	ZS(L,I)	ZCPR(L,J)	ZSPR(L,I)	TZER(I)	THCO(L,I)	THSI(L,I)
Dive	5	.5	0	0	0	0	0	.14	0	0
		.6	-	-	-	-	-	-	-	-
		.7	0	0	0	0	0	.10	0	0
		.8	-	-	-	-	-	-	-	-
		.9	0	0	0	0	0	.07	0	0
		1.0	-	-	-	-	-	-	-	-
		0	-	-	-	-	-	-	-	-
		.1	0	0	0	0	0	.38	0	-.04
		.2	-	-	-	-	-	-	-	-
		.3	0	0	0	0	0	.34	0	-.04
Pullout		.4	-	-	-	-	-	-	-	-
Fwd. Flt.	6	.5	0	0	0	0	0	.31	0	-.04
		.6	-	-	-	-	-	-	-	-
		.7	0	0	0	0	0	.27	0	-.04
		.8	-	-	-	-	-	-	-	-
		.9	0	0	0	0	0	.24	0	-.04
		1.0	-	-	-	-	-	-	-	-
		0	-	-	-	-	-	-	-	-
		.1	0	0	0	0	0	.38	0	-.22
		.2	-	-	-	-	-	-	-	-
		.3	0	0	0	0	0	.35	0	-.22
Maximum		.4	-	-	-	-	-	-	-	-
Fwd. Flt.	8	.5	0	0	0	0	0	.31	0	-.22
		.6	-	-	-	-	-	-	-	-
		.7	0	0	0	0	0	.28	0	-.22
		.8	-	-	-	-	-	-	-	-
		.9	0	0	0	0	0	.24	0	-.22
		1.0	-	-	-	-	-	-	-	-

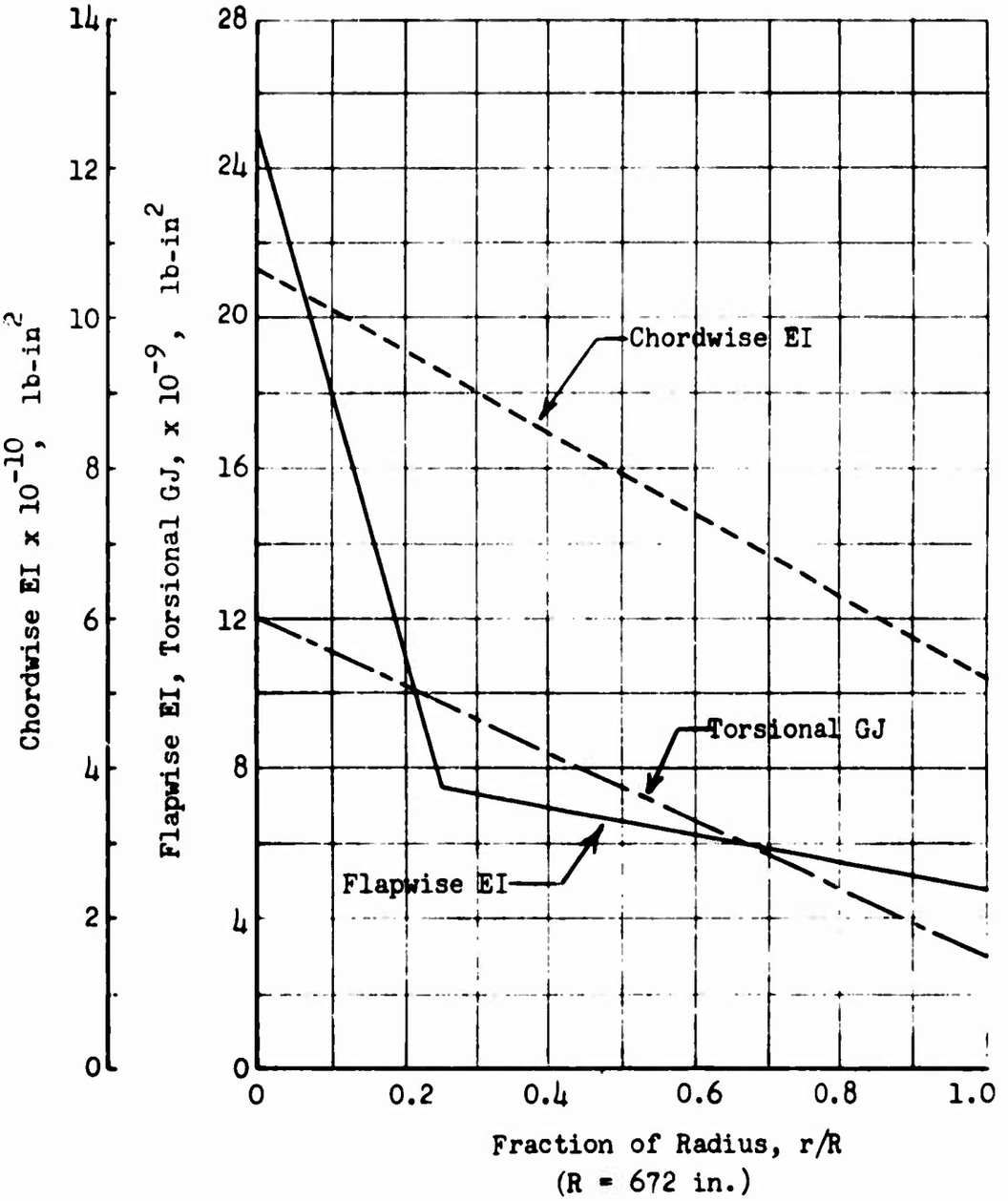

Figure 6. Rotor Blade Stiffness (EI, GJ) Versus Radius.

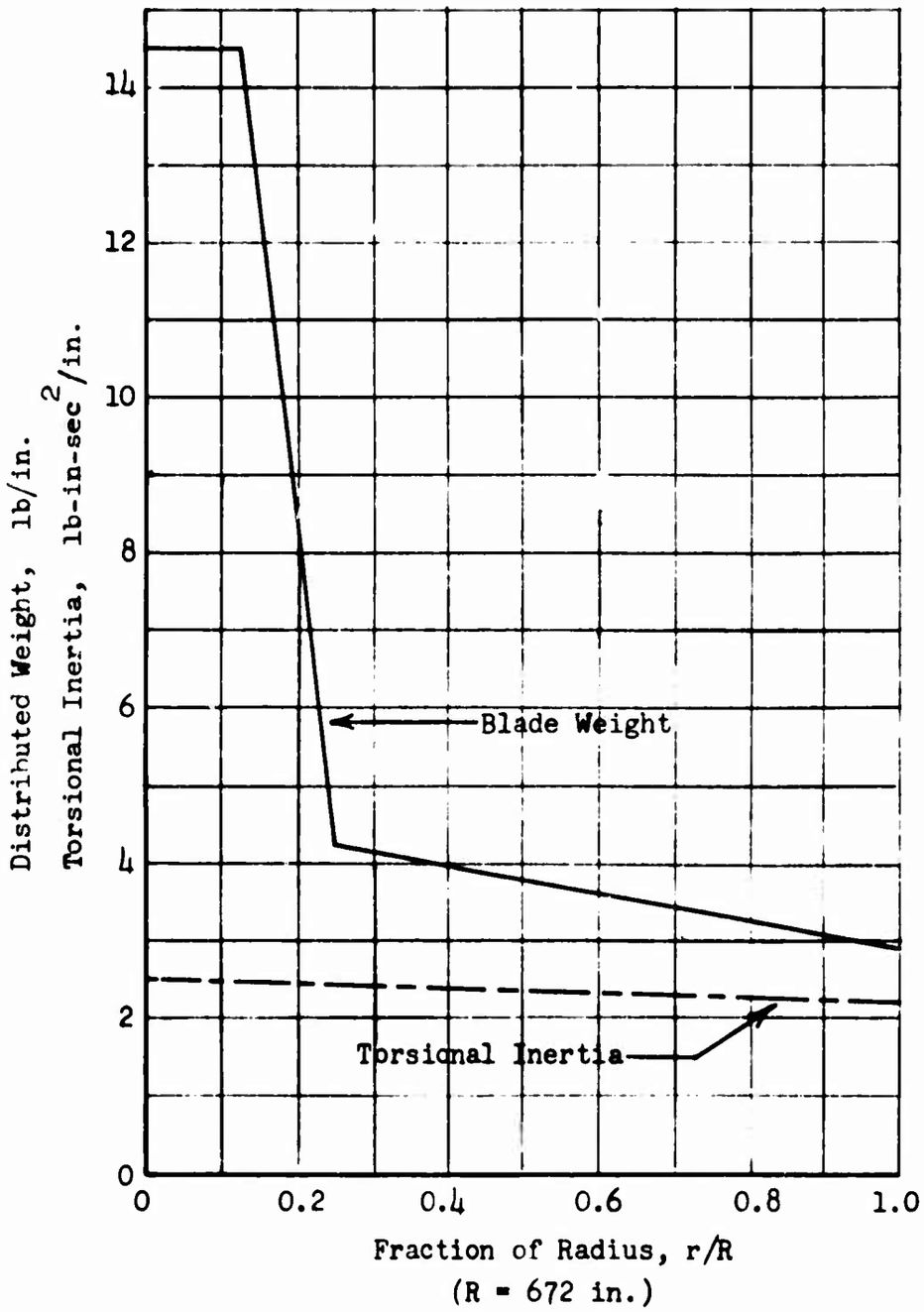

Figure 7. Rotor Blade Weight and Torsional Inertia Versus Radius.

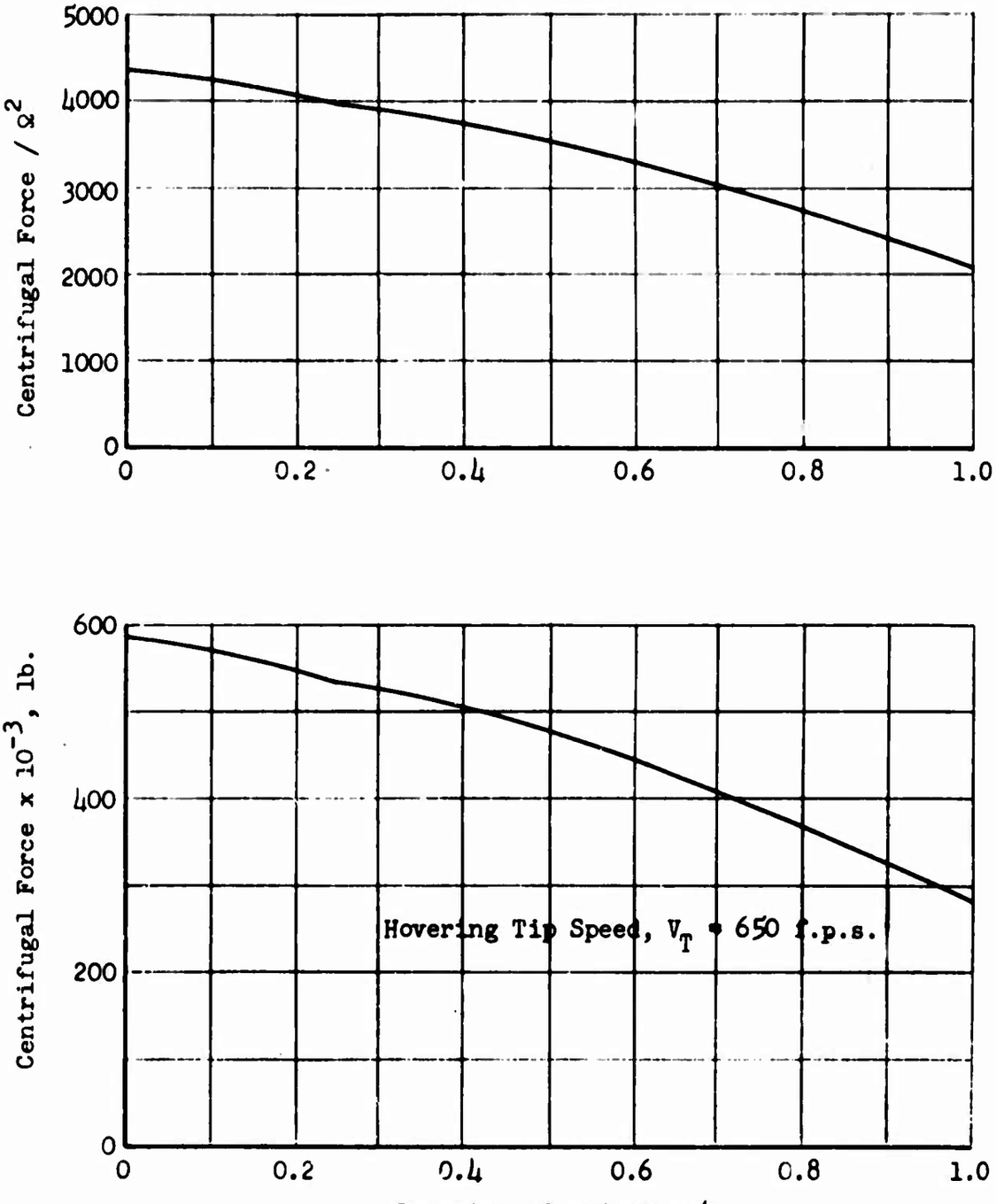

Figure 8. Centrifugal Force Versus Radius.

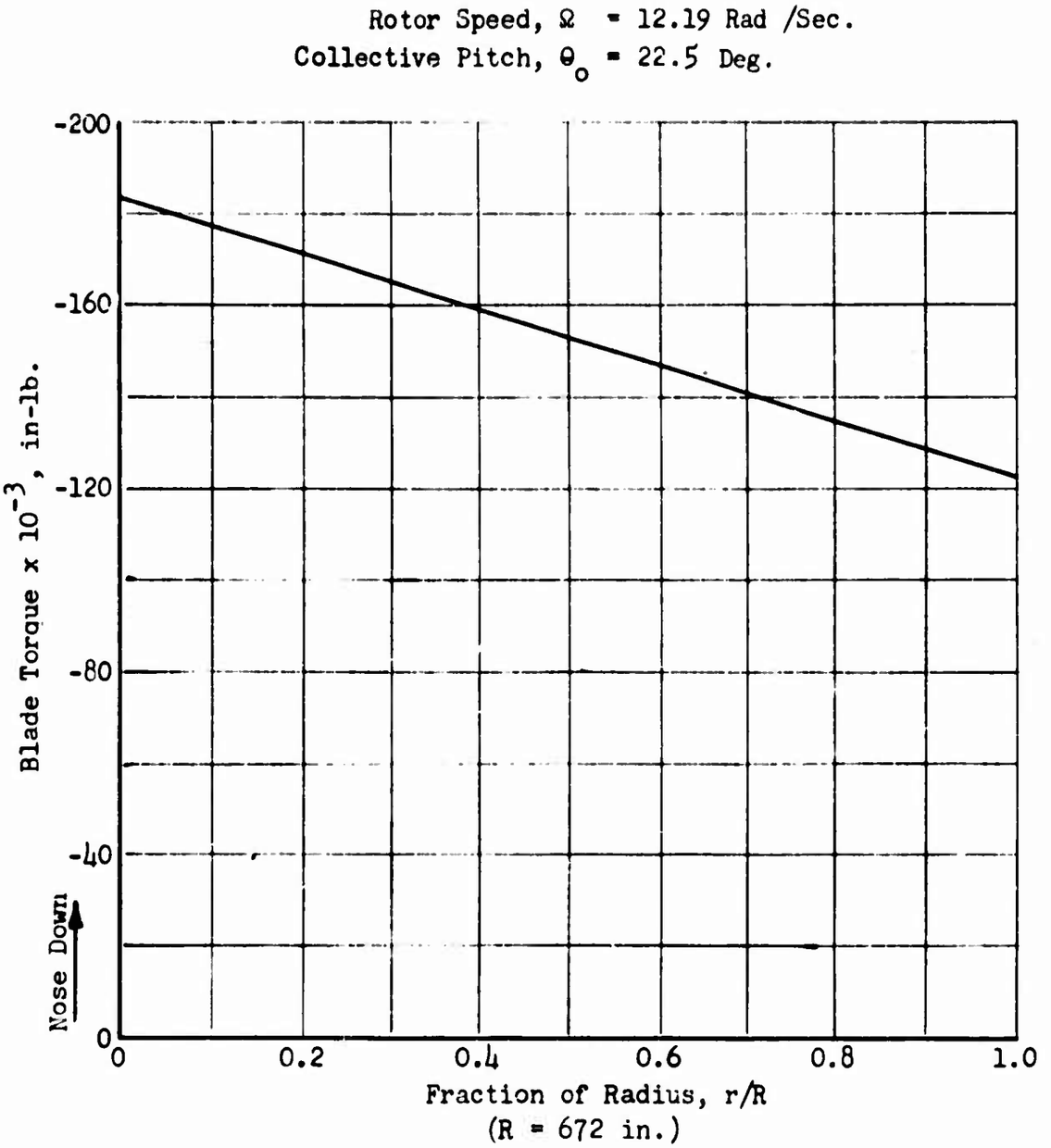

Figure 9. Rotor Blade Torque Versus Radius.

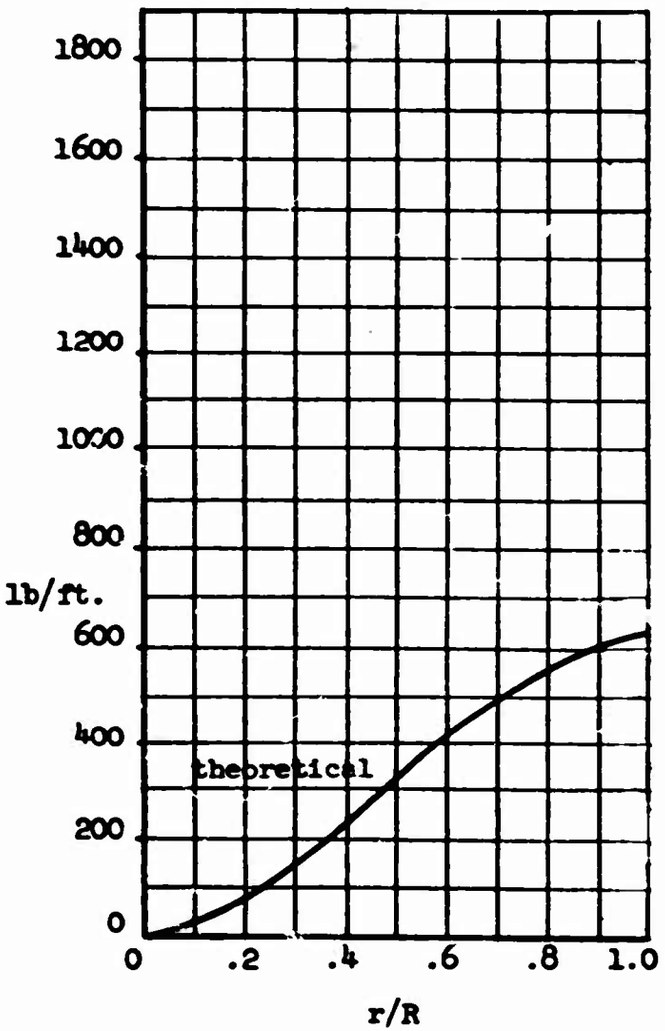

Figure 10. Lift - Zero Harmonic (Steady)
Hover
Condition 2

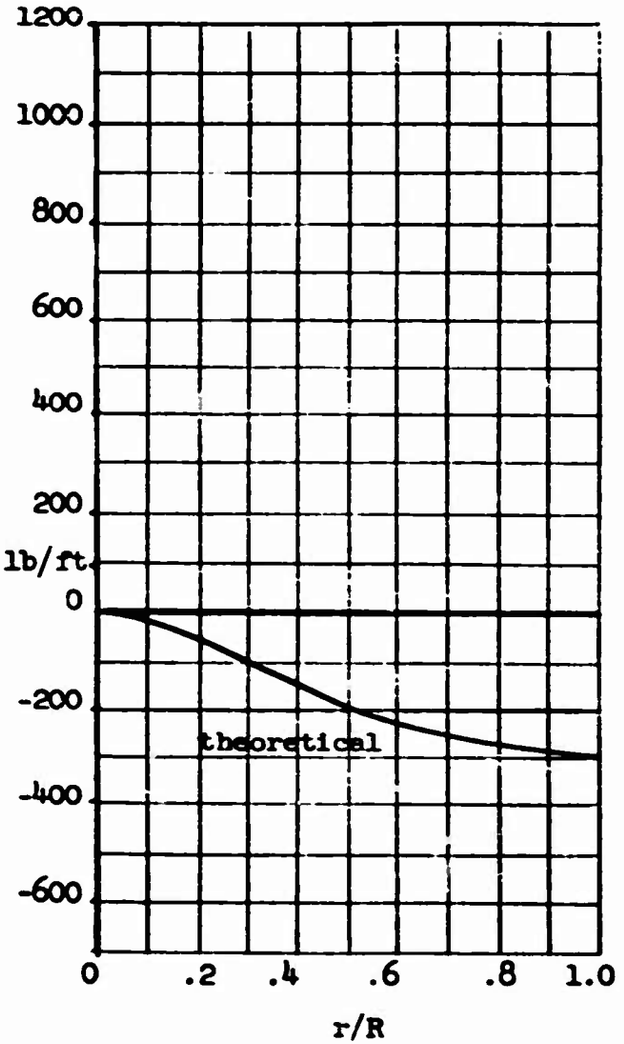

Figure 11. Lift - Zero Harmonic
Pushover
(-0.5g, 0 m.p.h.)
Condition 5

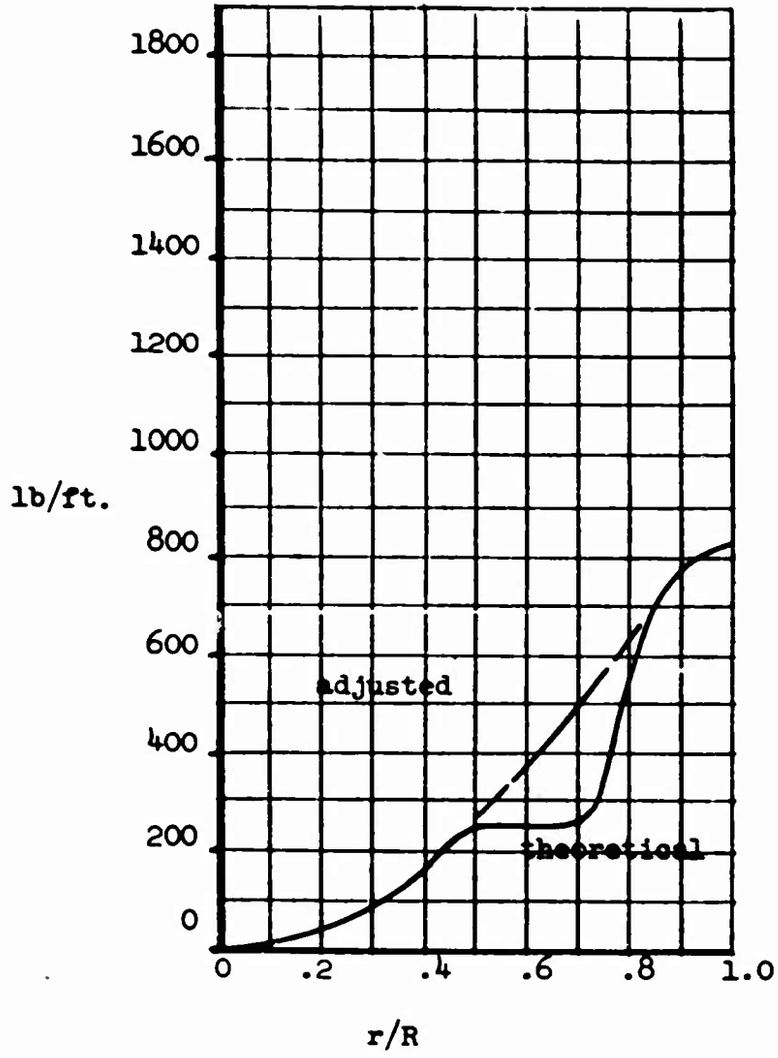

Figure 12. Lift - Zero Harmonic (Steady)
Forward Flight
(1g, 41 m.p.h.)
Condition 3

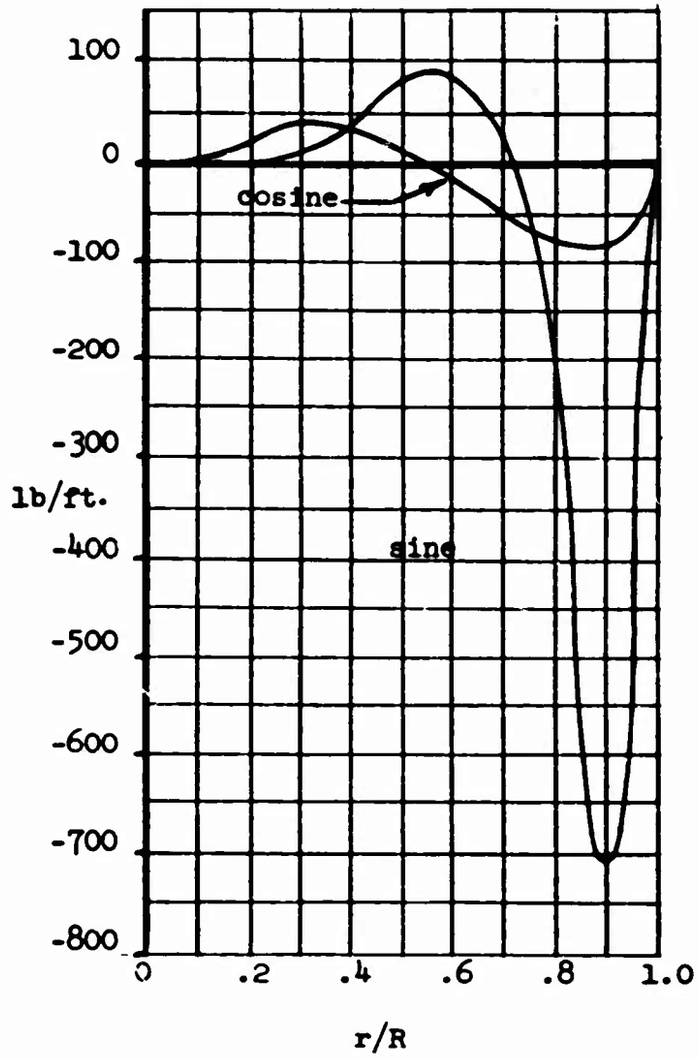

Figure 13. Lift - First Harmonic
Forward Flight
(1g, 41 m.p.h.)
Condition 3

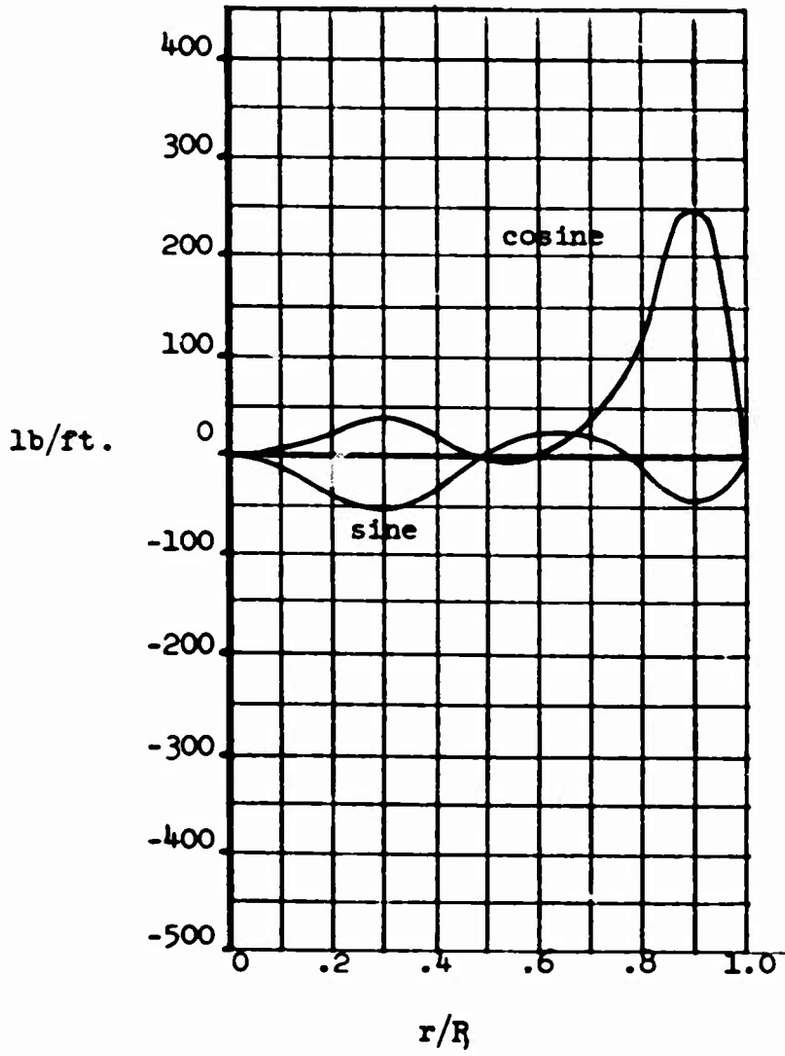

Figure 14. Lift - Second Harmonic
Forward Flight
(1g, 41 m.p.h.)
Condition 3

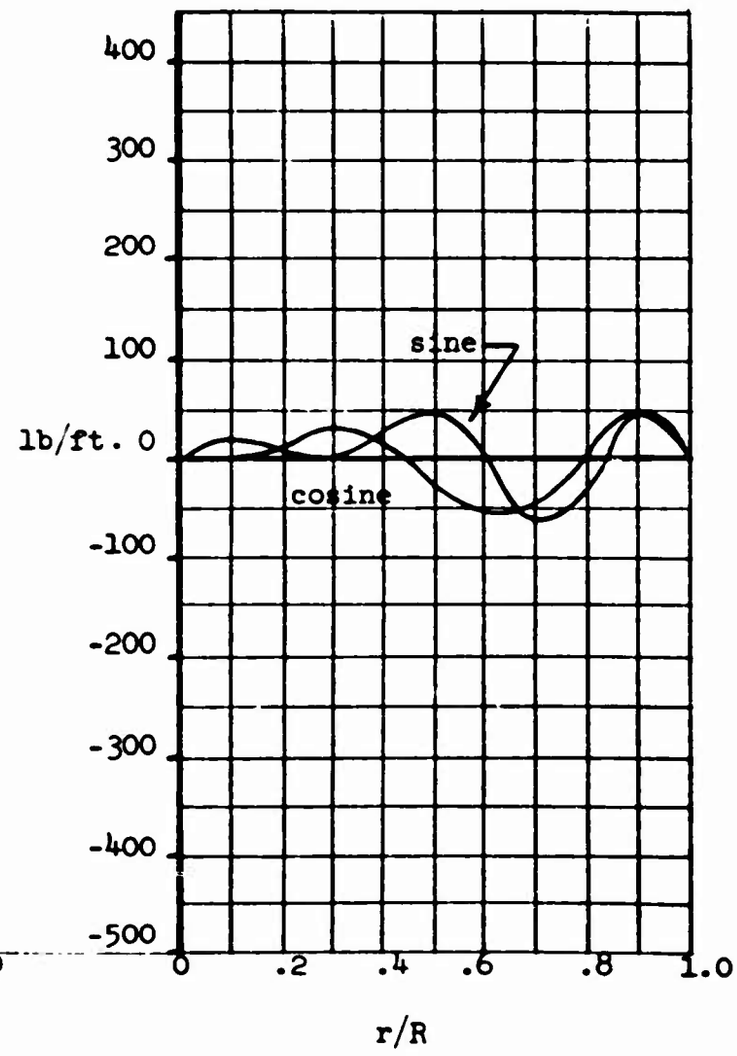

Figure 15. Lift - Third Harmonic
Forward Flight
(1g, 41 m.p.h.)
Condition 3

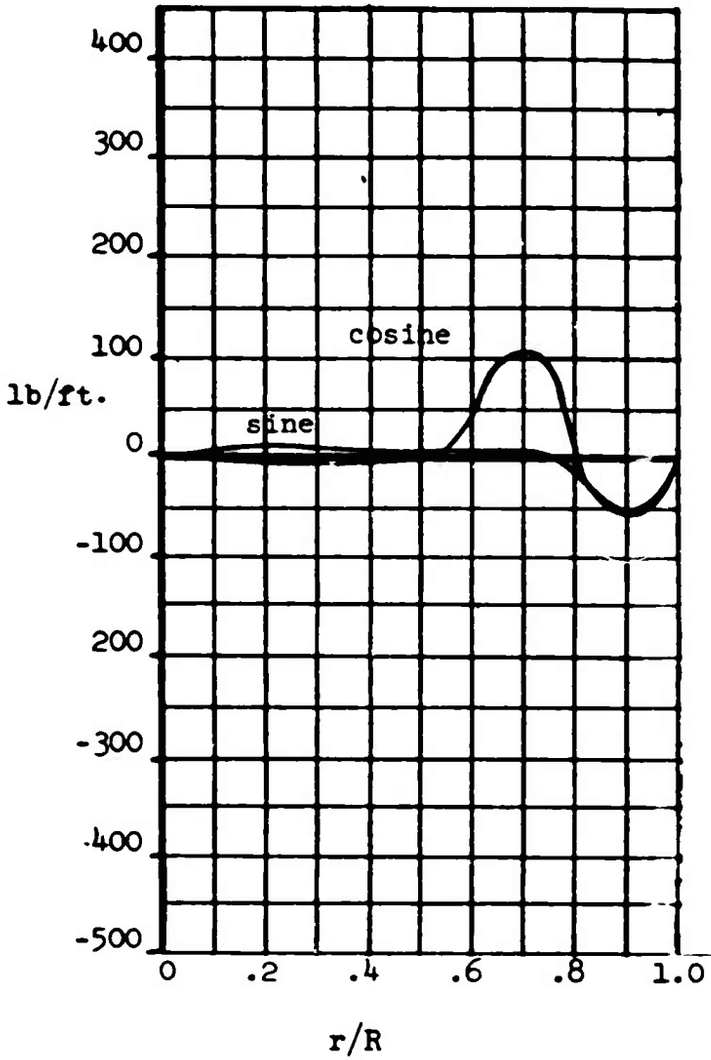

Figure 16. Lift - Fourth Harmonic
Forward Flight
(1g, 41 m.p.h.)
Condition 3

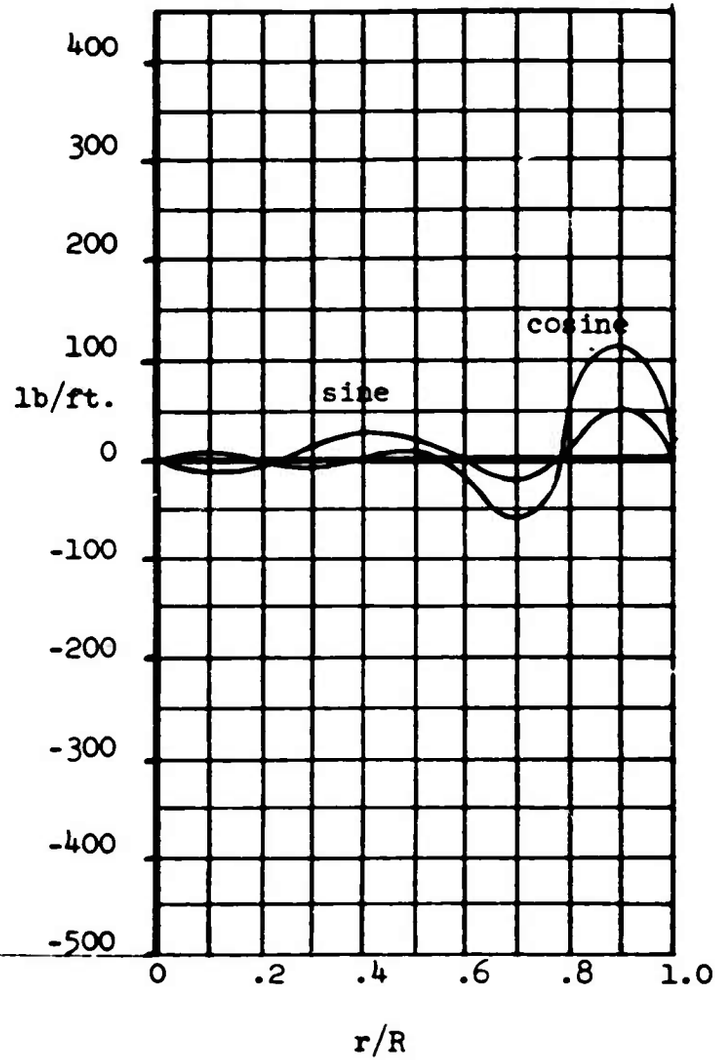

Figure 17. Lift - Fiftn Harmonic
Forward Flight
(1g, 41 m.p.h.)
Condition 3

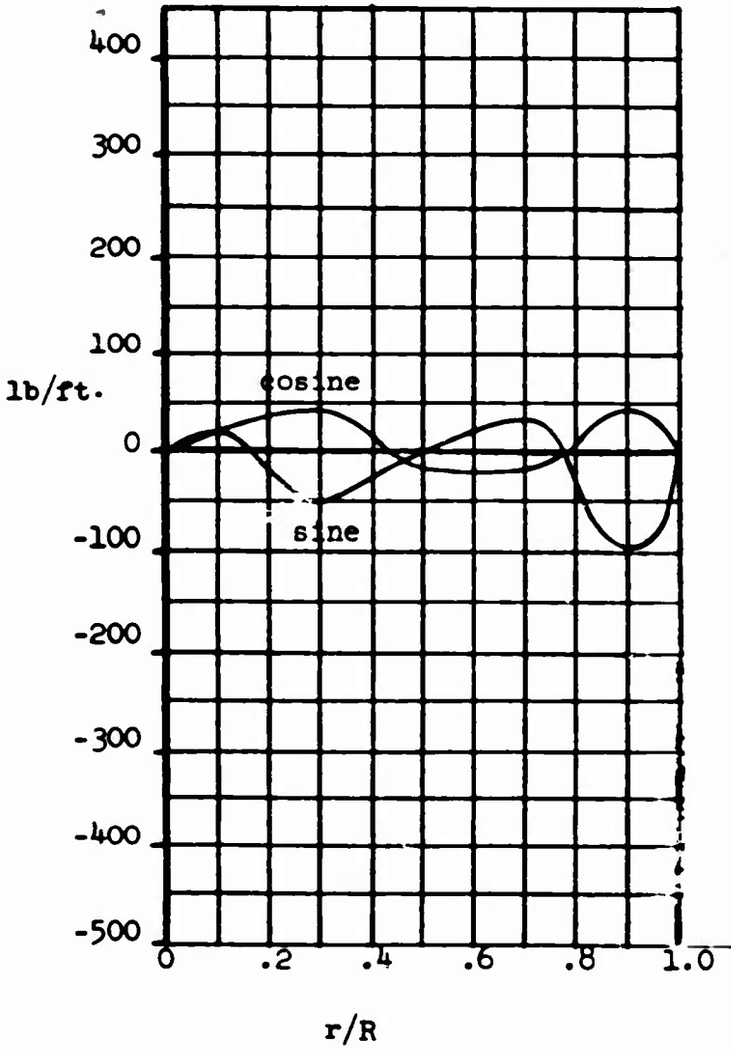

Figure 18. Lift - Sixth Harmonic
Forward Flight
(lg, 41 m.p.h.)
Condition 3

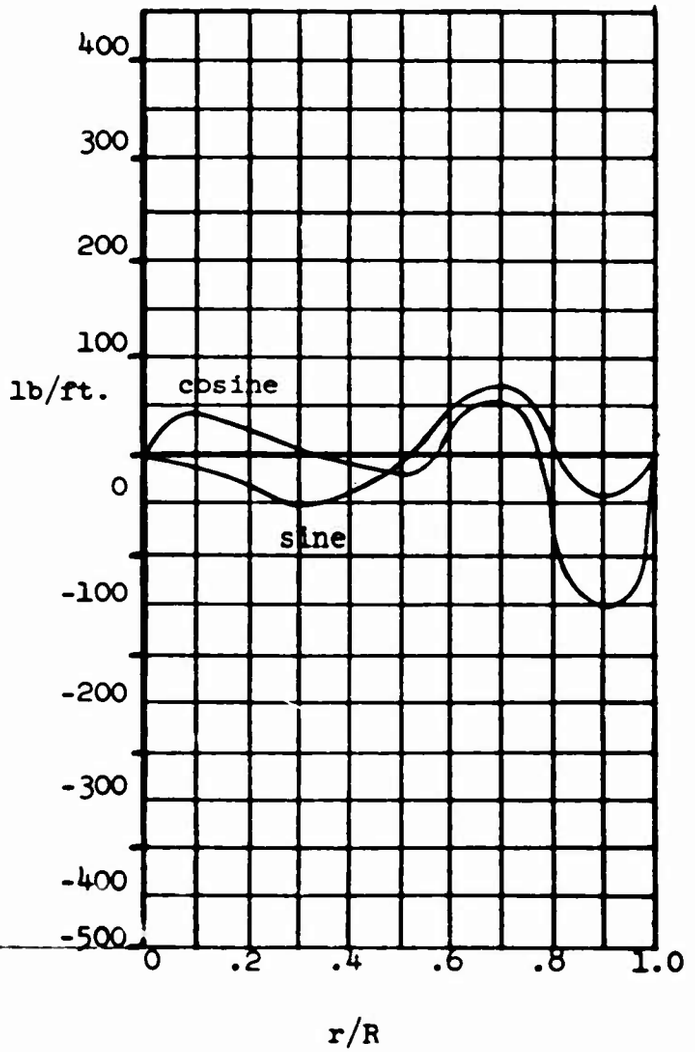

Figure 19. Lift - Seventh Harmonic
Forward Flight
(lg, 41 m.p.h.)
Condition 3

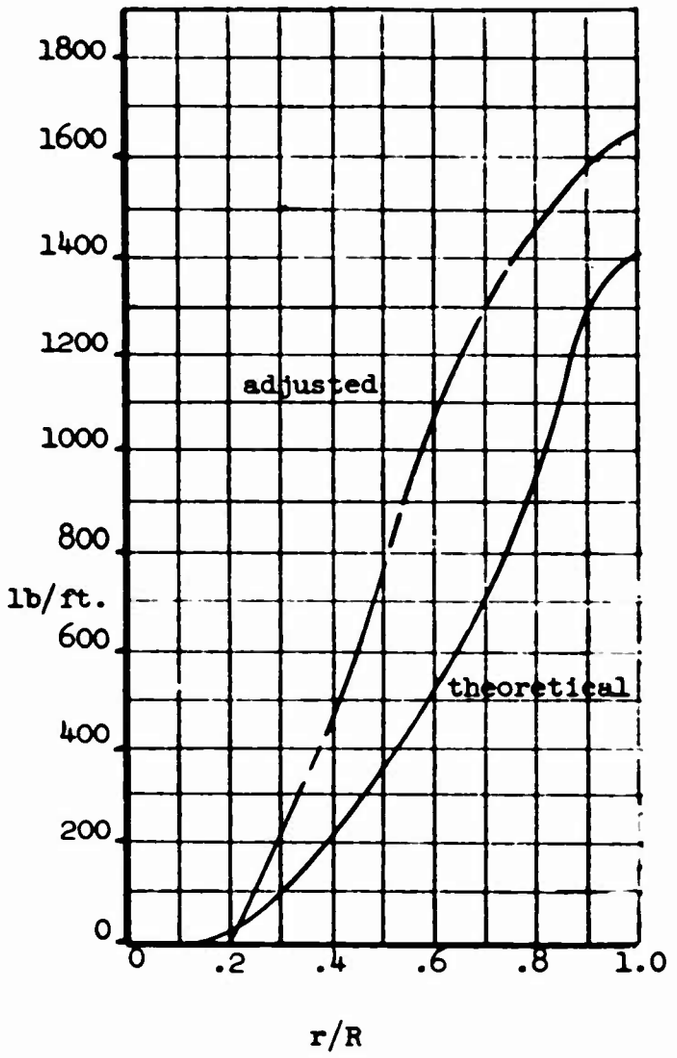

Figure 20. Lift - Zero Harmonic (Steady)
Forward Flight
(2.5g, 41 m.p.h.)
Condition 6

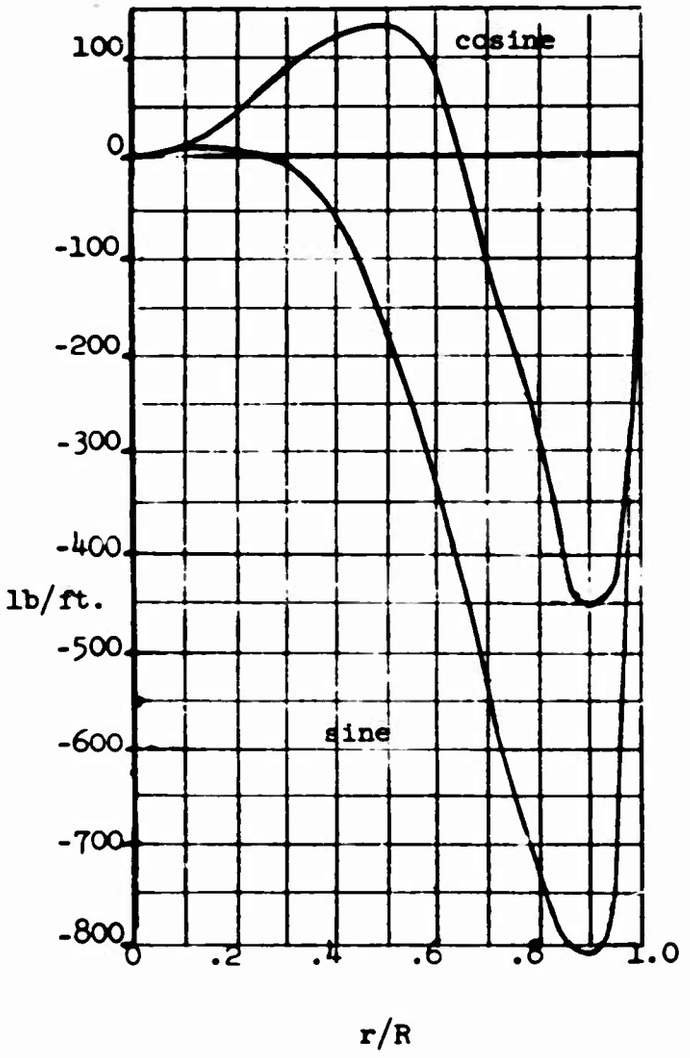

Figure 21. Lift - First Harmonic
Forward Flight
(2.5g, 41 m.p.h.)
Condition 6

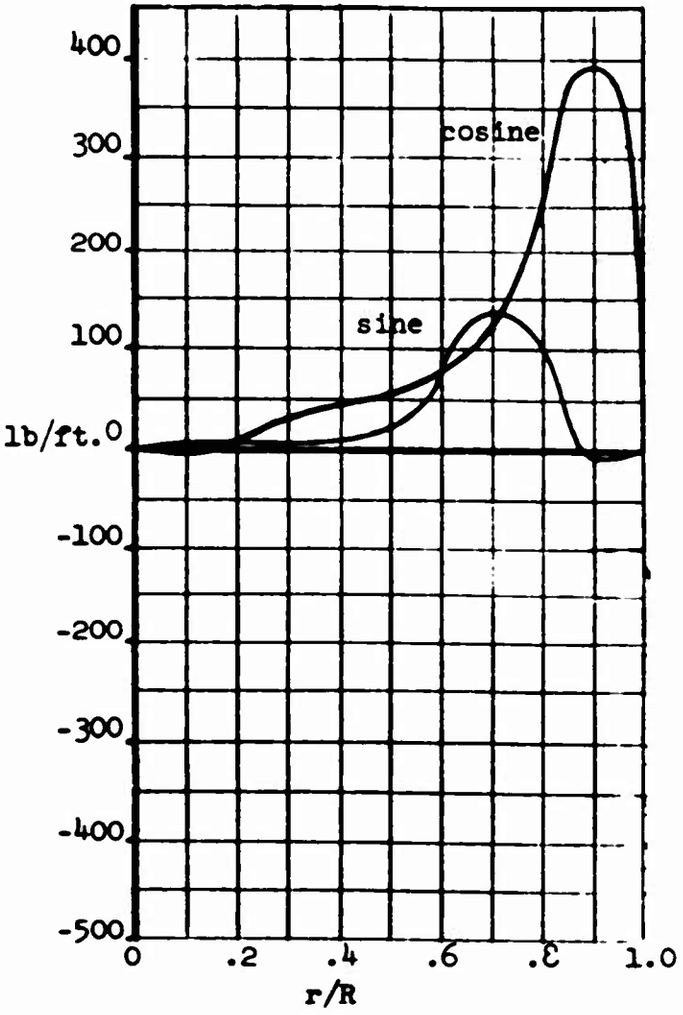

Figure 22. Lift - Second Harmonic
Forward Flight
(2.5g, 41 m.p.h.)
Condition 6

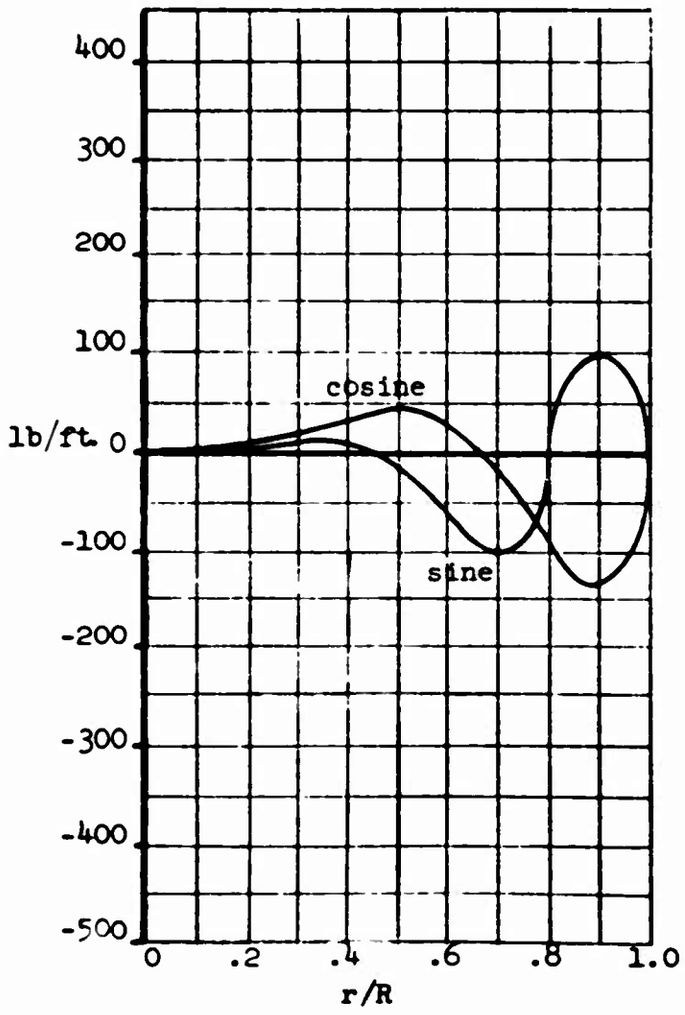

Figure 23. Lift - Third Harmonic
Forward Flight
(2.5g, 41 m.p.h.)
Condition 6

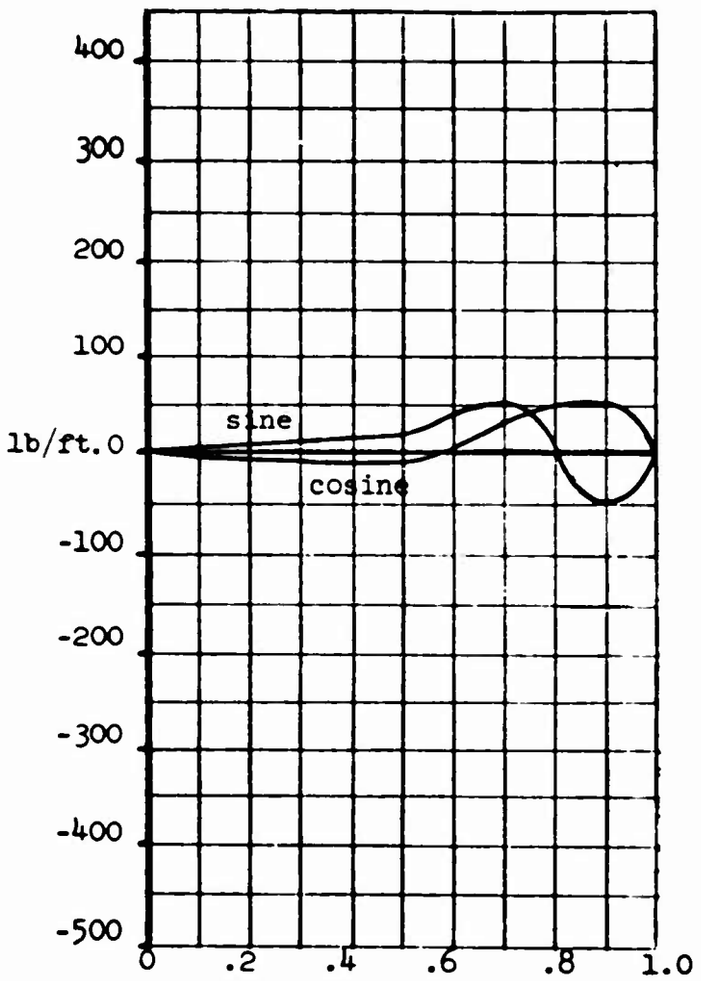

Figure 24. Lift - Fourth Harmonic
Forward Flight
(2.5g, 41 m.p.h.)
Condition 6

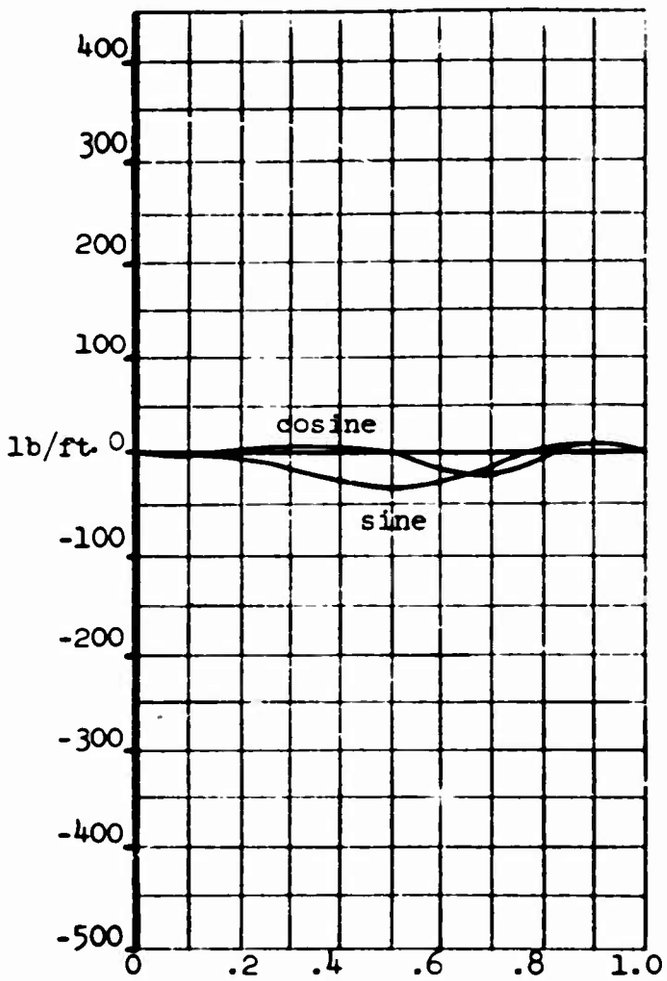

Figure 25. Lift - Fifth Harmonic
Forward Flight
(2.5g, 41 m.p.h.)
Condition 6

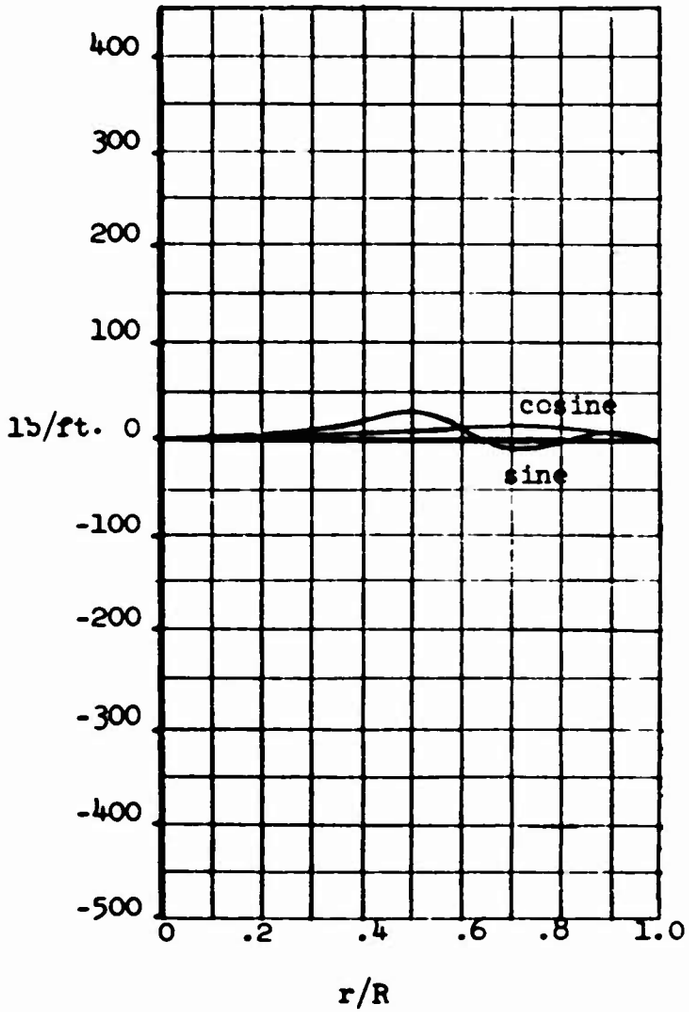

Figure 26. Lift - Sixth Harmonic
Forward Flight
(2.5g, 41 m.p.h.)
Condition 6

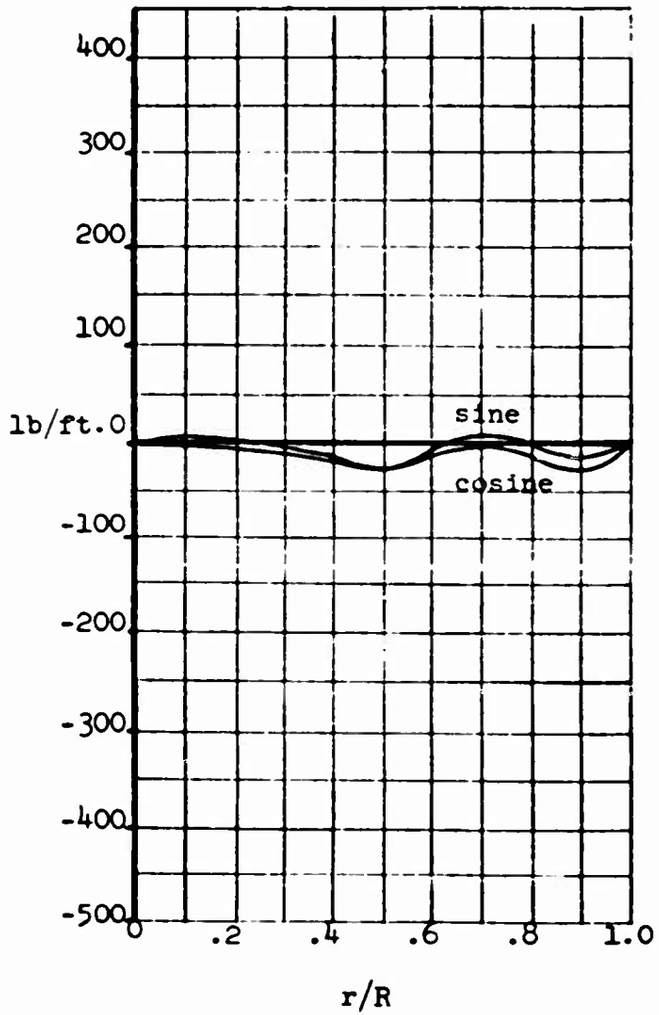

Figure 27. Lift - Seventh Harmonic
Forward Flight
2.5g, 41 m.p.h.)
Condition 6

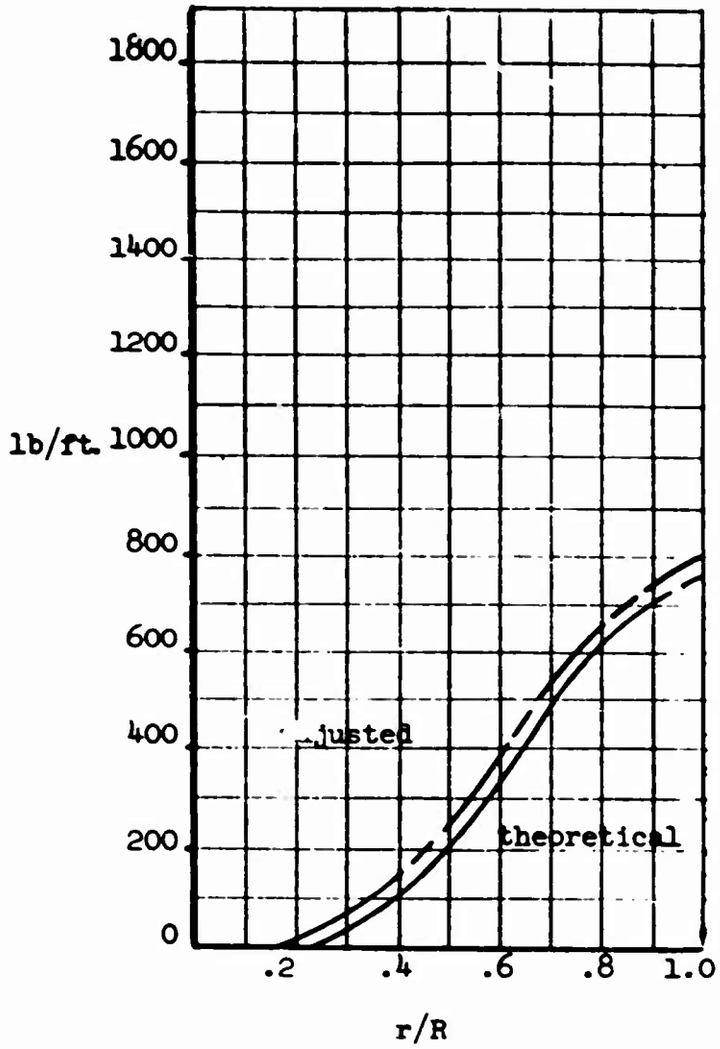

Figure 28. Lift - Zero Harmonic (Steady)
Forward Flight
(lg, 144 m.p.h.)
Condition 8

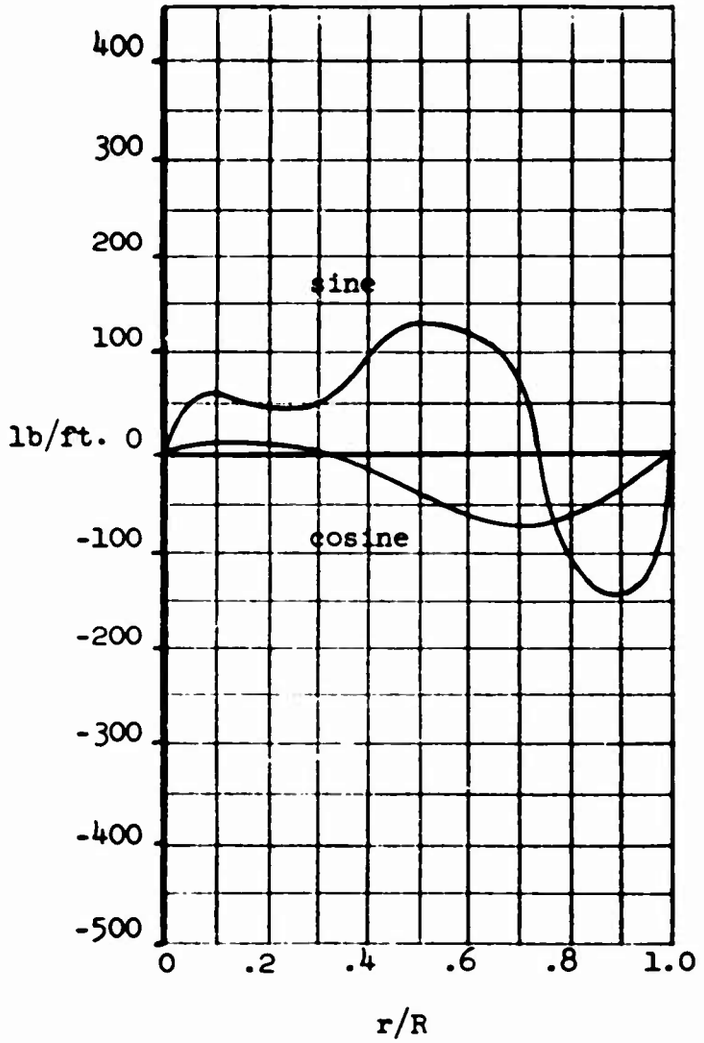

Figure 29. Lift - First Harmonic
Forward Flight
(lg, 144 m.p.h.)
Condition 8

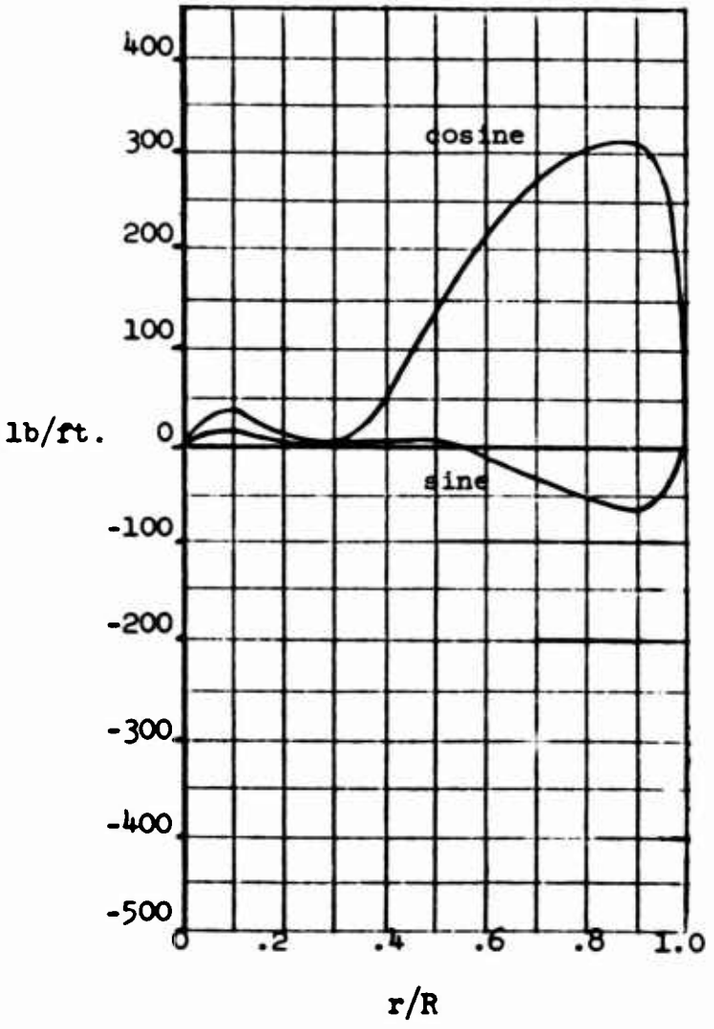

Figure 30. Lift - Second Harmonic
Forward Flight
(lg, 144 m.p.h.)
Condition 8

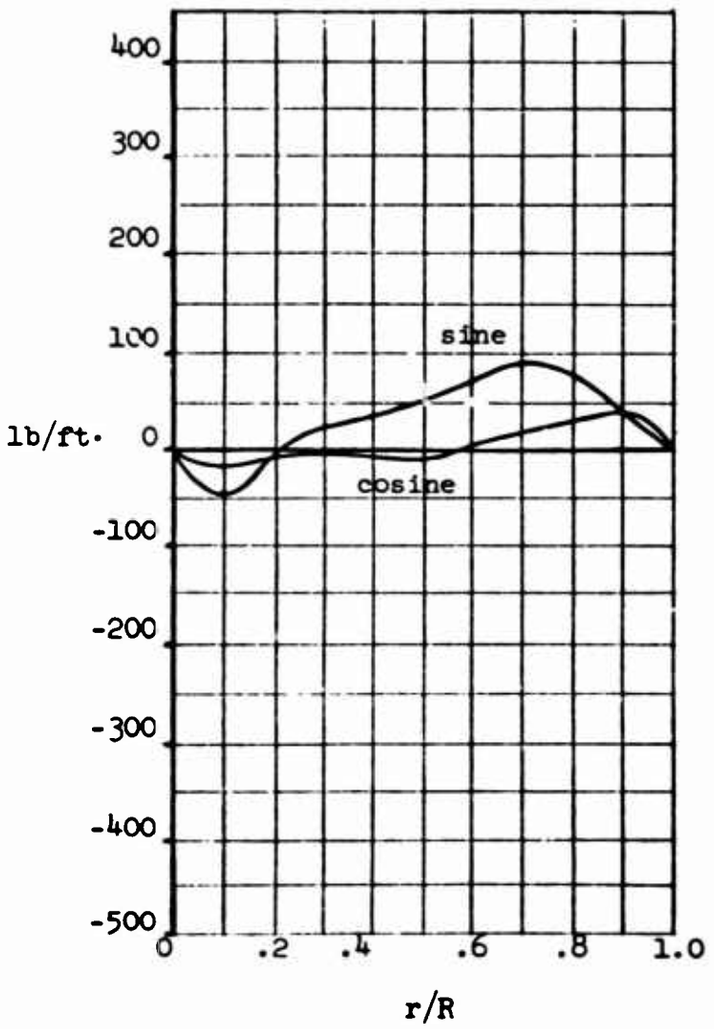

Figure 31. Lift - Third Harmonic
Forward Flight
(lg, 144 m.p.h.)
Condition 8

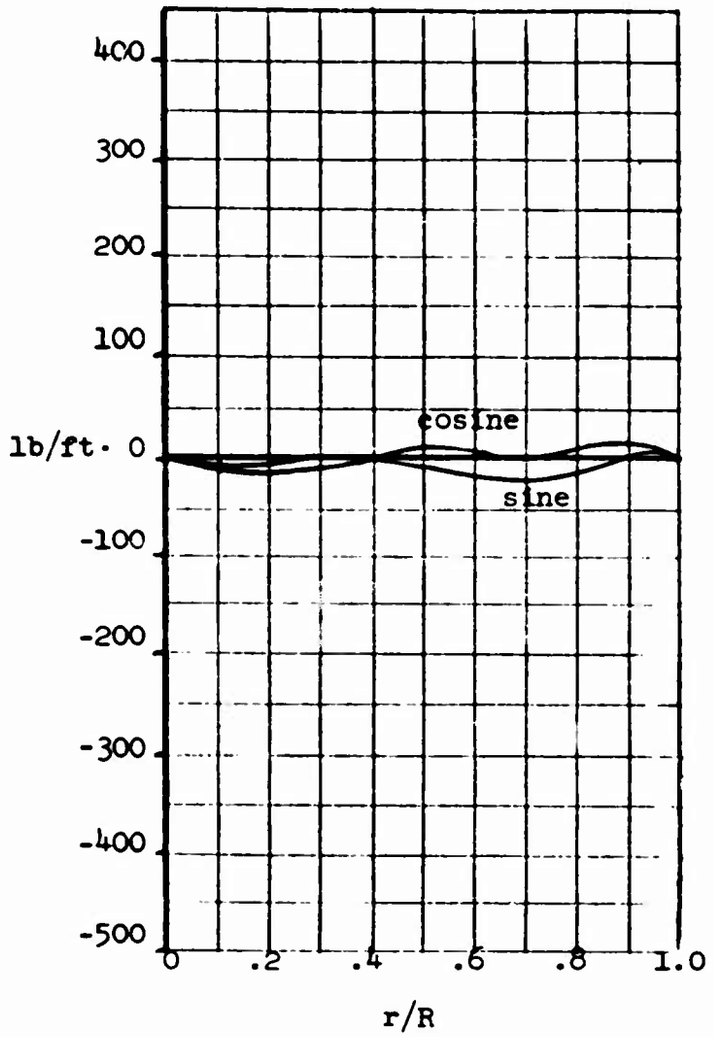

Figure 32. Lift - Fourth Harmonic
Forward Flight
(lg, 144 m.p.h.)
Condition 8

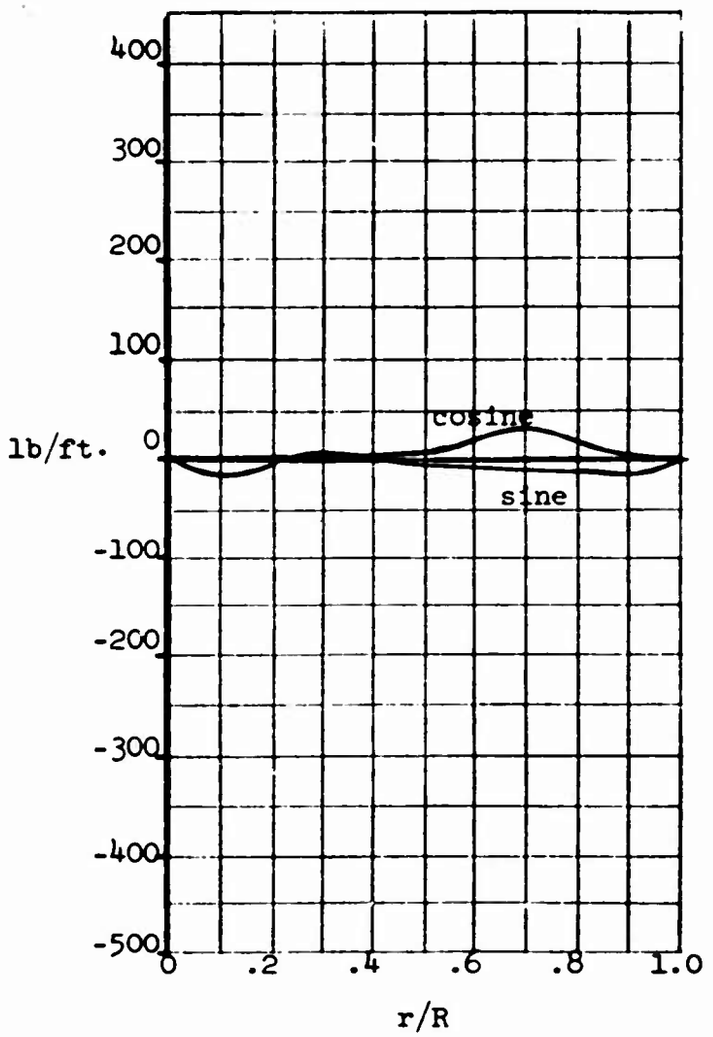

Figure 33. Lift - Fifth Harmonic
Forward Flight
(lg, 144 m.p.h.)
Condition 8

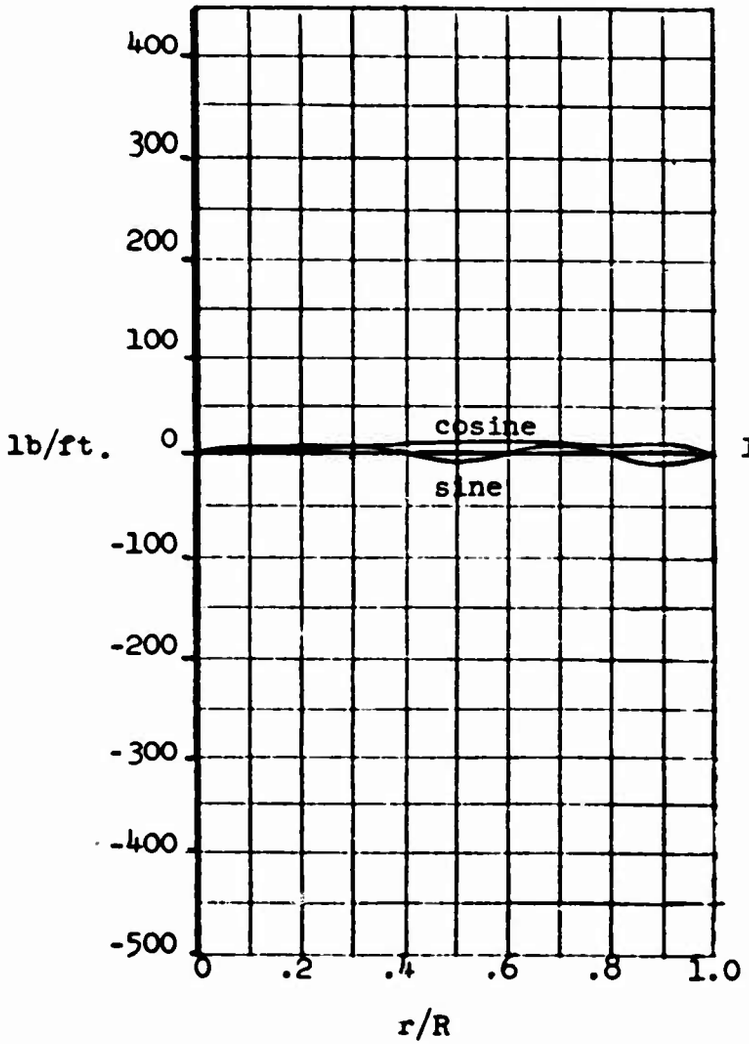

Figure 34. Lift - Sixth Harmonic
Forward Flight
(1g, 144 m.p.h.)
Condition 8

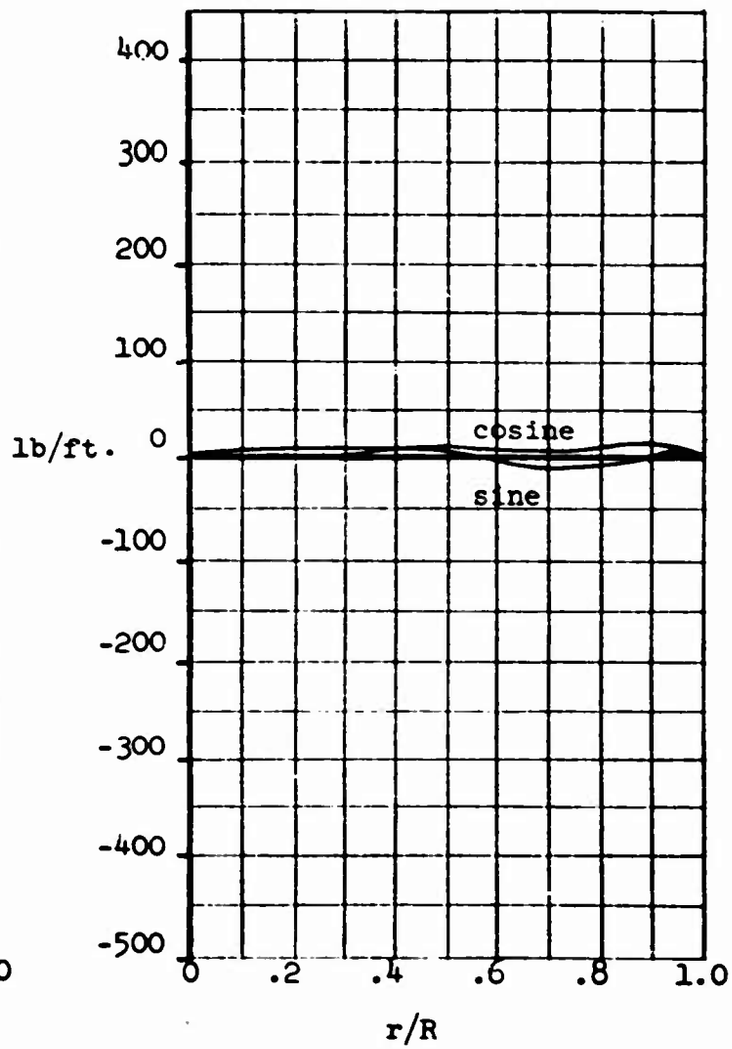

Figure 35. Lift - Seventh Harmonic
Forward Flight
(1g, 144 m.p.h.)
Condition 8

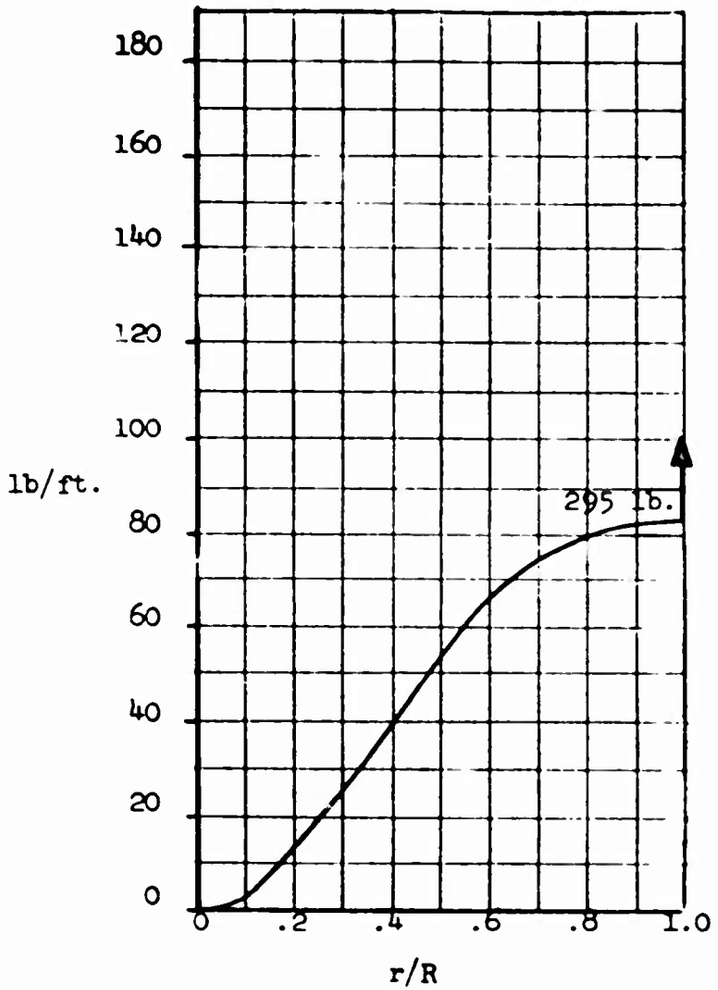

Figure 36. Drag - Zero Harmonic
Hover
Condition 2

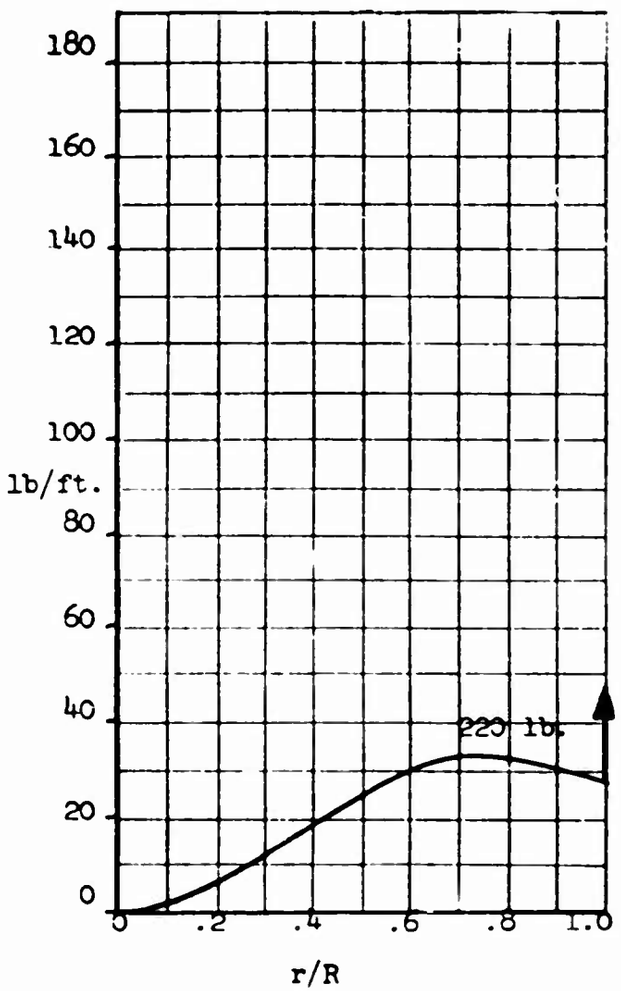

Figure 37. Drag - Zero Harmonic
Pushover (-0.5g, 0 m.p.h.)
Condition 5

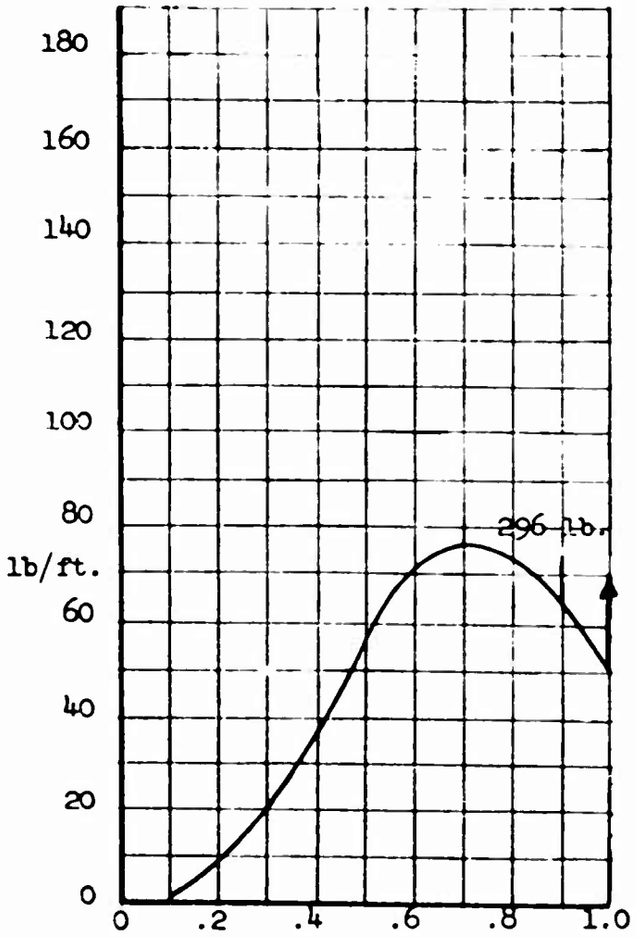

Figure 38. Drag - Zero Harmonic (Steady)
Forward Flight
(lg, 41 m.p.h.)
Condition 3

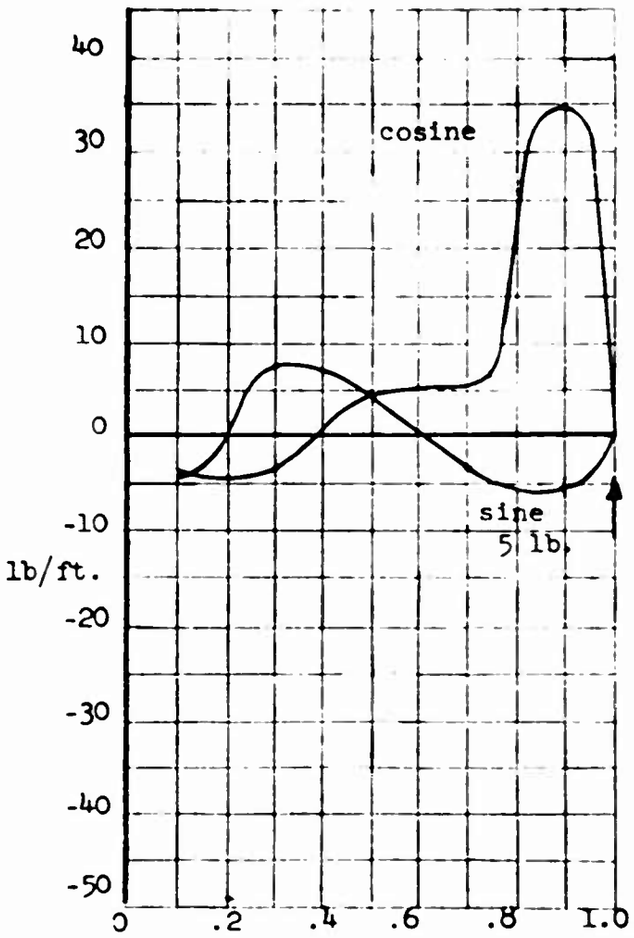

Figure 39. Drag - First Harmonic
Forward Flight
(lg, 41 m.p.h.)
Condition 3

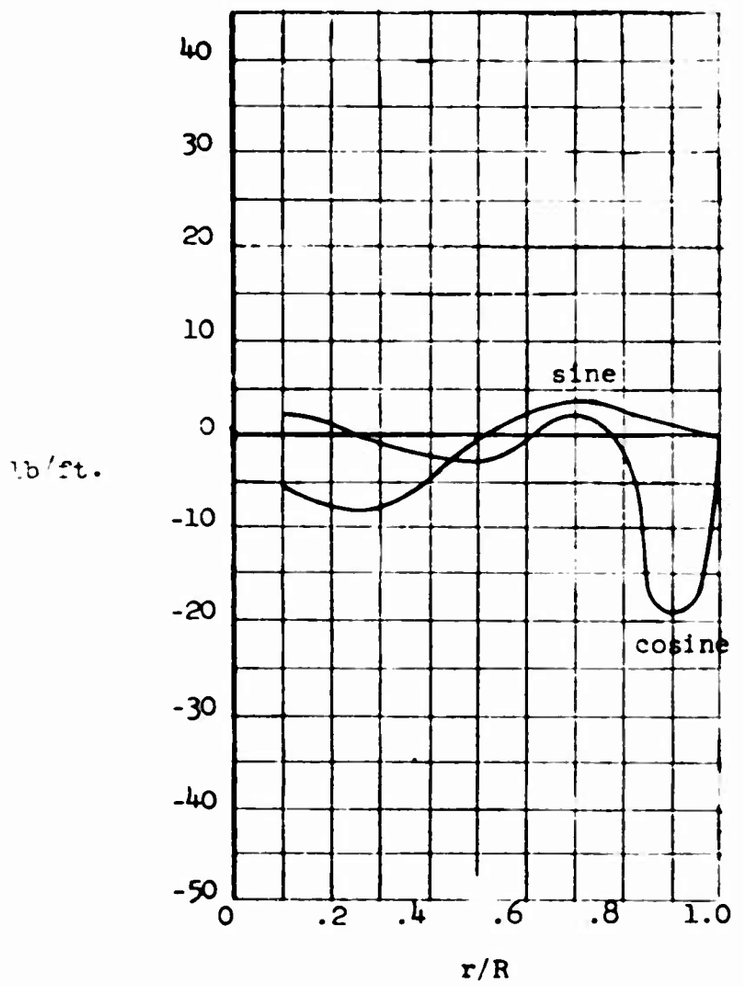

Figure 40. Drag - Second Harmonic
Forward Flight
(lg, 41 m.p.h.)
Condition 3

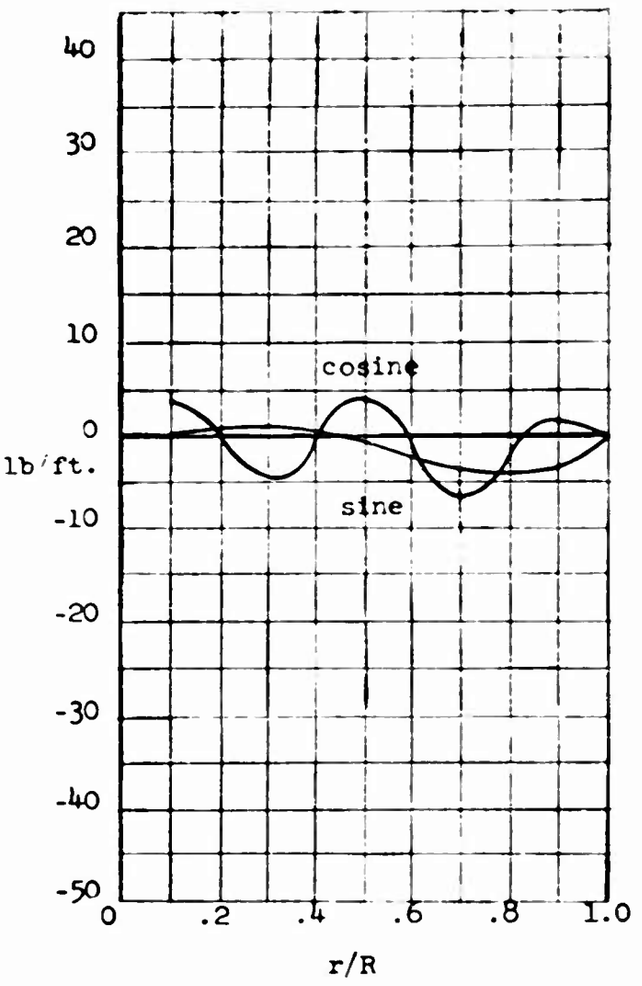

Figure 41. Drag - Third Harmonic
Forward Flight
(lg, 41 m.p.h.)
Condition 3

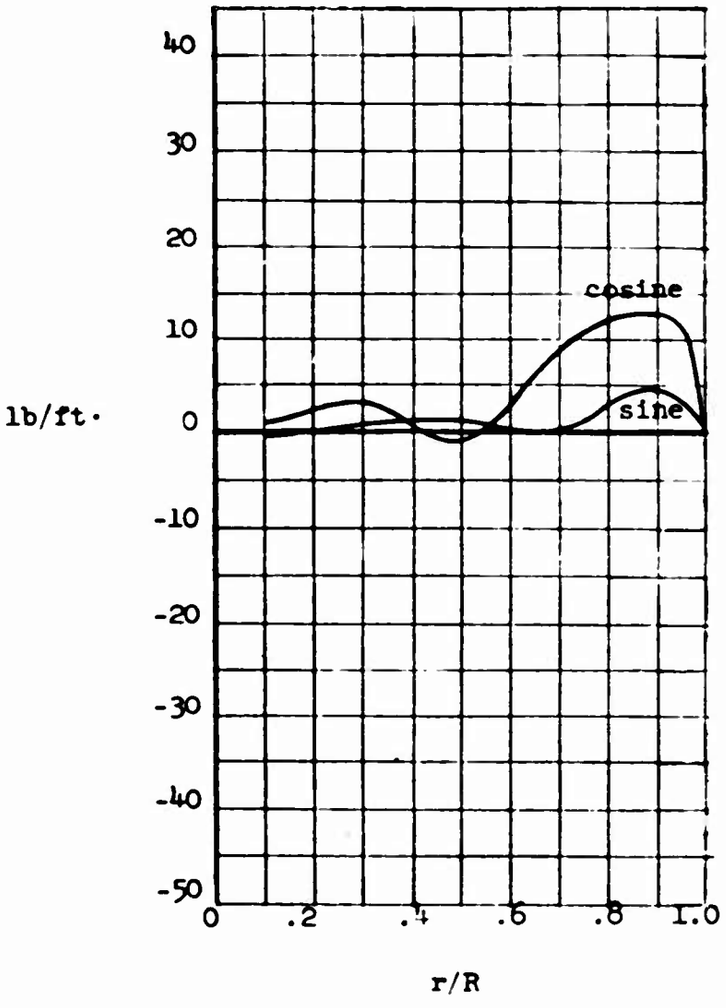

Figure 42. Drag - Fourth Harmonic
Forward Flight
(lg, 41 m.p.h.)
Condition 3

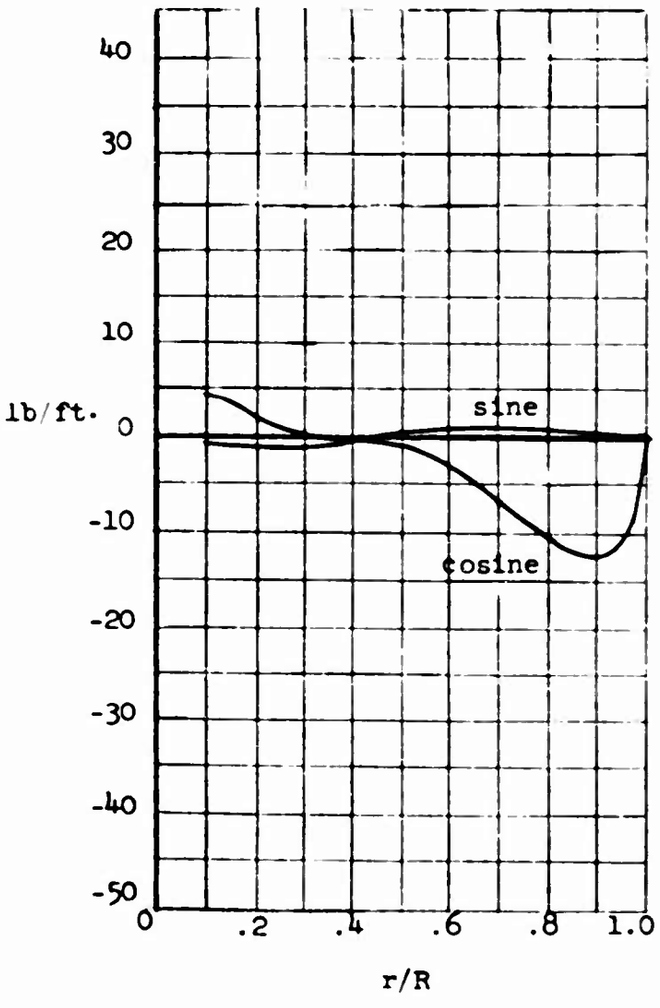

Figure 43. Drag - Fifth Harmonic
Forward Flight
(lg, 41 m.p.h.)
Condition 3

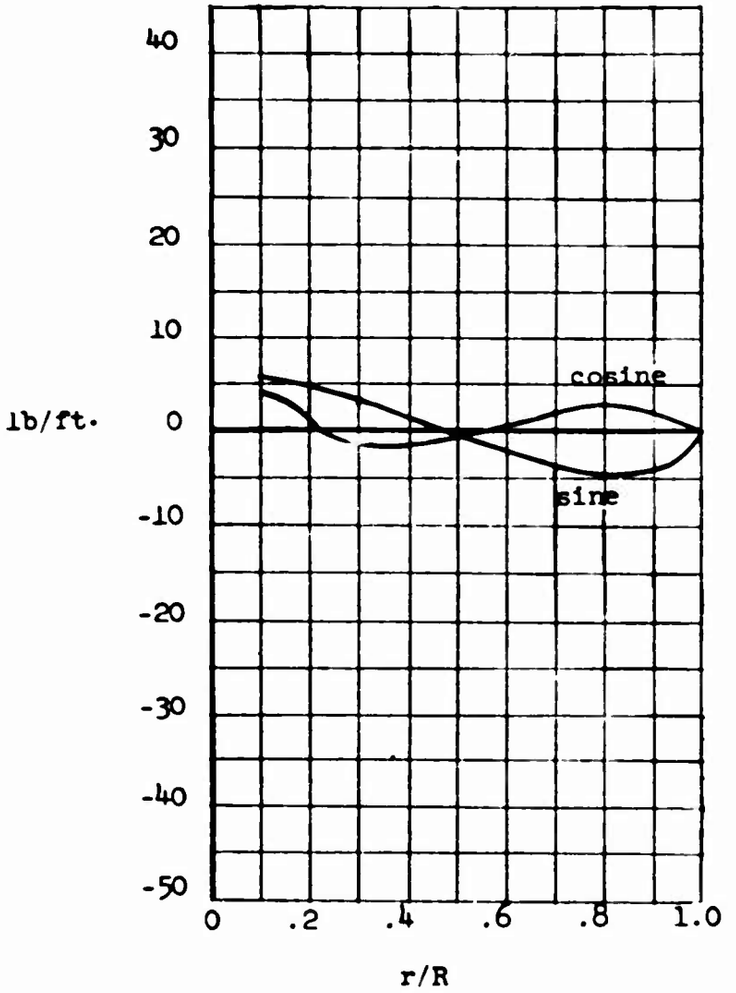

Figure 44. Drag - Sixth Harmonic
Forward Flight
(1g, 41 m.p.h.)
Condition 3

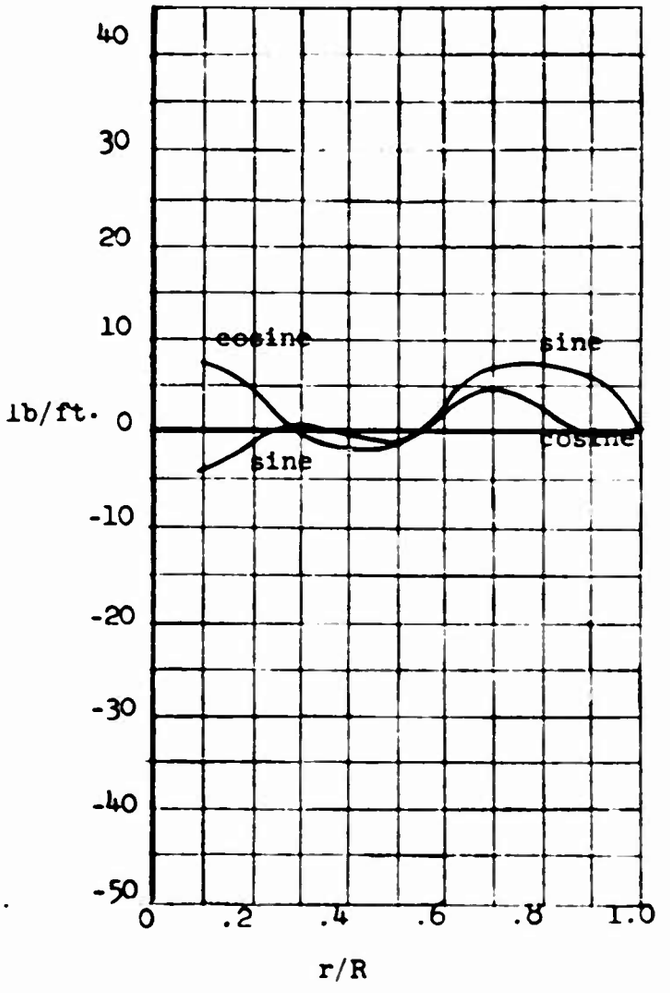

Figure 45. Drag - Seventh Harmonic
Forward Flight
(1g, 41 m.p.h.)
Condition 3

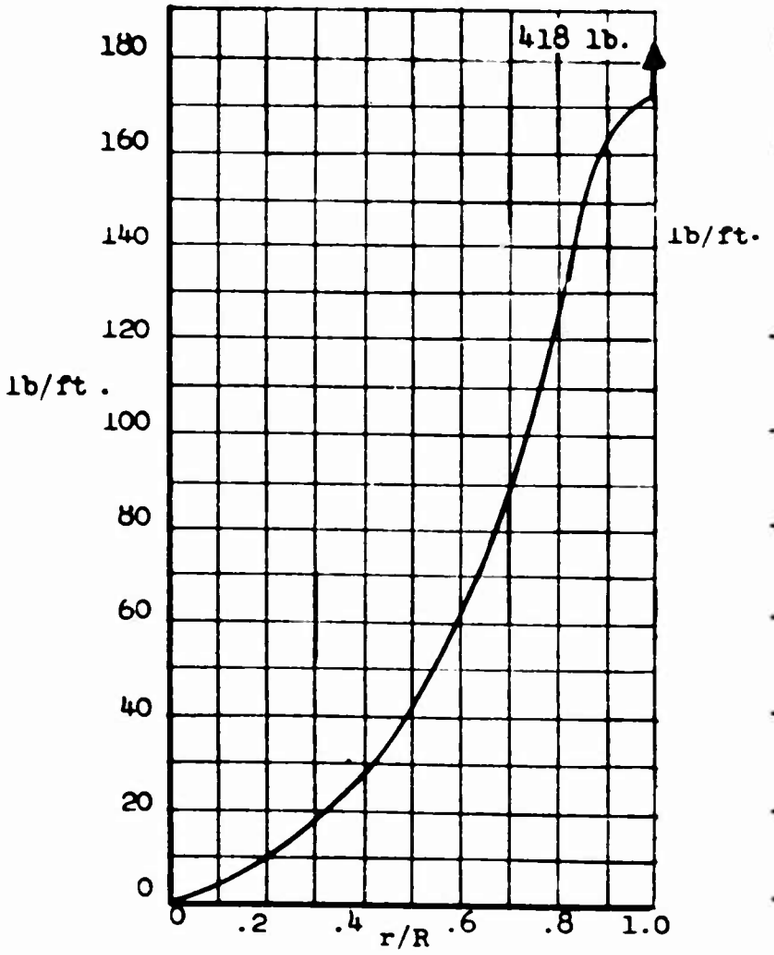

Figure 46. Drag - Zero Harmonic (Steady)
Forward Flight
(2.5g, 41 m.p.h.)
Condition 6

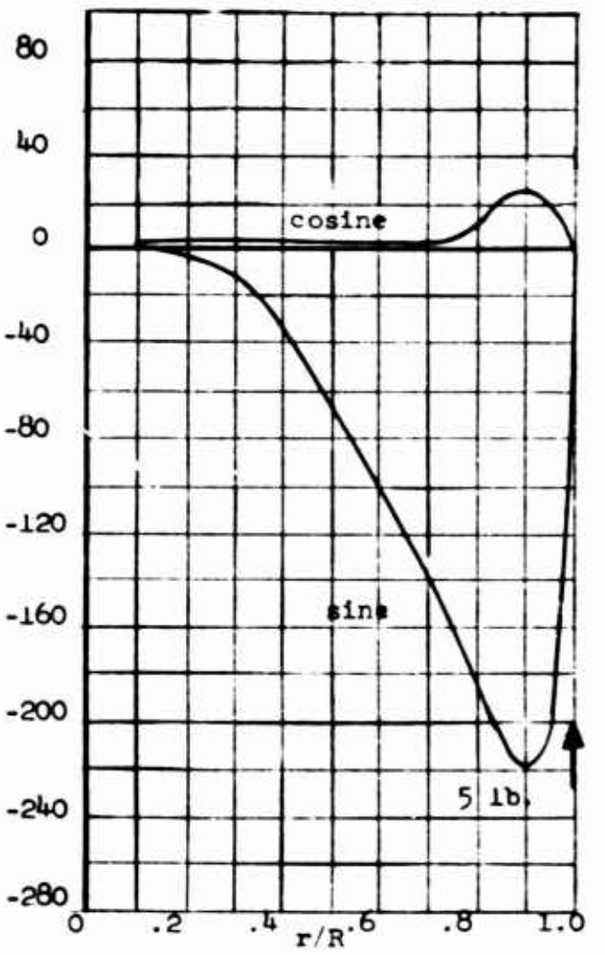

Figure 47. Drag - First Harmonic
Forward Flight
(2.5g, 41 m.p.h.)
Condition 6

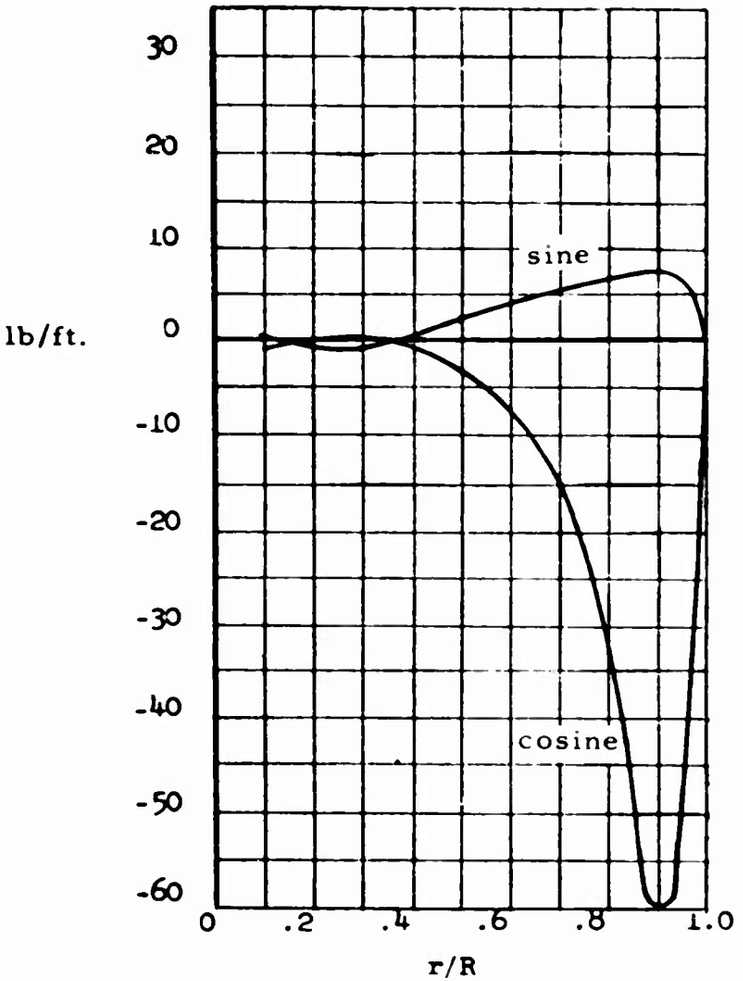

Figure 48. Drag - Second Harmonic
Forward Flight
(2.5g, 41 m.p.h.)
Condition 6

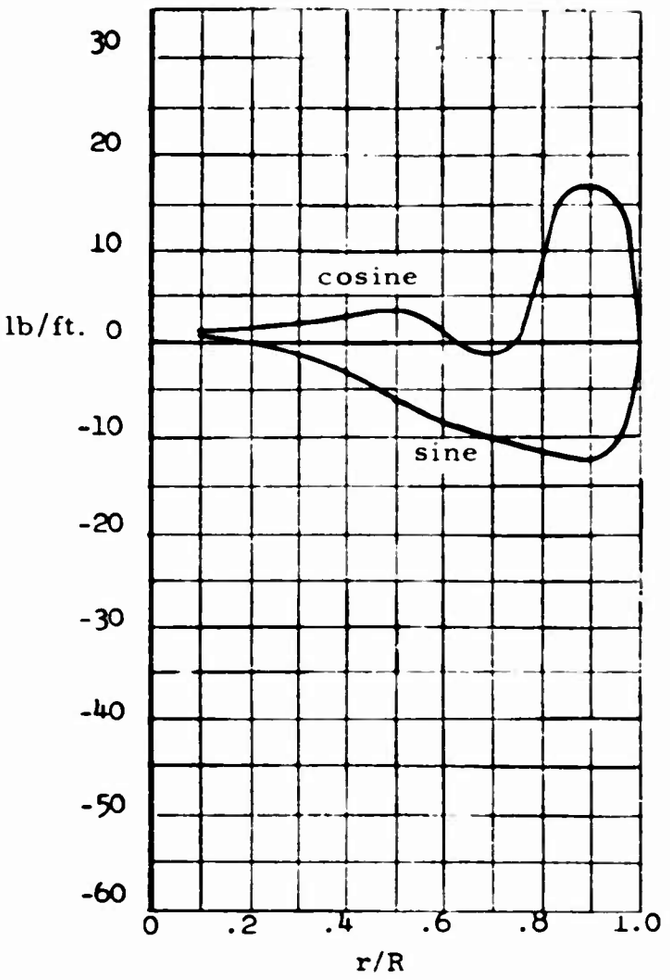

Figure 49. Drag - Third Harmonic
Forward Flight
(2.5g, 41 m.p.h.)
Condition 6

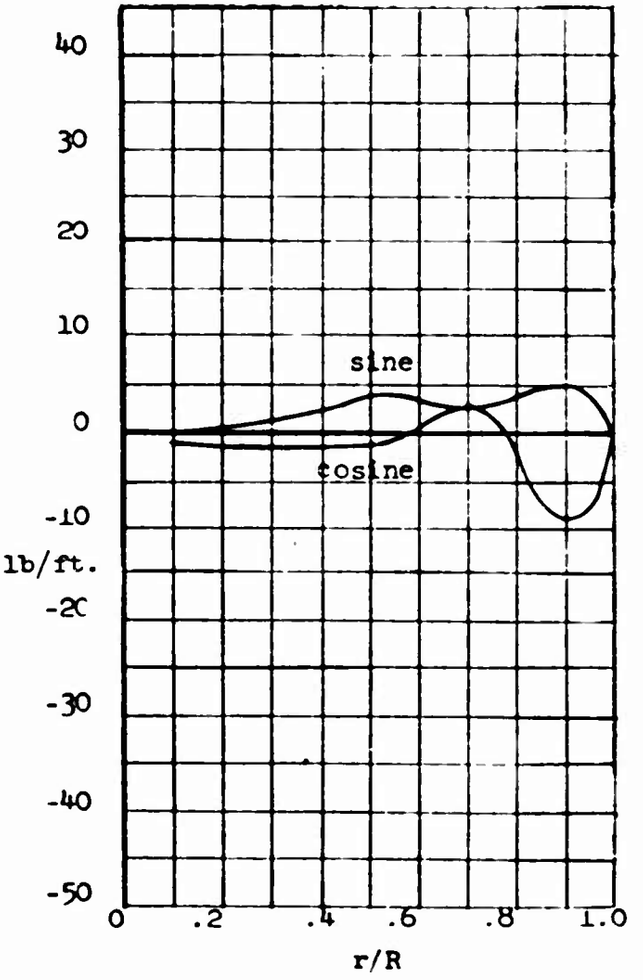

Figure 50. Drag - Fourth Harmonic
Forward Flight
(2.5g, 41 m.p.h.)
Condition 6

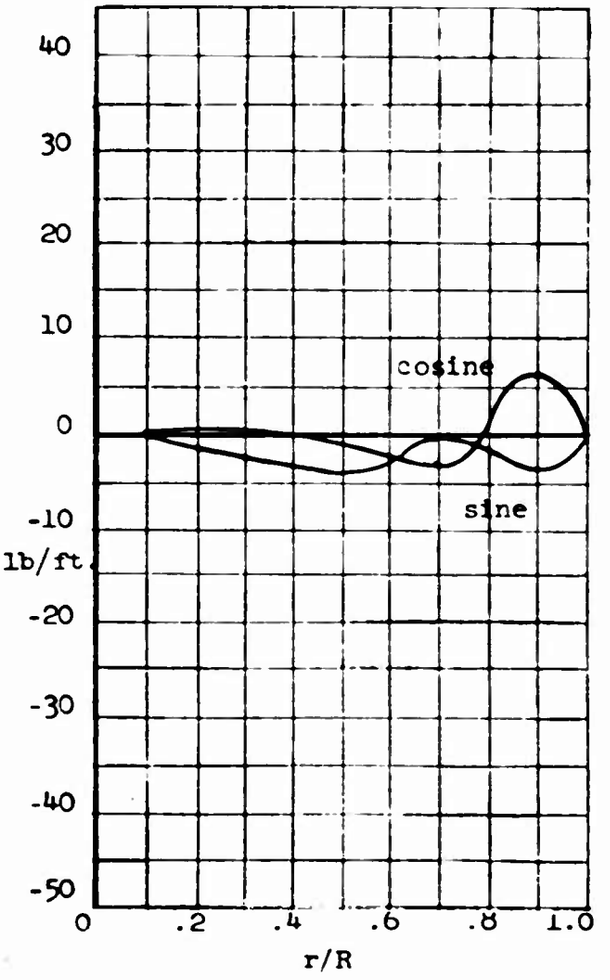

Figure 51. Drag - Fifth Harmonic
Forward Flight
(2.5g, 41 m.p.h.)
Condition 6

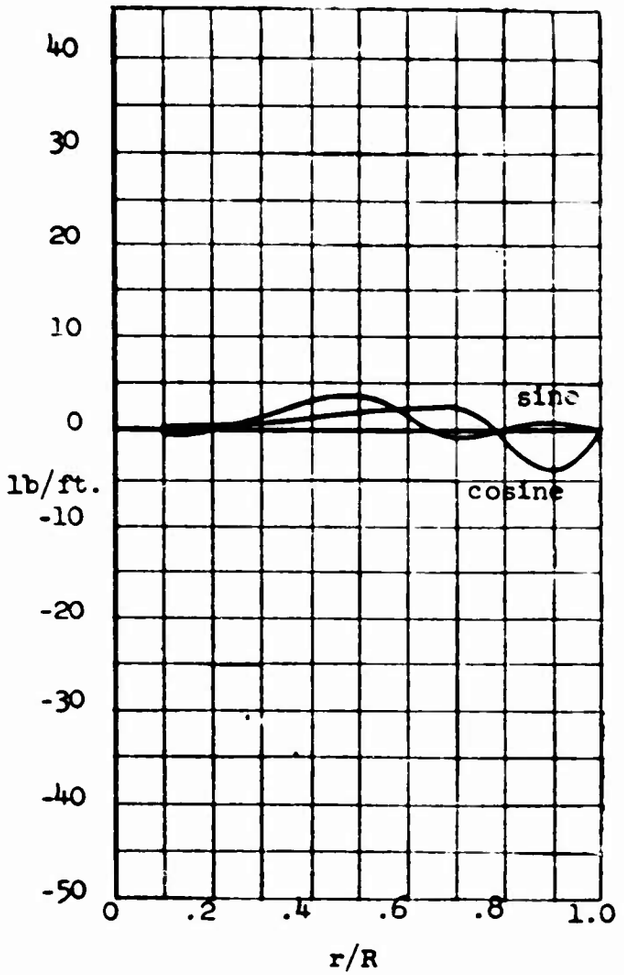

Figure 52. Drag - Sixth Harmonic
Forward Flight
(2.5g, 41 m.p.h.)
Condition 6

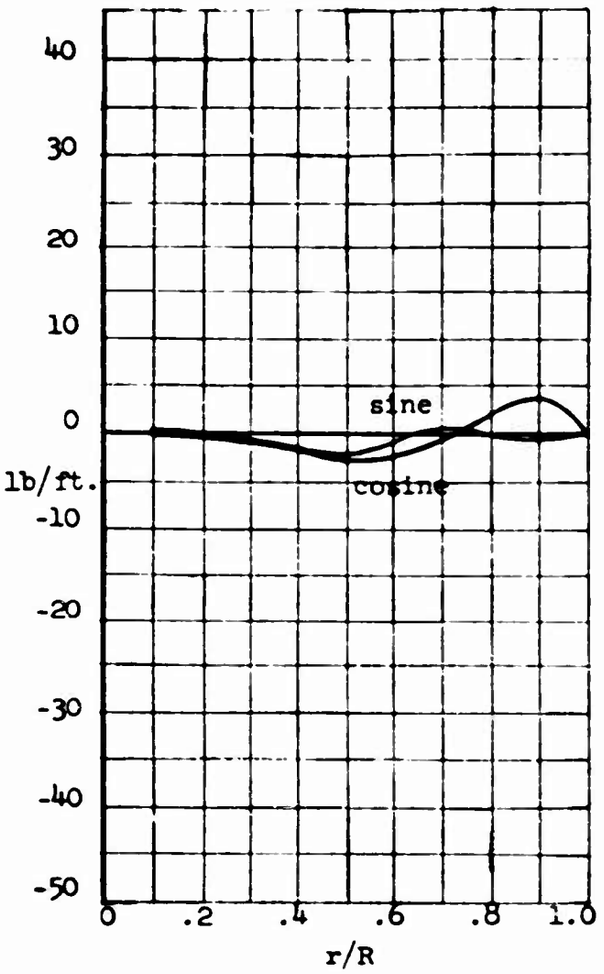

Figure 53. Drag - Seventh Harmonic
Forward Flight
(2.5g, 41 m.p.h.)
Condition 6

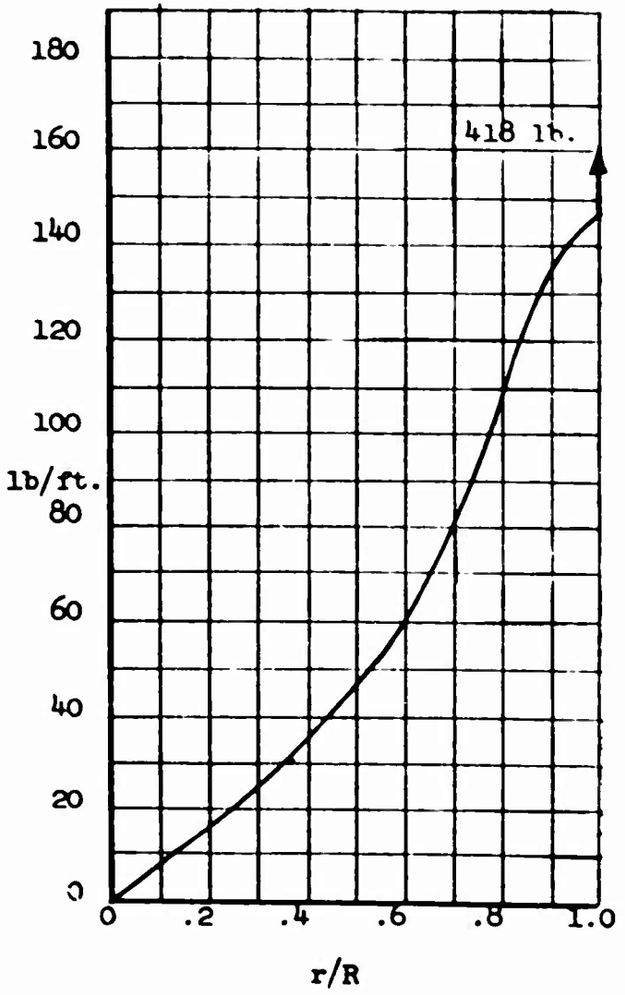

Figure 54. Drag - Zero Harmonic (Steady)
Forward Flight
(lg, 144 m.p.h.)
Condition 8

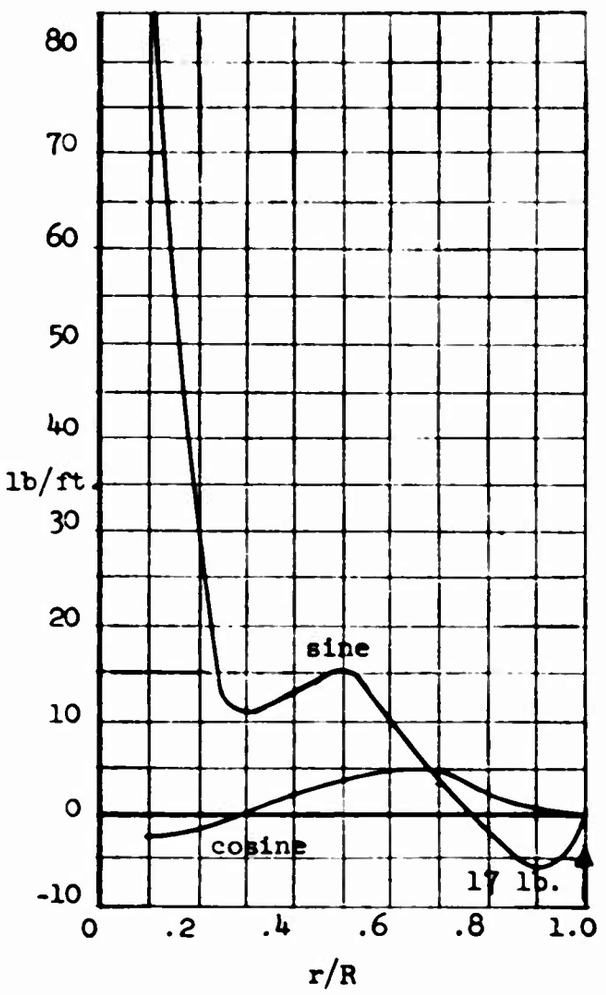

Figure 55. Drag - First Harmonic
Forward Flight
(lg, 144 m.p.h.)
Condition 8

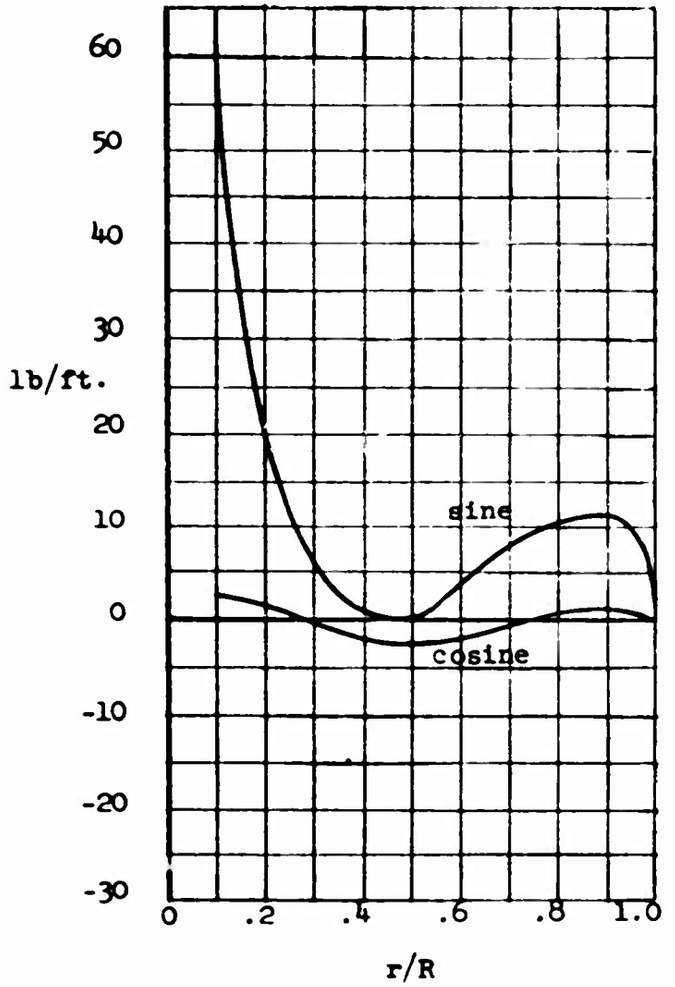

Figure 56. Drag - Second Harmonic
Forward Flight
(lg, 144 m.p.h.)
Condition 8

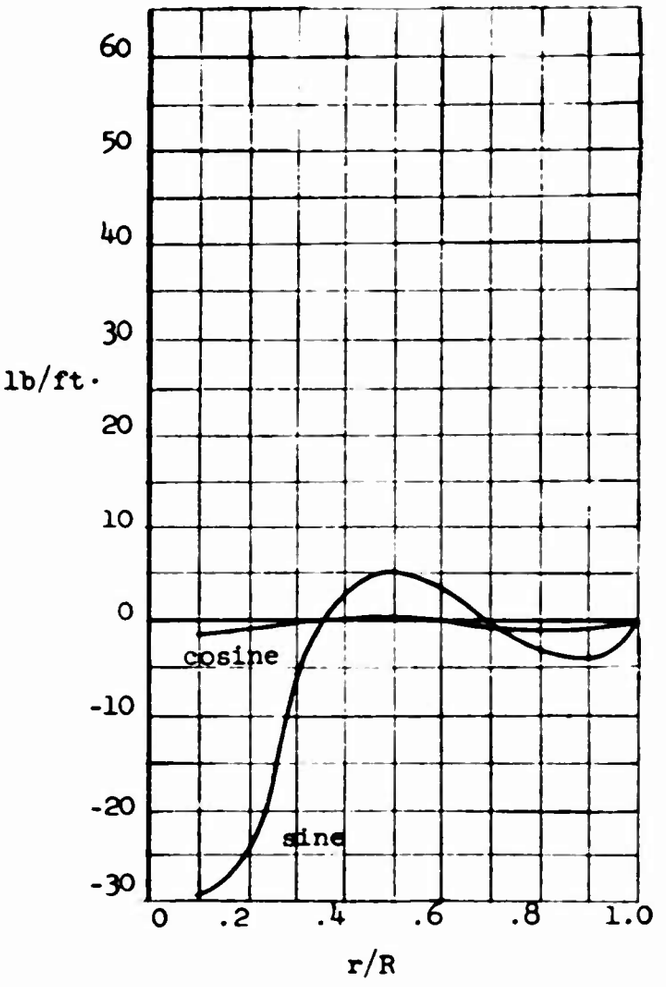

Figure 57. Drag - Third Harmonic
Forward Flight
(lg, 144 m.p.h.)
Condition 8

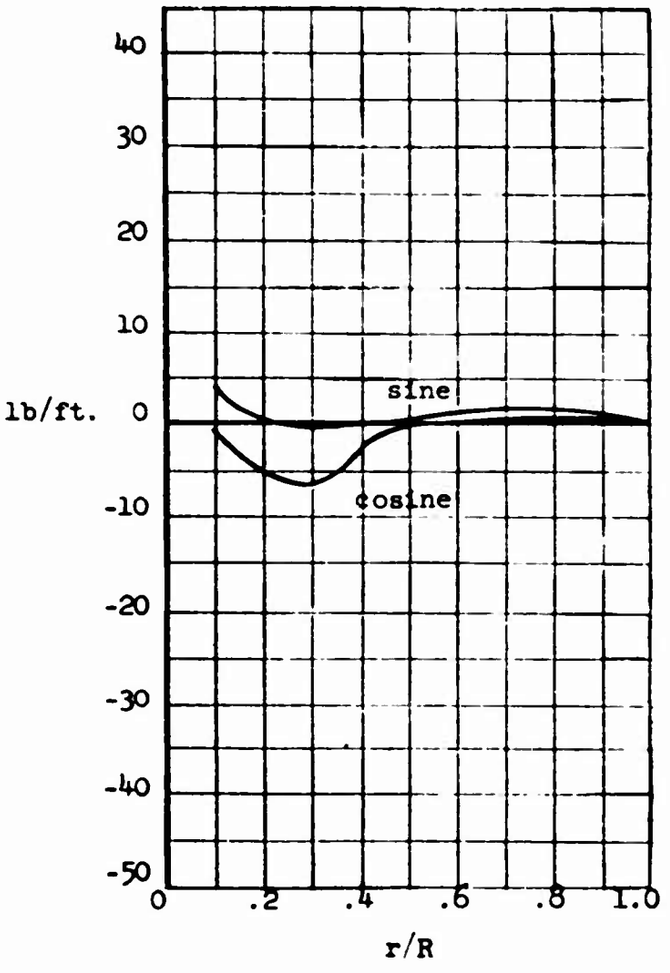

Figure 58. Drag - Fourth Harmonic
Forward Flight
(1g, 144 m.p.h.)
Condition 8

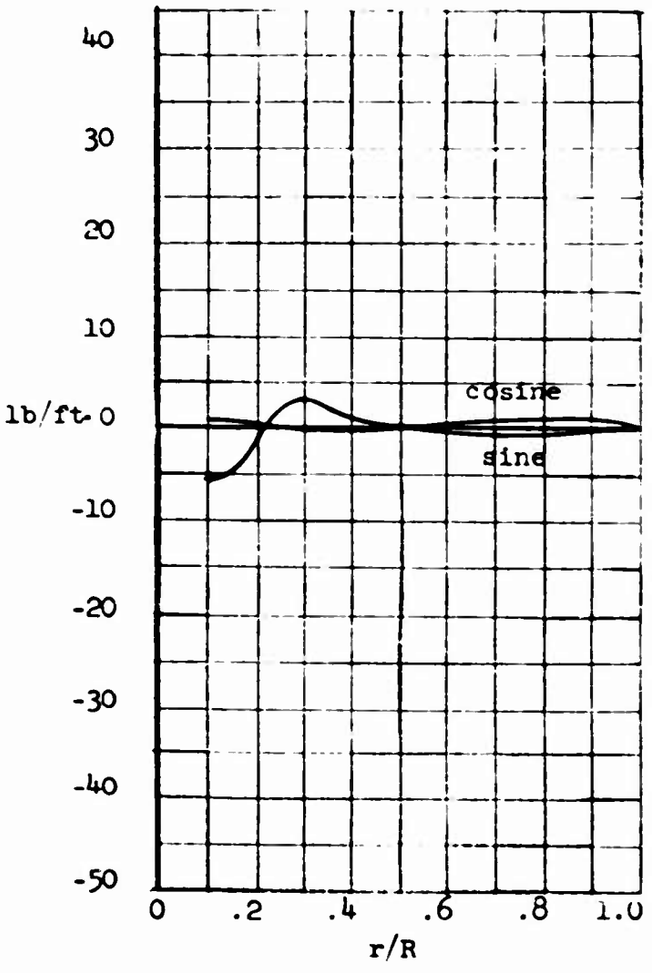

Figure 59. Drag - Fifth Harmonic
Forward Flight
(1g, 144 m.p.h.)
Condition 8

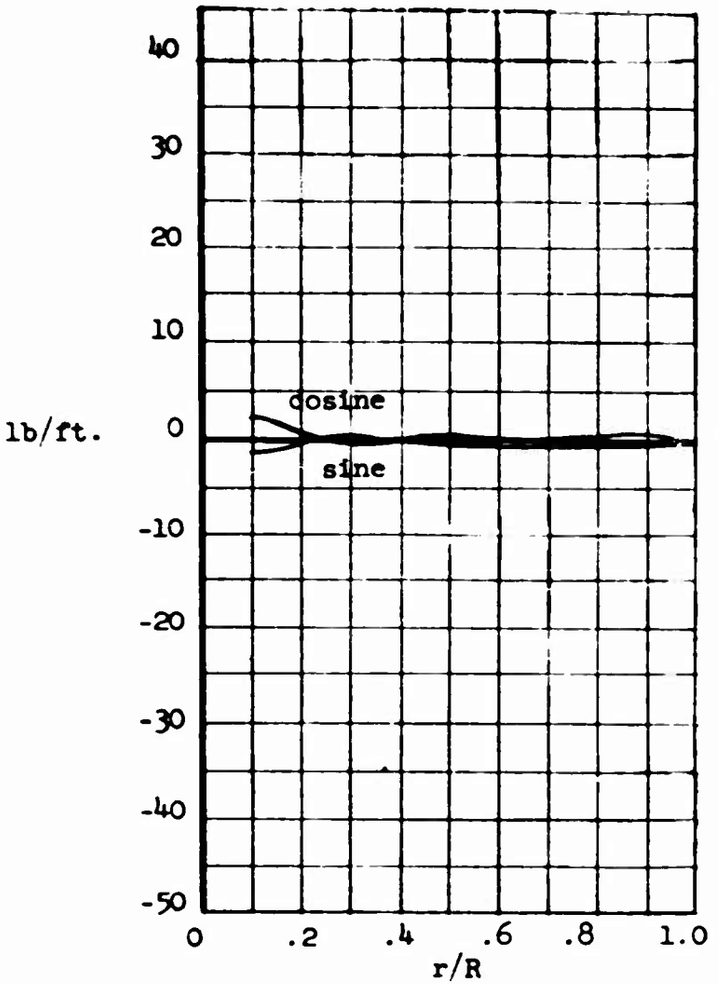

Figure 60. Drag - Sixth Harmonic
Forward Flight
(1g, 144 m.p.h.)
Condition 8

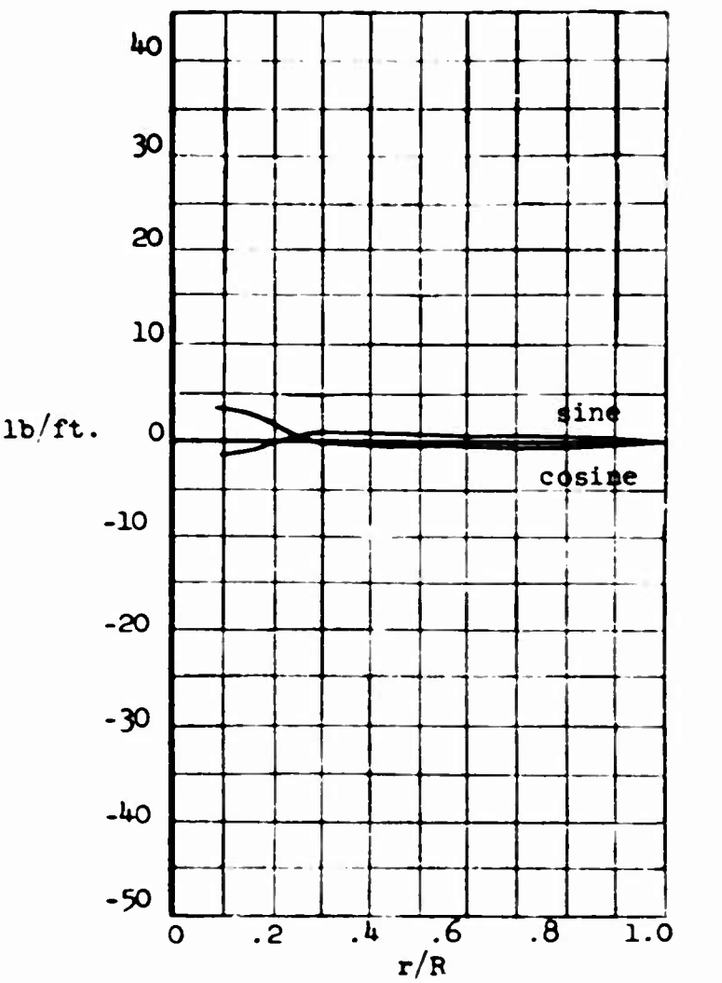

Figure 61. Drag - Seventh Harmonic
Forward Flight
(1g, 144 m.p.h.)
Condition 8

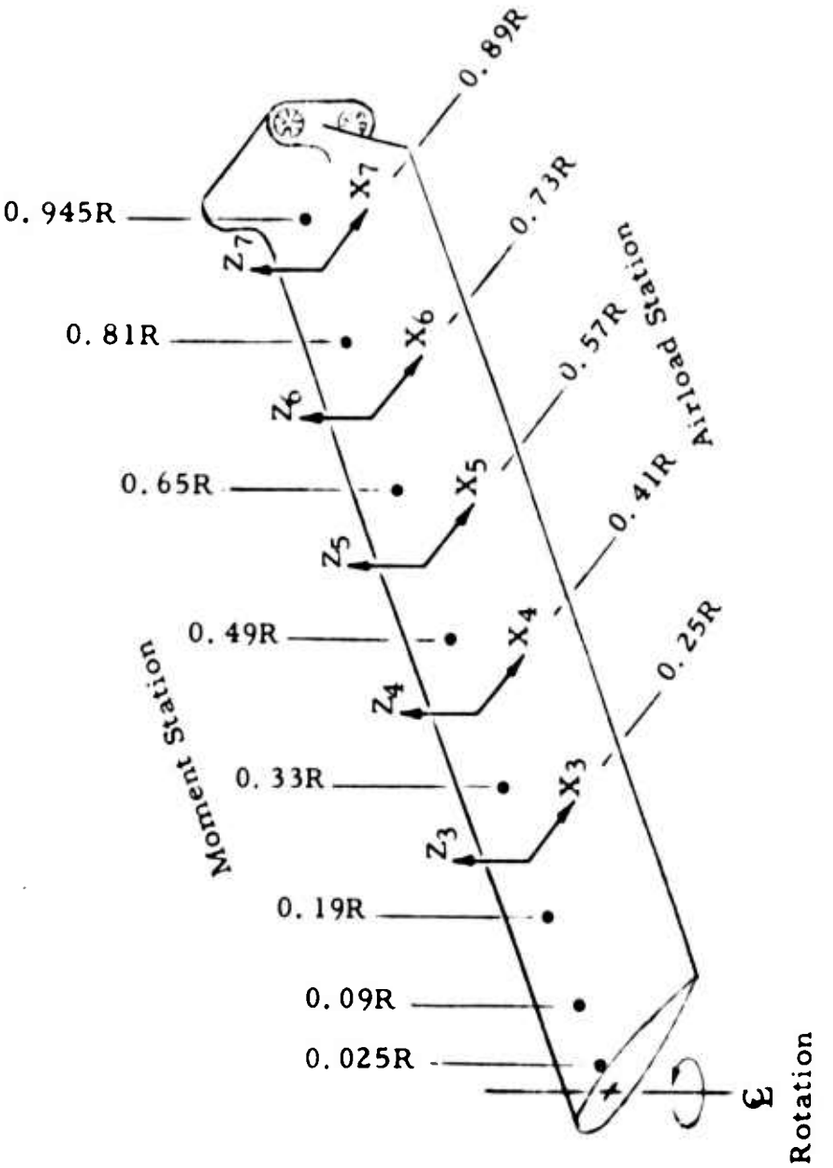

Figure 62. Airload and Moment Stations for Harmonic Airloads Study.

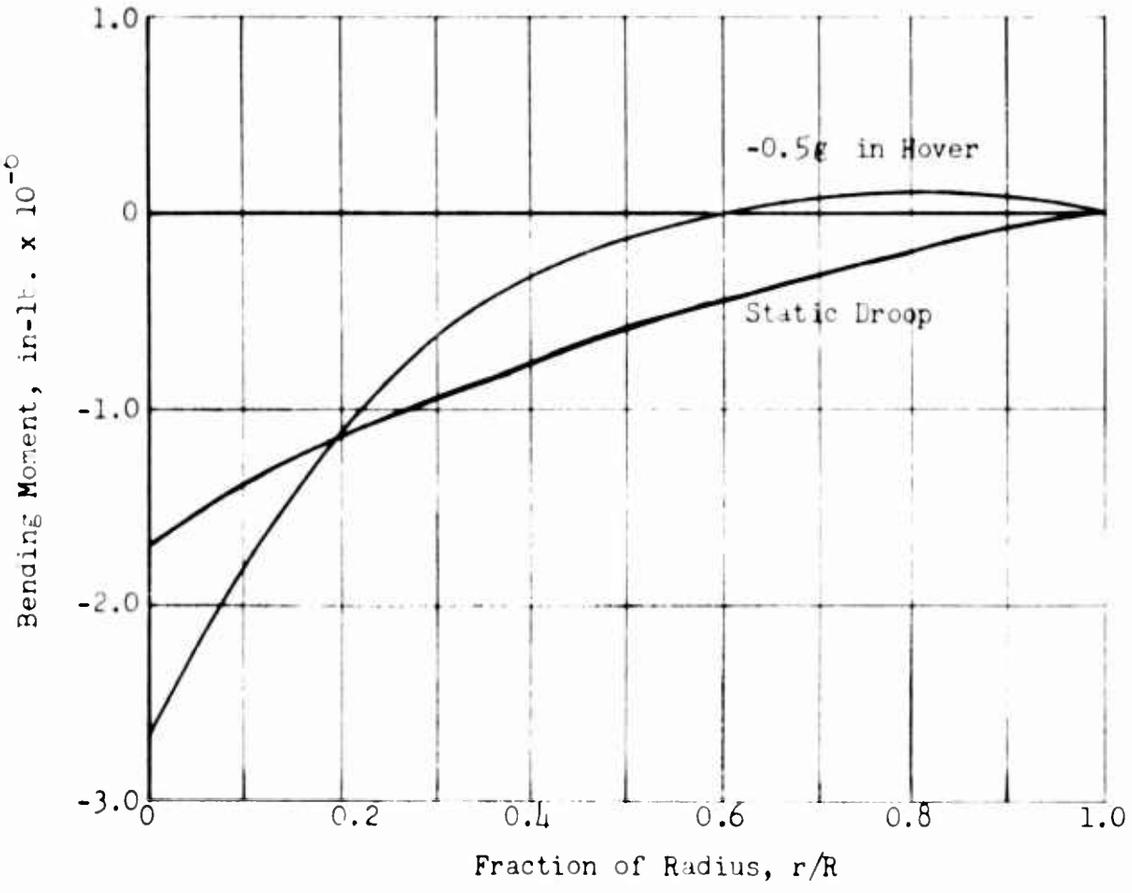

Figure 63. Flapwise Bending Moment Versus Radius.

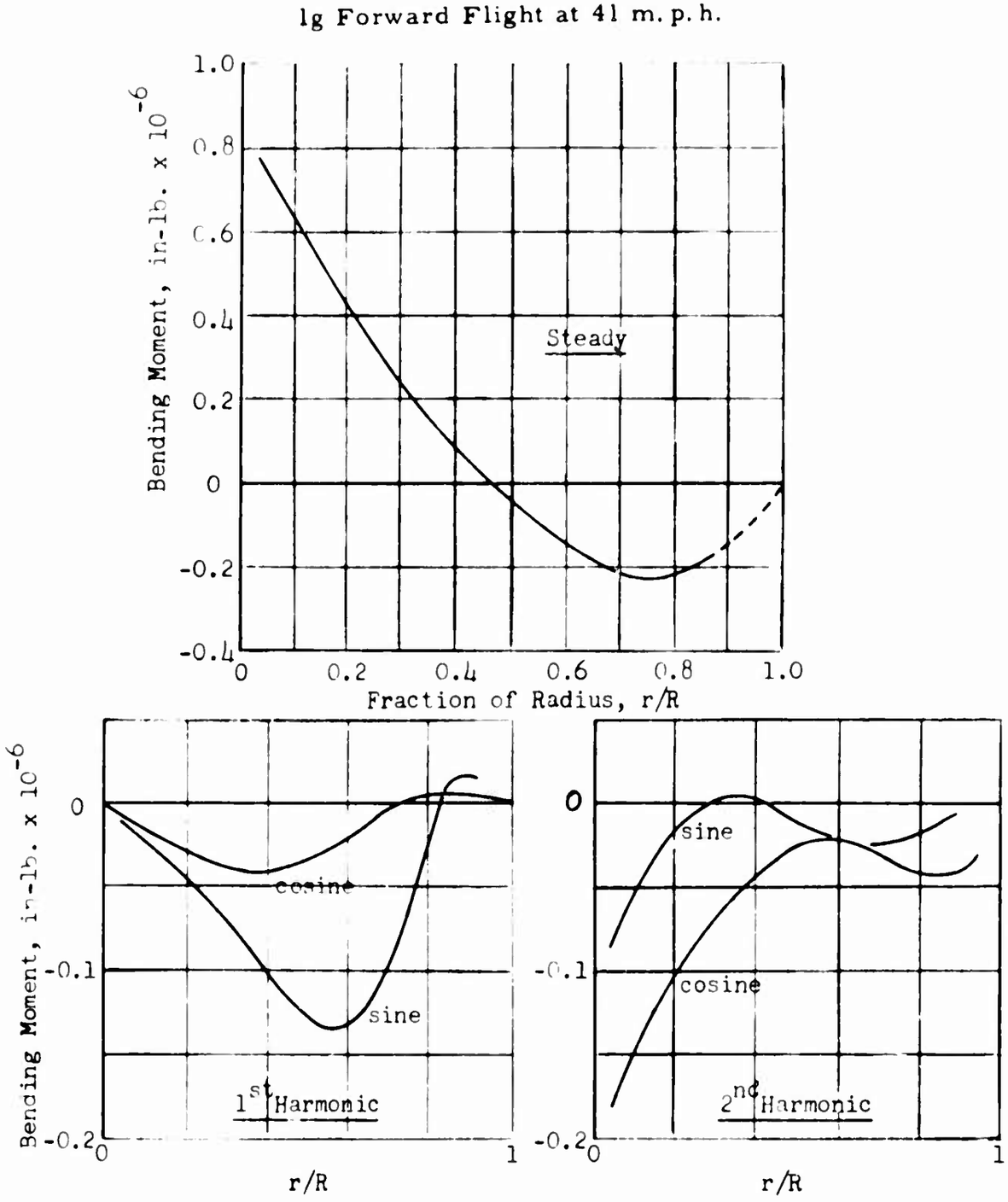

Figure 64. Flapwise Bending Moment Versus Radius.

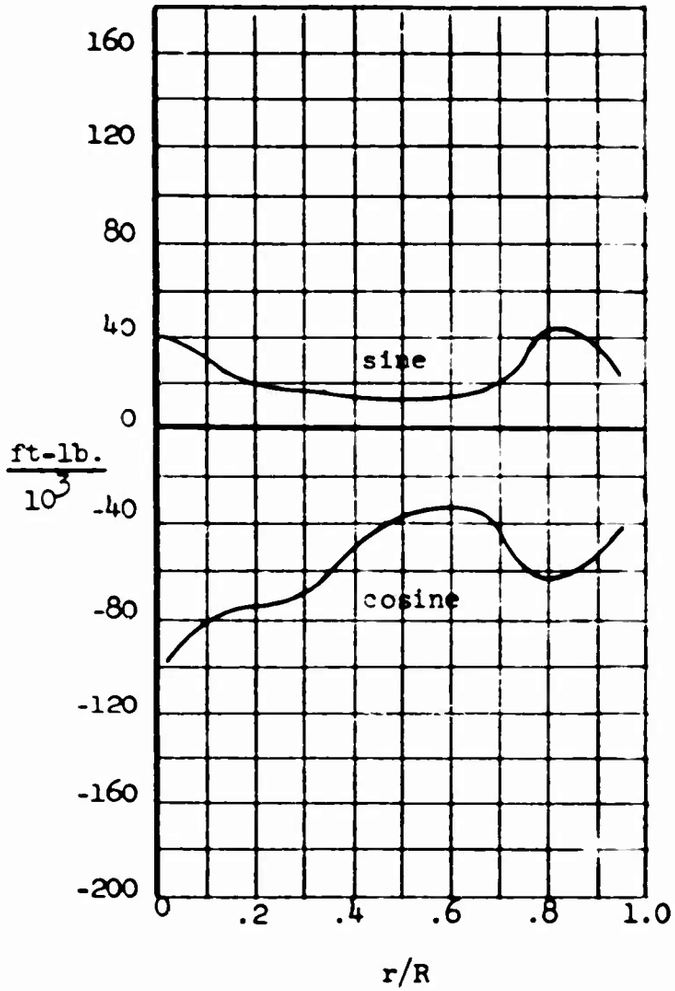

Figure 65. Flapwise Moment - Second Harmonic - Forward Flight (lg, 41 m.p.h.) Condition 3

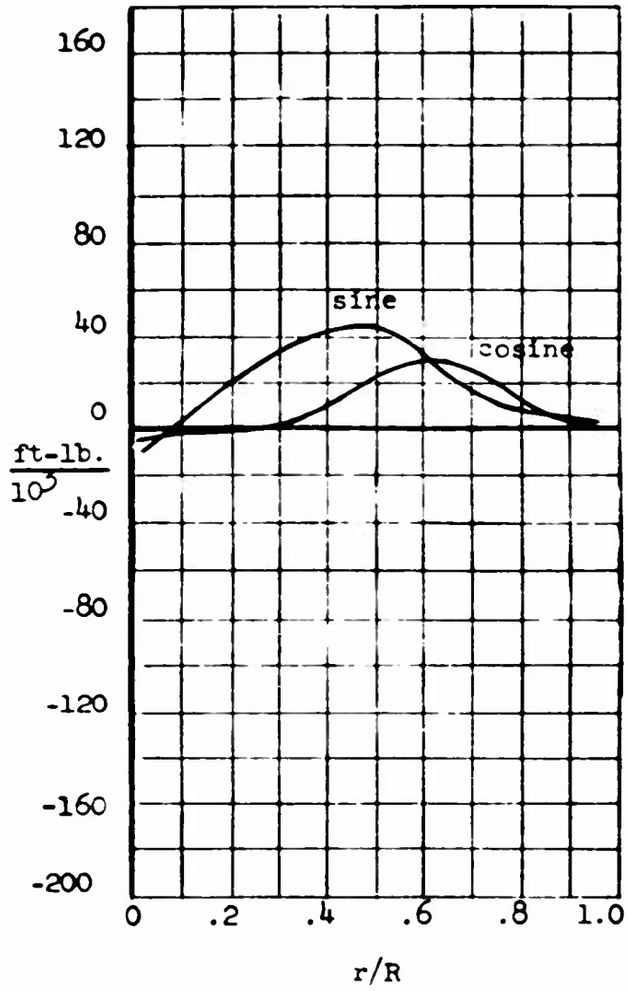

Figure 66. Flapwise Moment - Third Harmonic - Forward Flight (lg, 41 m.p.h.) Condition 3

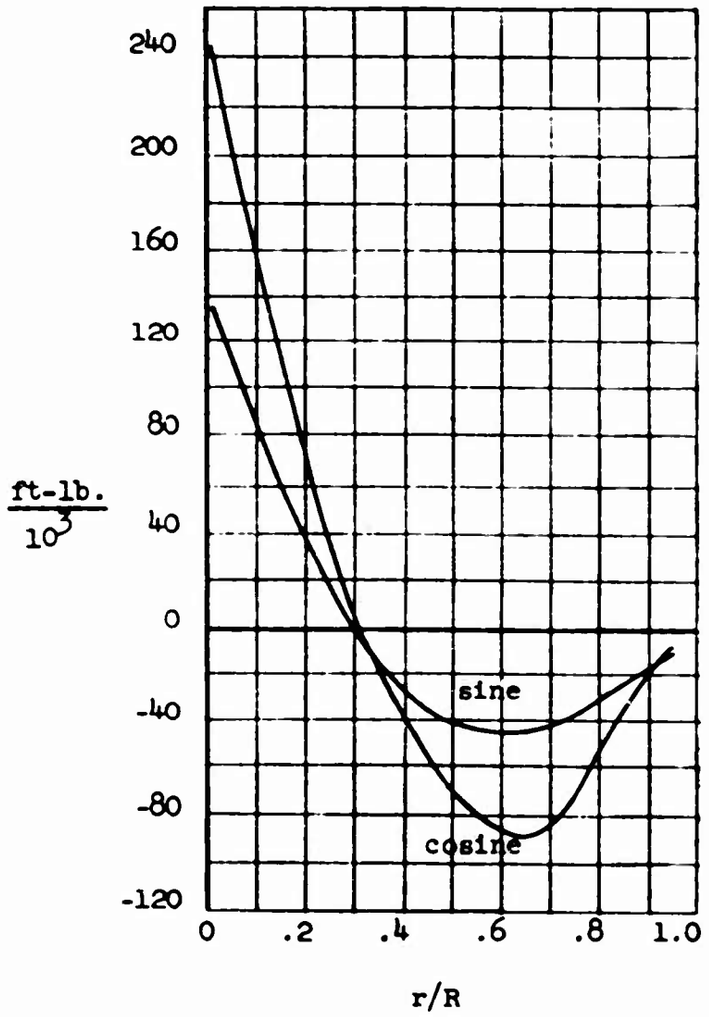

Figure 67. Flapwise Moment - Fourth Harmonic - Forward Flight (lg, 41 m.p.h.) Condition 3

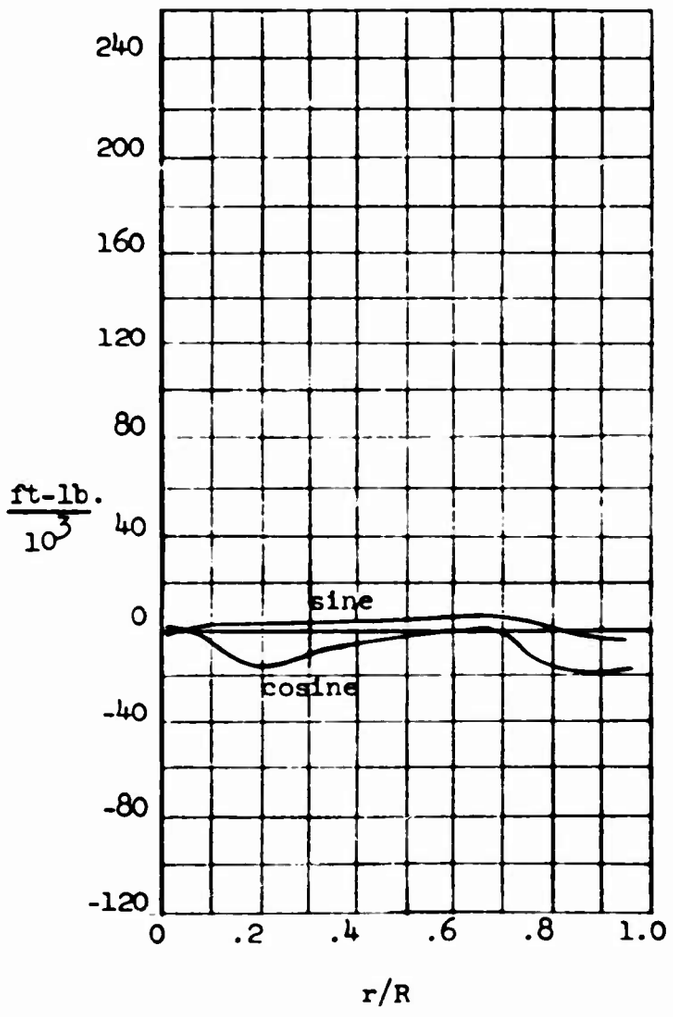

Figure 68. Flapwise Moment - Fifth Harmonic - Forward Flight (lg, 41 m.p.h.) Condition 3

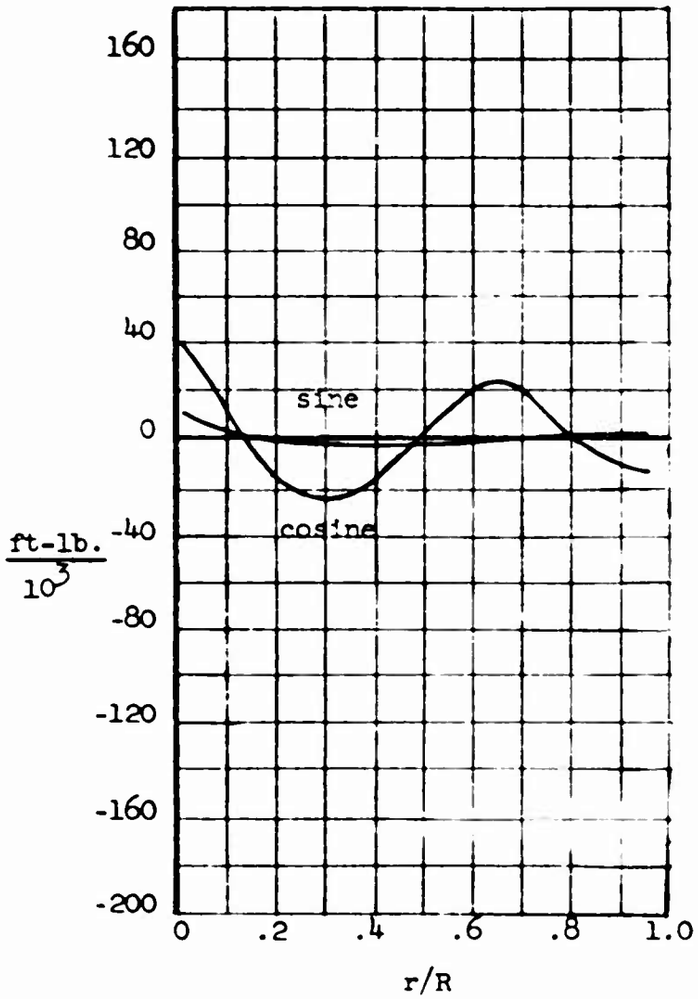

Figure 69. Flapwise Moment - Sixth Harmonic - Forward Flight (lg, 41 m.p.h.) Condition 3

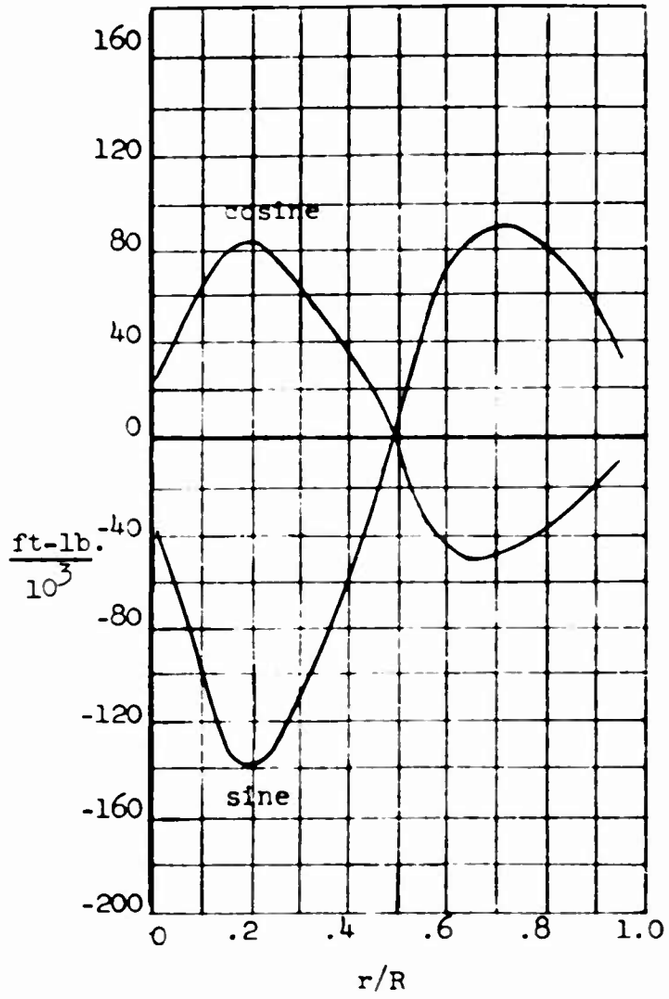

Figure 70. Flapwise Moment - Seventh Harmonic - Forward Flight (lg, 41 m.p.h.) Condition 3

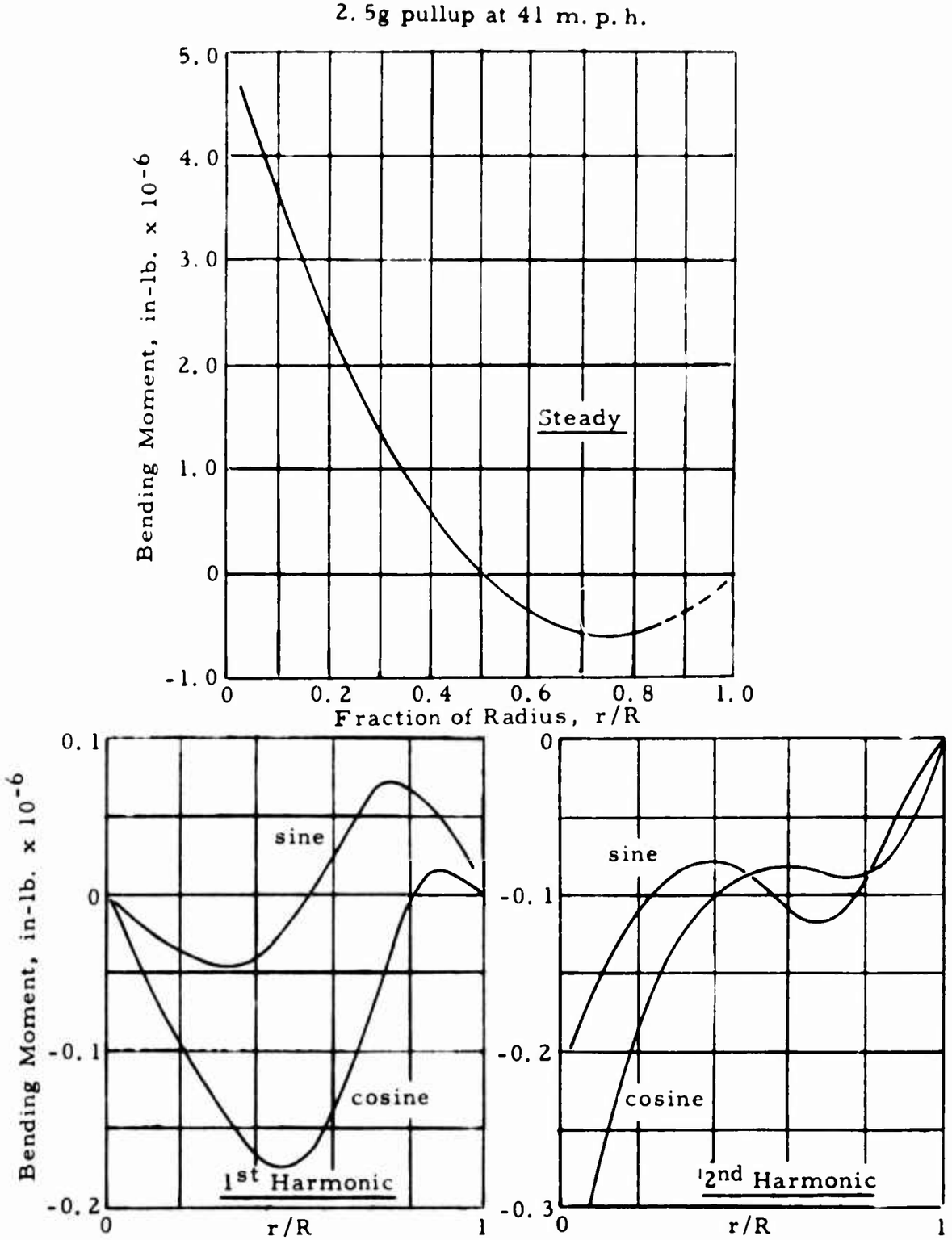

Figure 71. Flapwise Bending Moment Versus Radius.

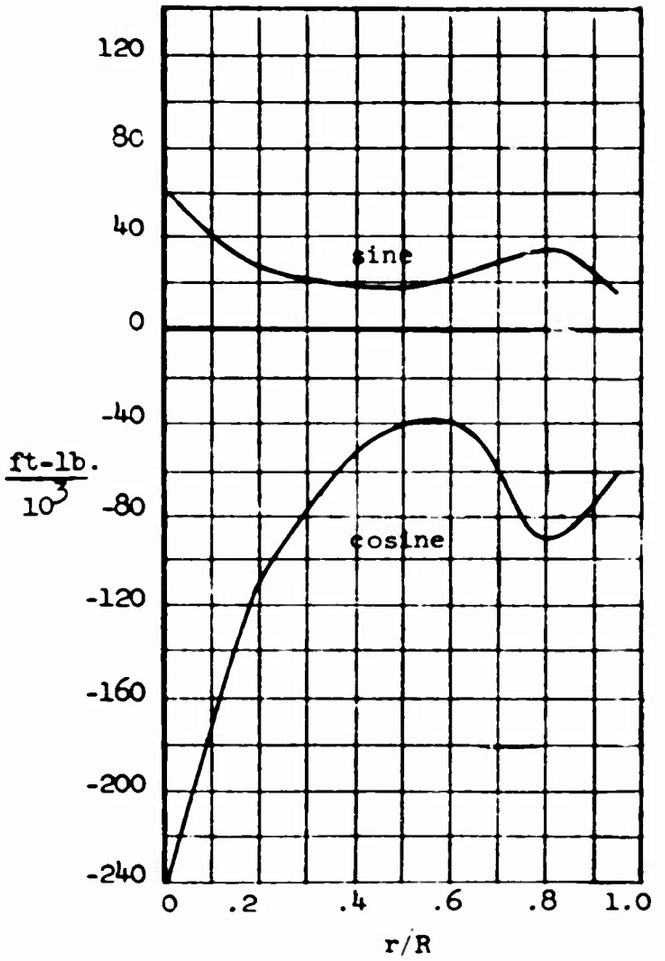

Figure 72. Flapwise Moment - Second Harmonic - Forward Flight (2.5g, 41 m.p.h.) Condition 6

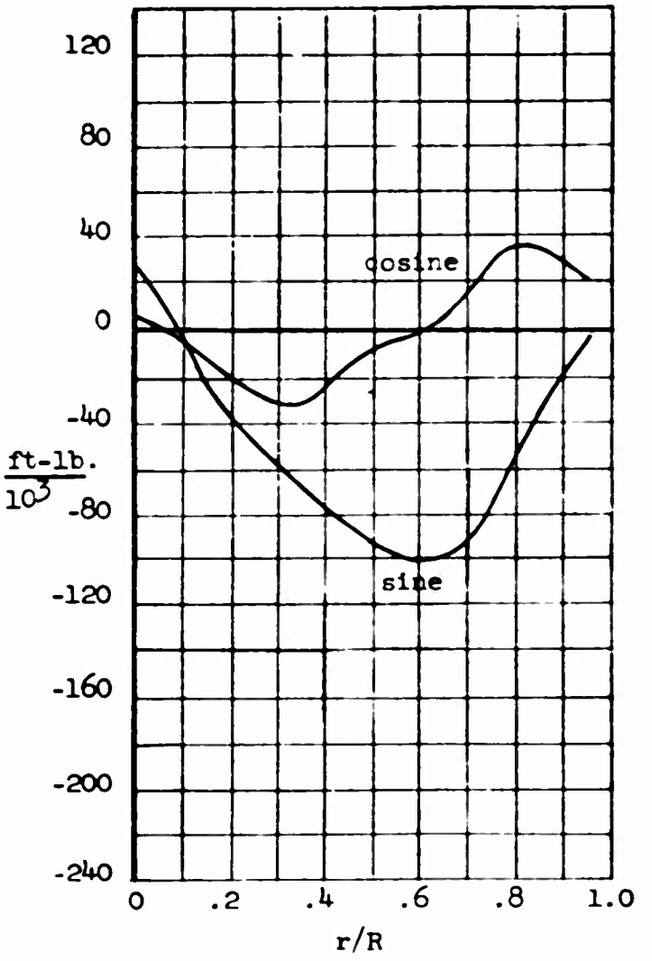

Figure 73. Flapwise Moment - Third Harmonic - Forward Flight (2.5g, 41 m.p.h.) Condition 6

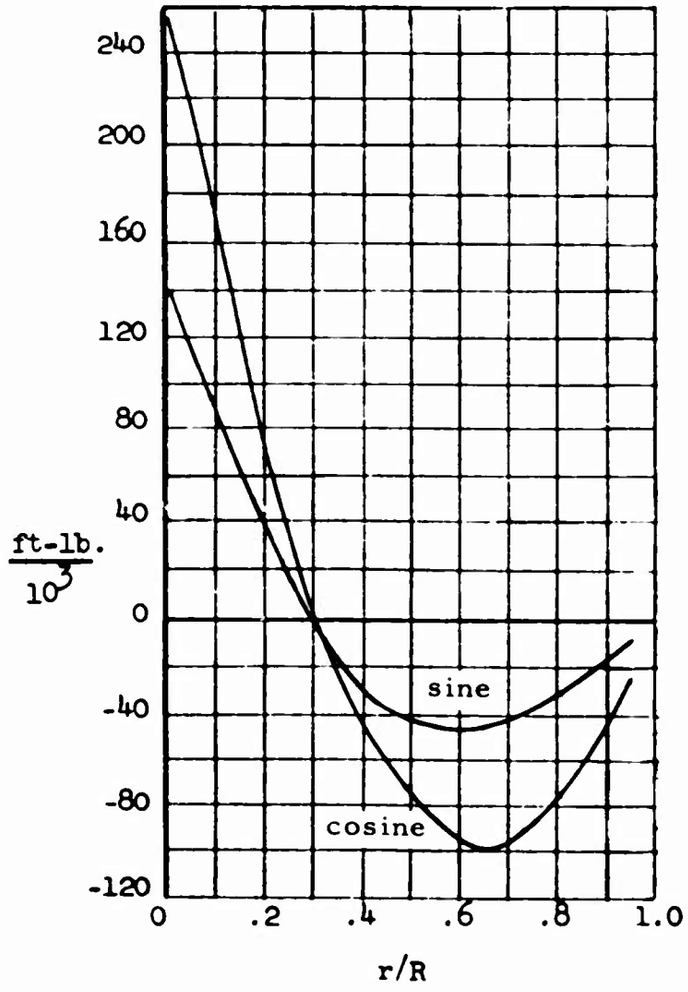

Figure 74. Flapwise Moment - Fourth Harmonic - Forward Flight (2.5g, 41 m.p.h.) Condition 6

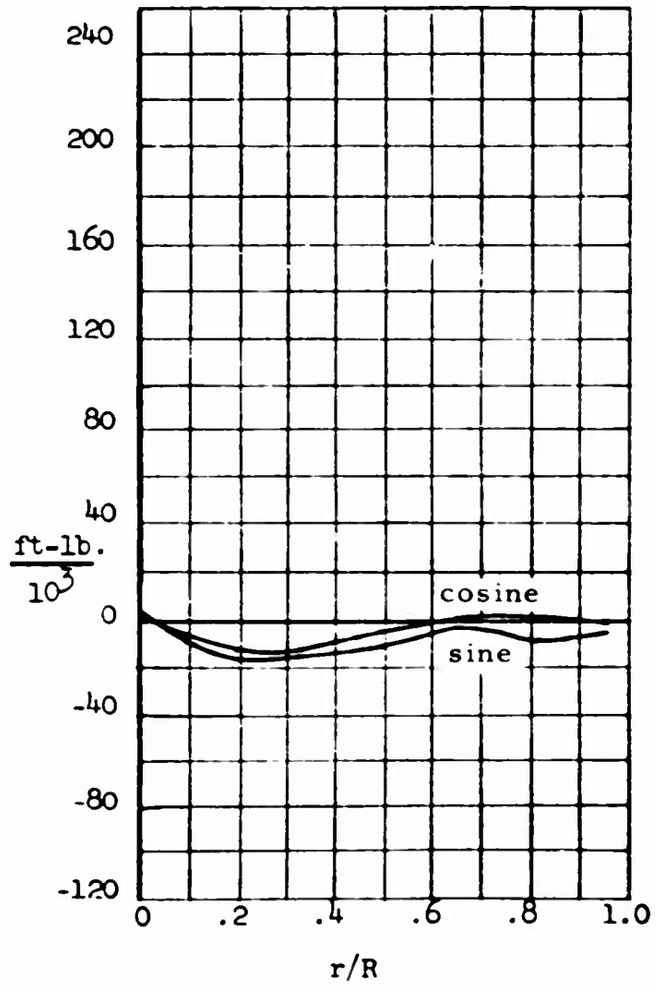

Figure 75. Flapwise Moment - Fifth Harmonic - Forward Flight (2.5g, 41 m.p.h.) Condition 6

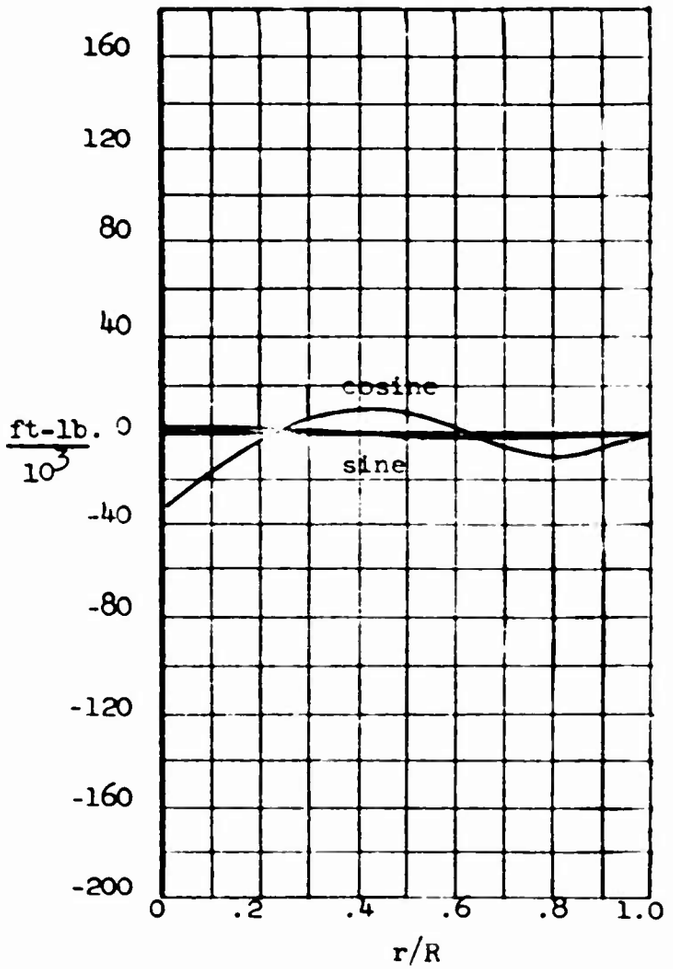

Figure 76. Flapwise Moment - Sixth Harmonic - Forward Flight (2.5g, 41 m.p.h.) Condition 6

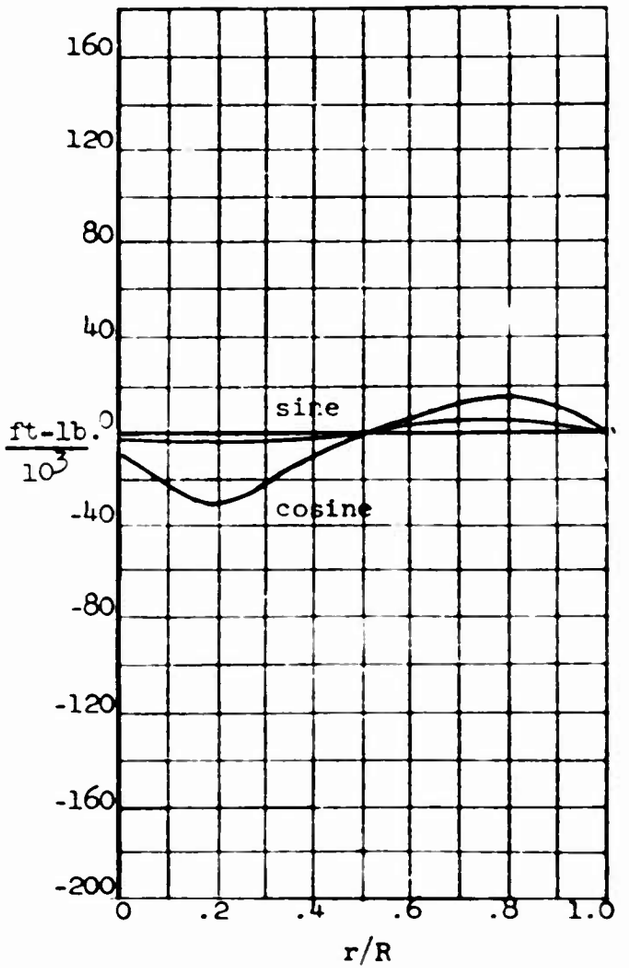

Figure 77. Flapwise Moment - Seventh Harmonic - Forward Flight (2.5g, 41 m.p.h.) Condition 6

lg Forward Flight at 144 m.p.h.

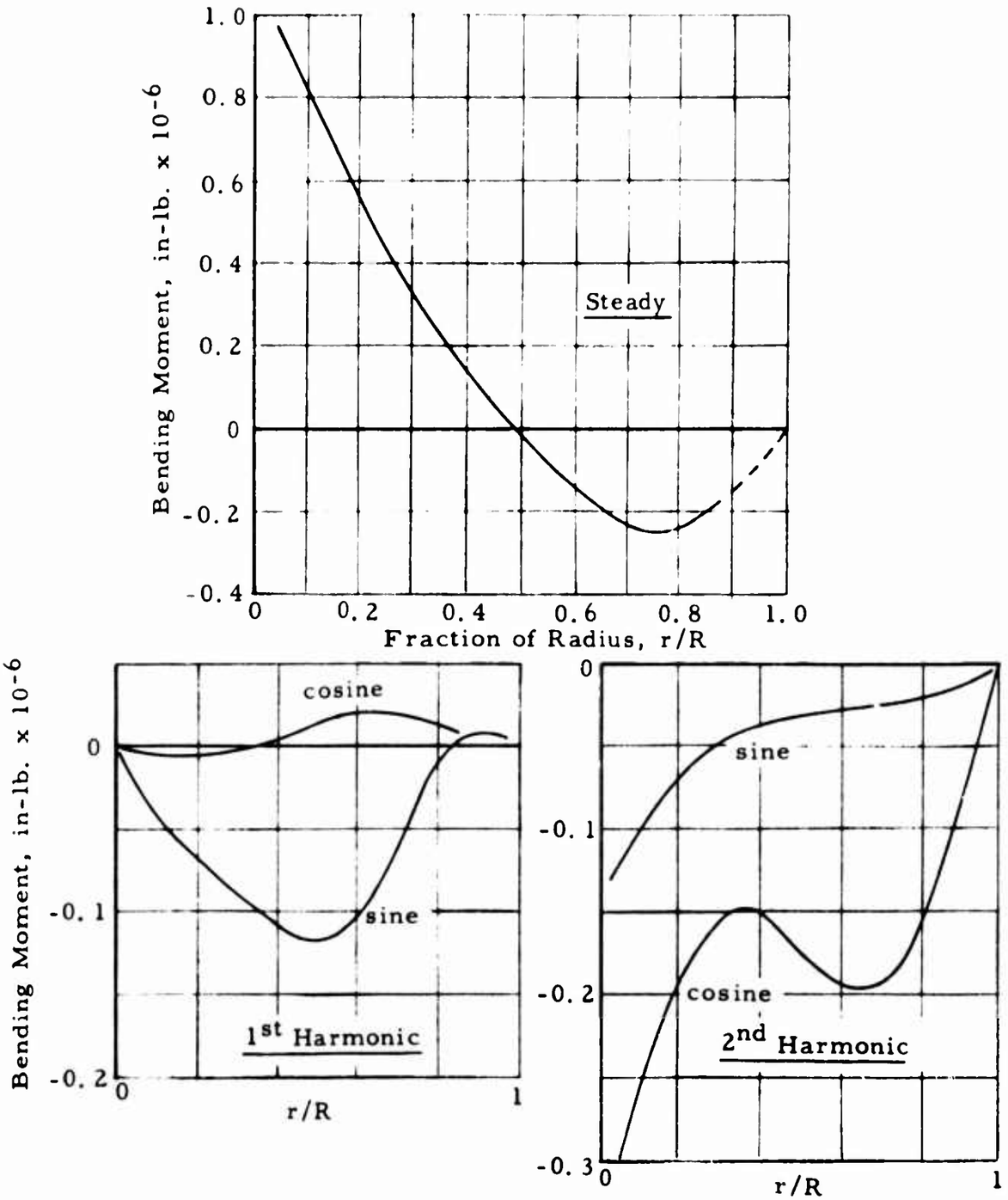

Figure 78. Flapwise Bending Moment Versus Radius.

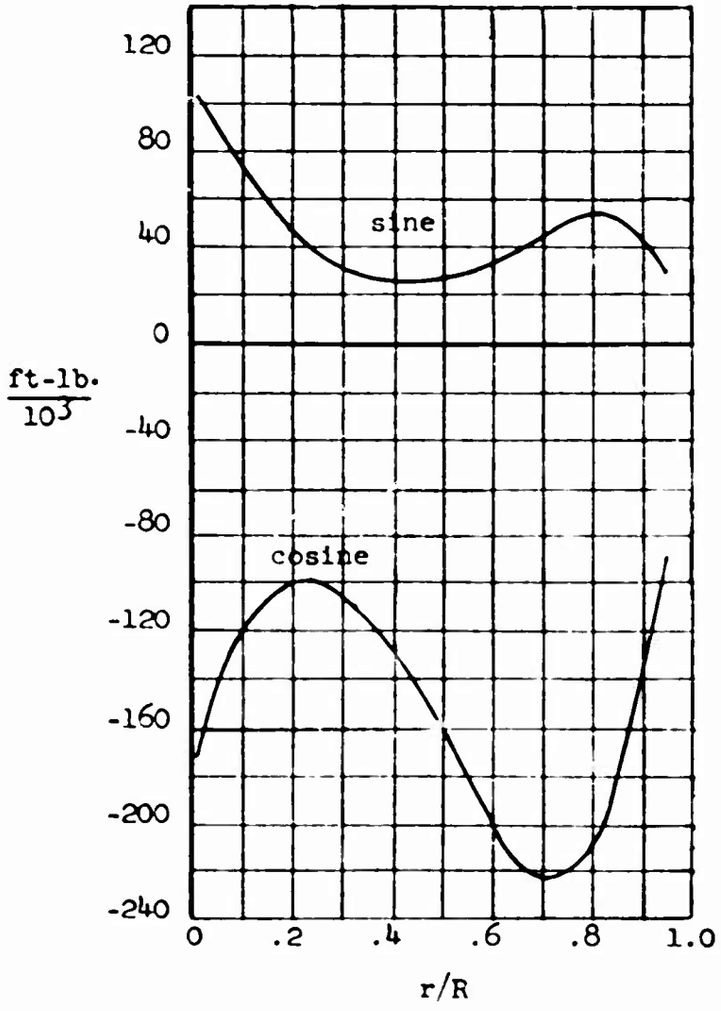

Figure 79. Flapwise Moment - Second Harmonic - Forward Flight (1g, 144 m.p.h.) Condition 8

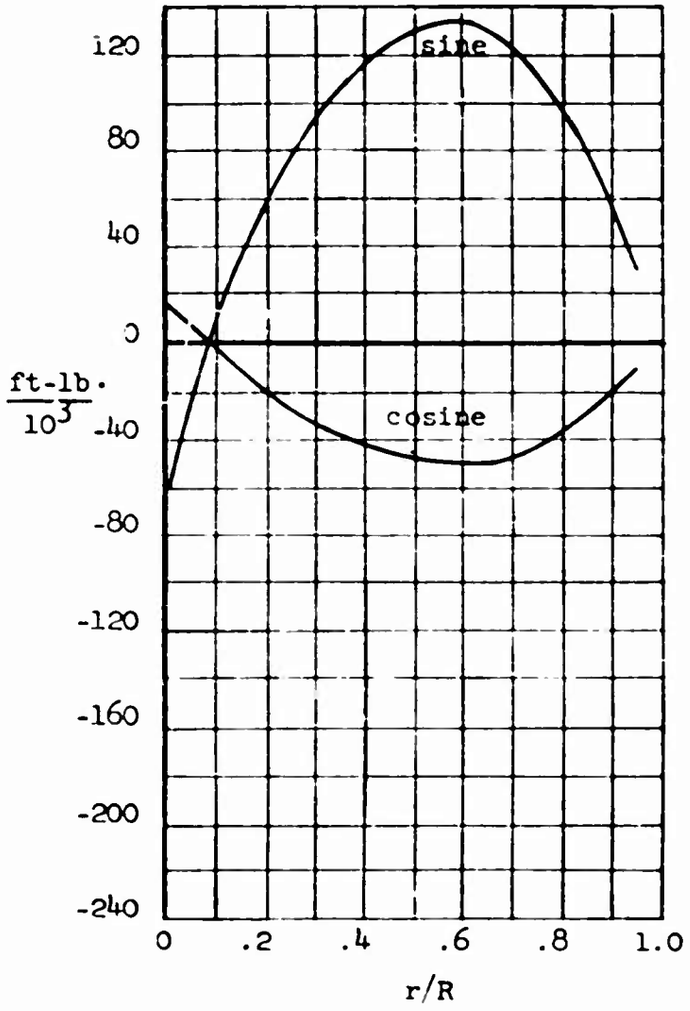

Figure 80. Flapwise Moment - Third Harmonic - Forward Flight (1g, 144 m.p.h.) Condition 8

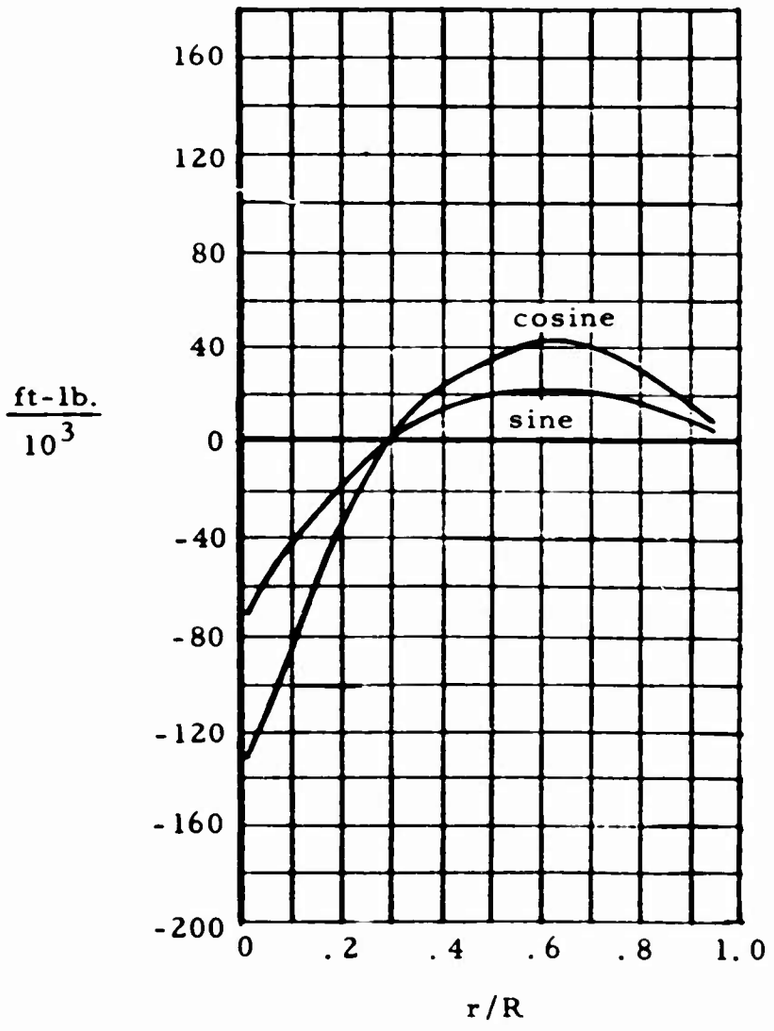

Figure 81. Flapwise Moment - Fourth Harmonic - Forward Flight (lg, 144 m. p. h.) Condition 8

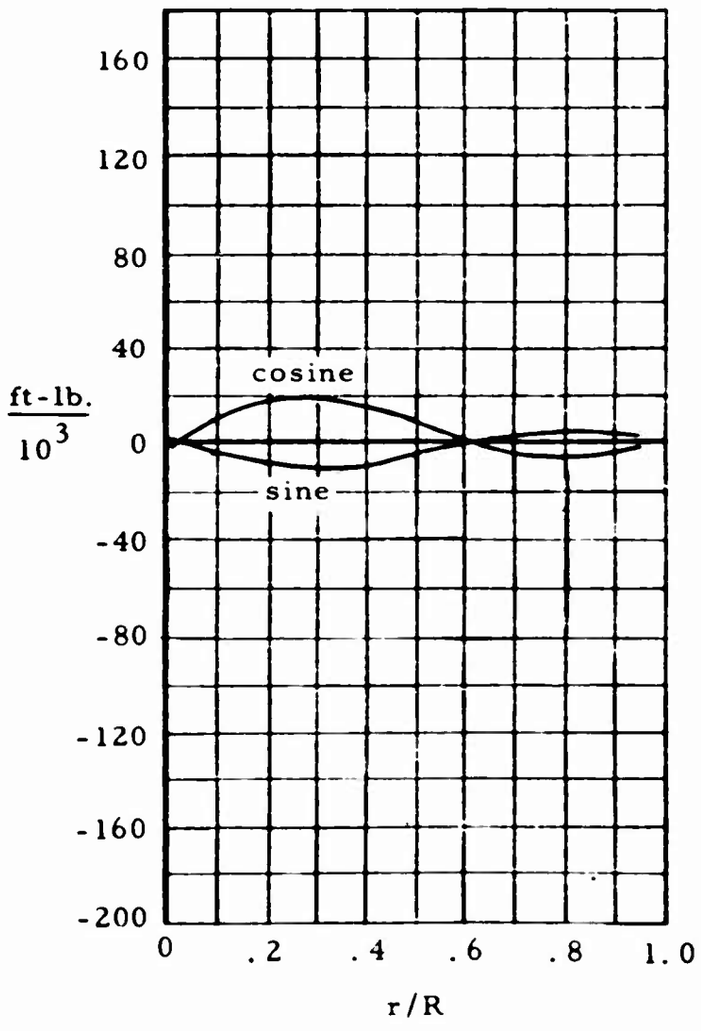

Figure 82. Flapwise Moment - Fifth Harmonic - Forward Flight (lg, 144 m. p. h.) Condition 8

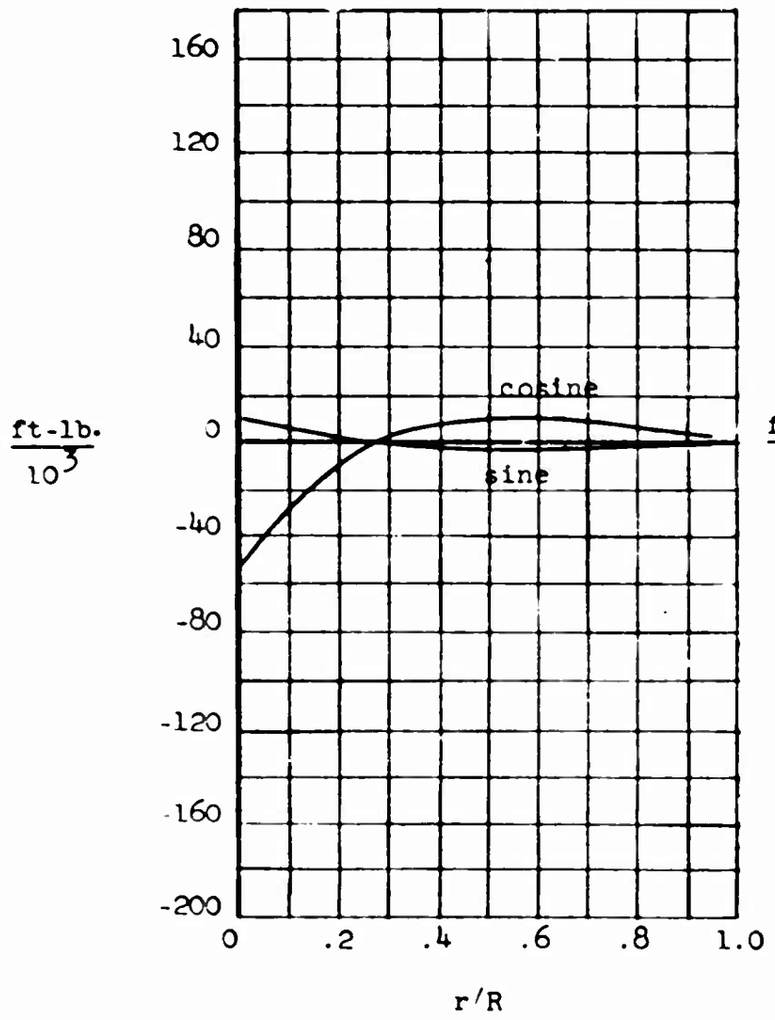

Figure 83. Flapwise Moment - Sixth Harmonic - Forward Flight (lg, 144 m.p.h.) Condition 8

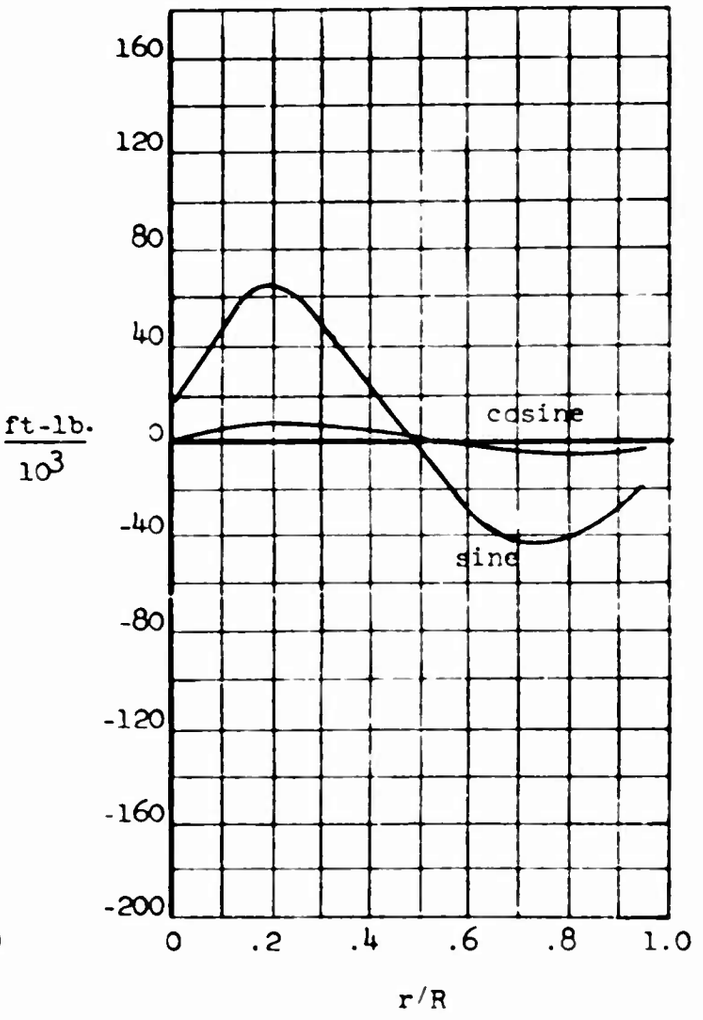

Figure 84. Flapwise Moment - Seventh Harmonic - Forward Flight (lg, 144 m.p.h.) Condition 8

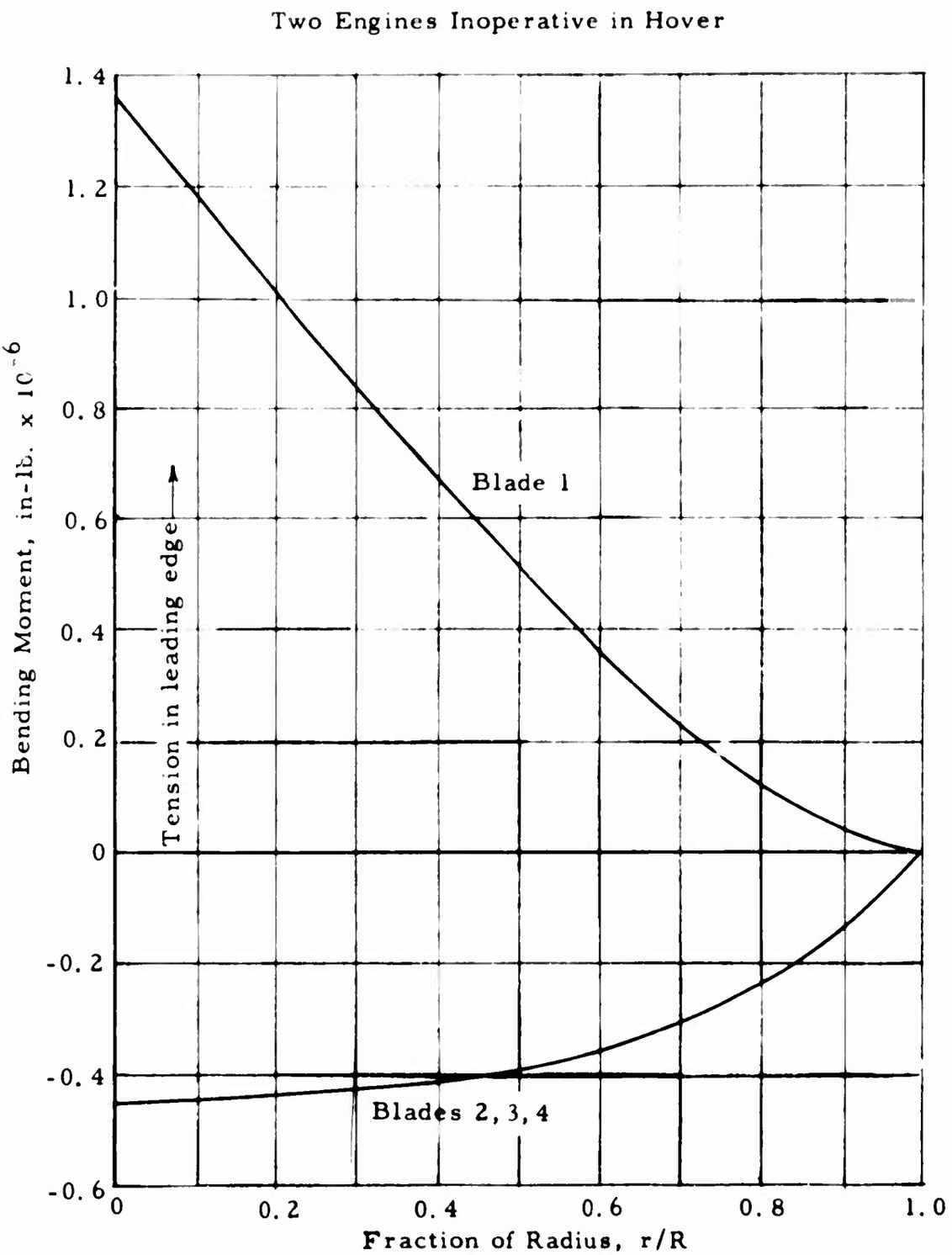

Figure 85. In-Plane Bending Moment Versus Radius.

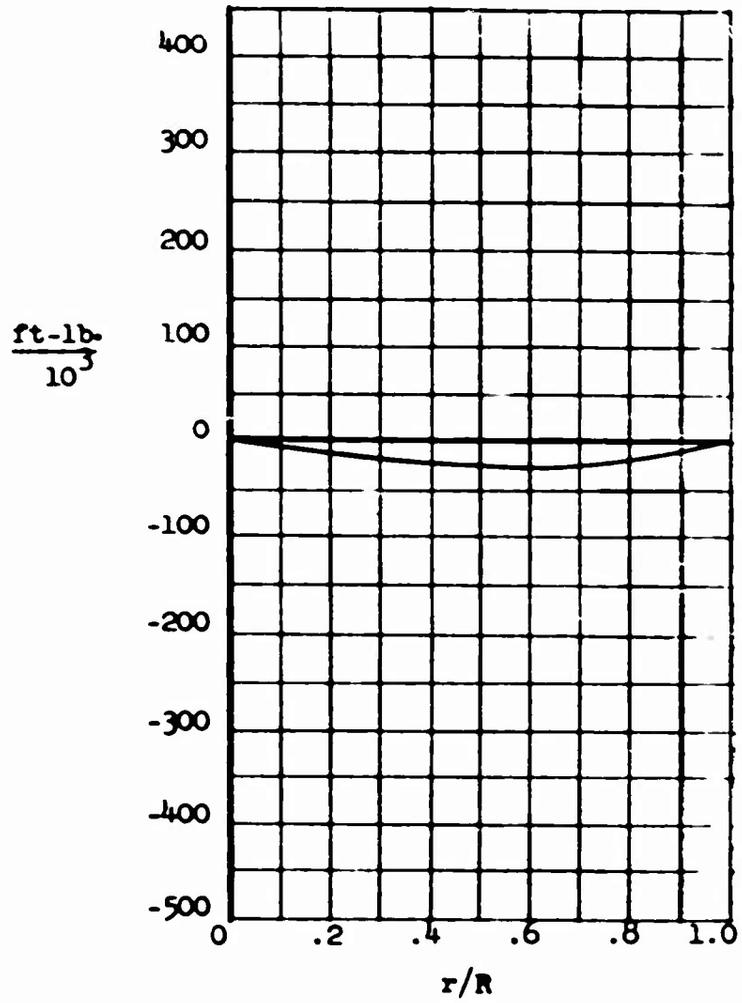

Figure 86. Chordwise Moment (Steady) Forward Flight (2.5g, 41 m.p.h.) Condition 6

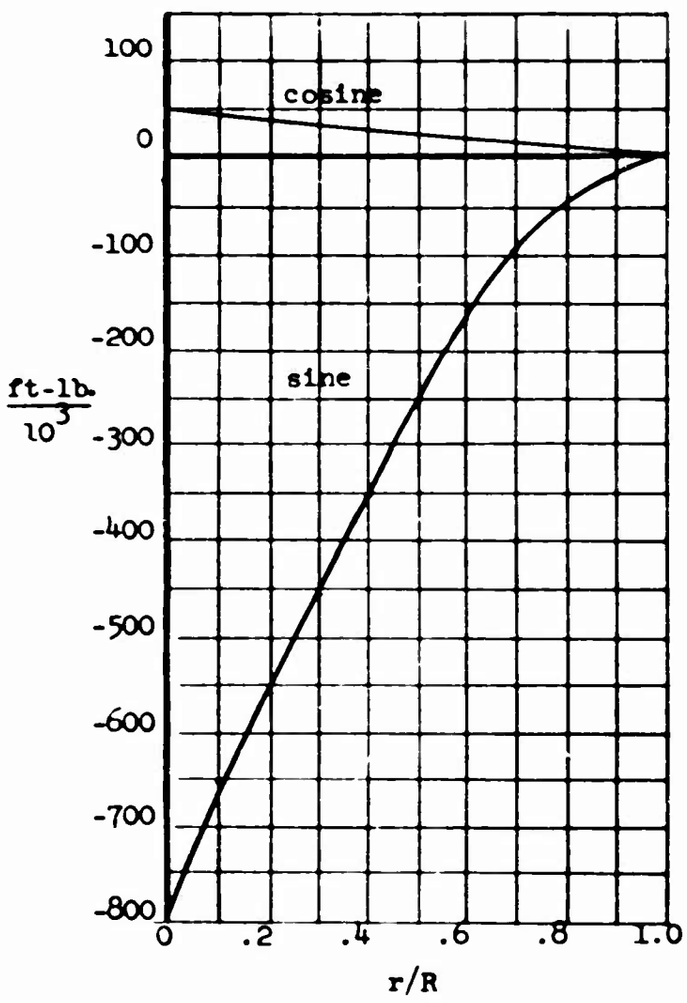

Figure 87. Chordwise Moment - First Harmonic - Forward Flight (1g, 144 m.p.h.) Condition 8

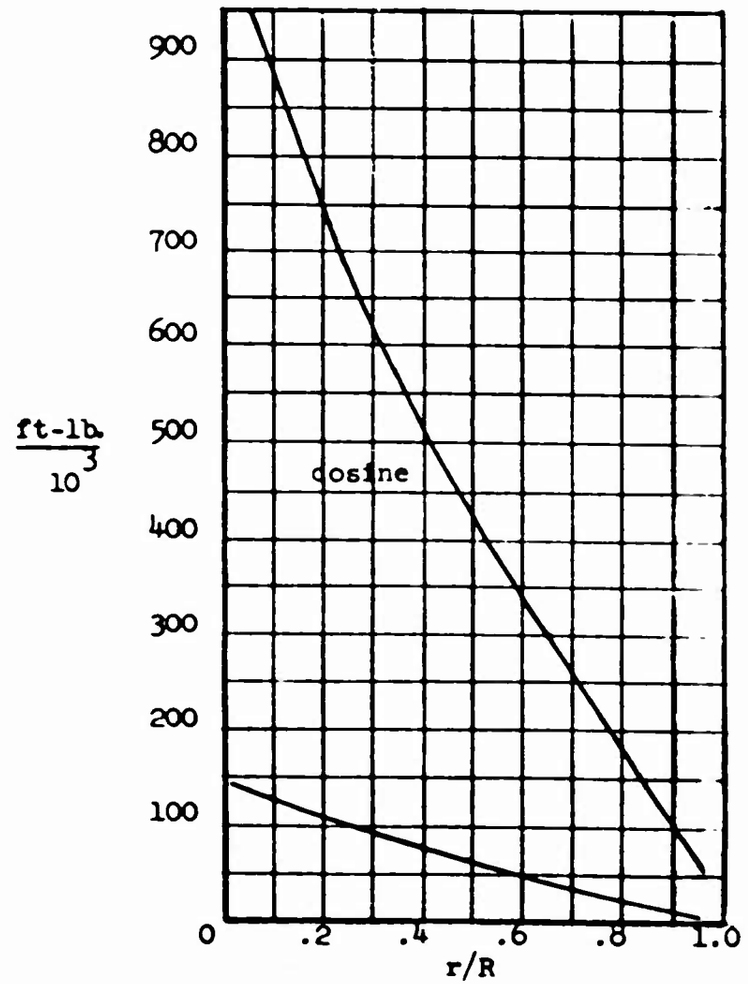

Figure 88. Chordwise Moment - Second Harmonic - Forward Flight (2.5g, 41 m.p.h.) Condition 6

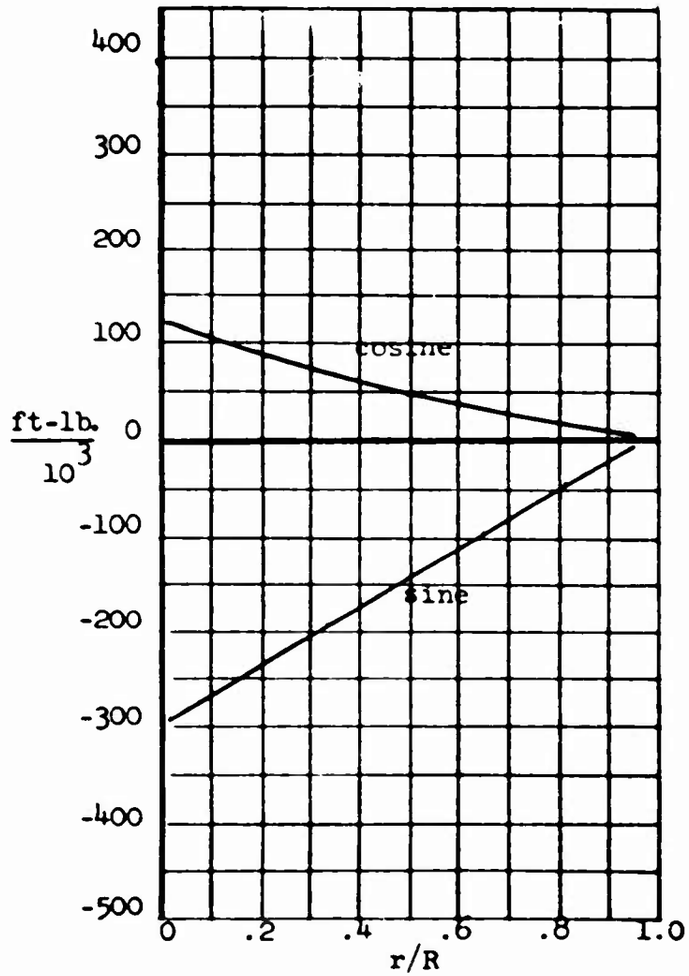

Figure 89. Chordwise Moment - Third Harmonic - Forward Flight (1g, 144 m.p.h.) Condition 8

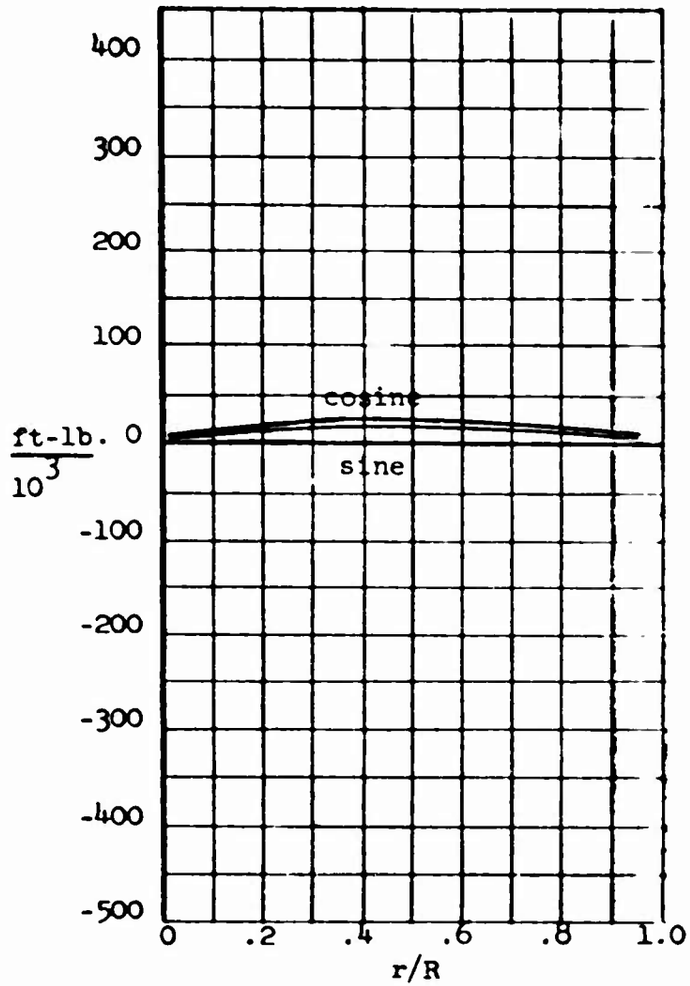

Figure 90. Chordwise Moment - Fourth Harmonic - Forward Flight (2.5g, 41 m.p.h.) Condition 6

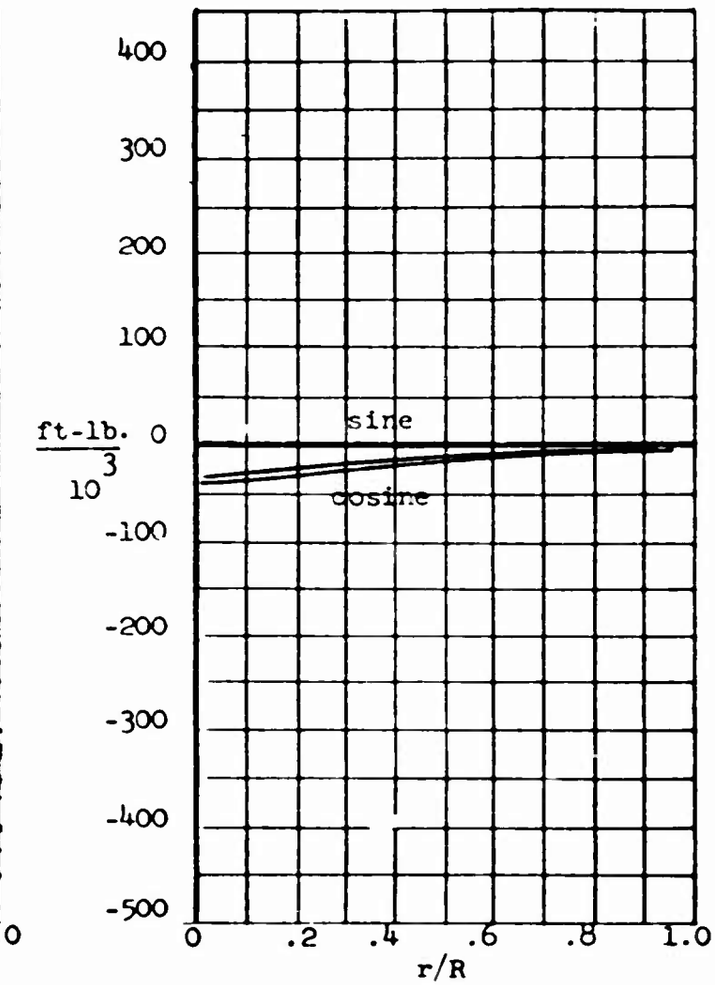

Figure 91. Chordwise Moment - Fifth Harmonic - Forward Flight (1g, 144 m.p.h.) Condition 8

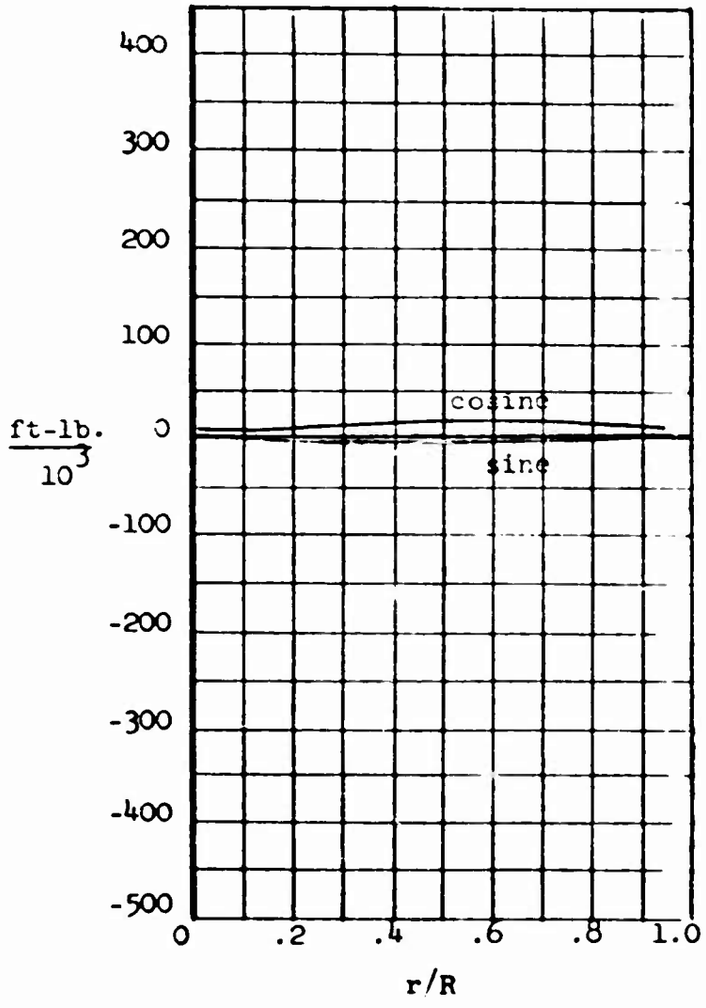

Figure 92. Chordwise Moment - Sixth Harmonic - Forward Flight (2.5g, 41 m.p.h.) Condition 6

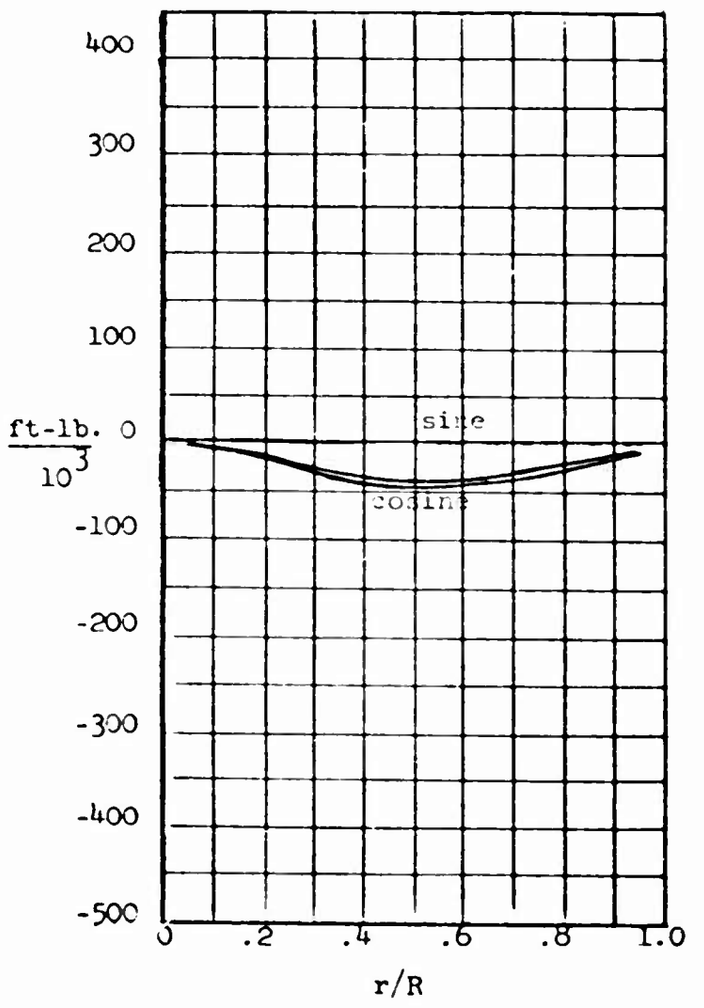

Figure 93. Chordwise Moment - Seventh Harmonic - Forward Flight (1g, 144 m.p.h.) Condition 8

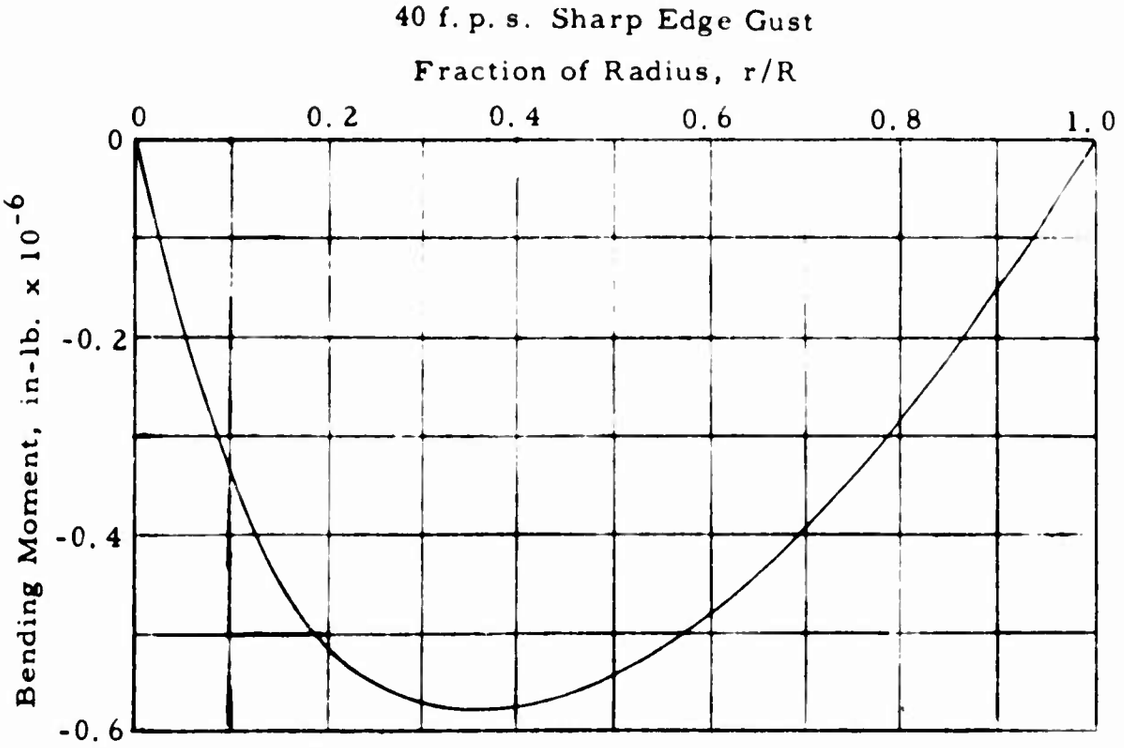

Figure 94. Transient In-Plane Bending Moment Versus Radius.

6.0 REFERENCES

1. A Method for Computing Rotary-Wing Airload Distribution in Forward Flight, TREC Technical Report 62-44, U. S. Army Transportation Research Command*, Fort Eustis, Virginia, November 1962.

2. Evaluation of the Induced Velocity Field of An Idealized Helicopter Rotor, NACA Advanced Restricted Report No. L5E10, June 1945.

3. Mayo, Alton P., "Matrix Method for Obtaining Spanwise Moments and Deflections of Torsionally Rigid Rotor Blades with Arbitrary Loadings," NACA Technical Note No. 4304, August 1958.

4. Direct Analog Computer Study of a Tip Turbojet Rotor System, The MacNeal-Schwendler Corporation, San Marino, California, February 1964. (Available at U. S. Army Transportation Research Command,* Fort Eustis, Virginia.)

*Changed to U. S. Army Aviation Materiel Laboratories in March 1965.

Unclassified

Security Classification

DOCUMENT CONTROL DATA - R&D

(Security classification of title, body of abstract and indexing annotation must be entered when the overall report is classified)

1 ORIGINATING ACTIVITY (Corporate author) Hiller Aircraft Company, Inc. Palo Alto, California	2a REPORT SECURITY CLASSIFICATION Unclassified 2b GROUP

3 REPORT TITLE

Heavy-Lift Tip Turbojet Rotor System, "Static and Dynamic Loads", Volume IV

4 DESCRIPTIVE NOTES (Type of report and inclusive dates)

5 AUTHOR(S) (Last name, first name, initial)

6 REPORT DATE October 1965	7a TOTAL NO OF PAGES 103	7b NO OF REFS 4
8a CONTRACT OR GRANT NO DA 44-177-AMC-25(T) b PROJECT NO c Task 1M121401D14412 d	9a ORIGINATOR'S REPORT NUMBER(S) USAAVLABS Technical Report 64-68D 9b OTHER REPORT NO(S) (Any other numbers that may be assigned this report) Hiller Engineering Report No. 64-44	

10 AVAILABILITY/LIMITATION NOTICES

Qualified requesters may obtain copies of this report from DDC.
This report has been furnished to the Department of Commerce for sale to the public.

11 SUPPLEMENTARY NOTES	12 SPONSORING MILITARY ACTIVITY US Army Aviation Materiel Laboratories Fort Eustis, Virginia

13 ABSTRACT

Volume IV of Heavy-Lift Tip Turbojet Rotor System discusses aerodynamic and interia loadings for rotor blade and engine attachment design. Results of a blade air-load digital computer program are included wherein steady and harmonic airloads are derived. Excerpts from a direct analog computer study of the rotor system present transient blade loads.

DD FORM 1 JAN 64 1473

Unclassified

Security Classification

14 KEY WORDS	LINK A		LINK B		LINK C	
	ROLE	WT	ROLE	WT	ROLE	WT
Tip Turbojet Rotor System Static and Dynamic Loads						

INSTRUCTIONS

1. ORIGINATING ACTIVITY: Enter the name and address of the contractor, subcontractor, grantee, Department of Defense activity or other organization *(corporate author)* issuing the report.

2a. REPORT SECURITY CLASSIFICATION: Enter the overall security classification of the report. Indicate whether "Restricted Data" is included. Marking is to be in accordance with appropriate security regulations.

2b. GROUP: Automatic downgrading is specified in DoD Directive 5200.10 and Armed Forces Industrial Manual. Enter the group number. Also, when applicable, show that optional markings have been used for Group 3 and Group 4 as authorized.

3. REPORT TITLE: Enter the complete report title in all capital letters. Titles in all cases should be unclassified. If a meaningful title cannot be selected without classification, show title classification in all capitals in parenthesis immediately following the title.

4. DESCRIPTIVE NOTES: If appropriate, enter the type of report, e.g., interim, progress, summary, annual, or final. Give the inclusive dates when a specific reporting period is covered.

5. AUTHOR(S): Enter the name(s) of author(s) as shown on or in the report. Enter last name, first name, middle initial. If military, show rank and branch of service. The name of the principal author is an absolute minimum requirement.

6. REPORT DATE: Enter the date of the report as day, month, year, or month, year. If more than one date appears on the report, use date of publication.

7a. TOTAL NUMBER OF PAGES: The total page count should follow normal pagination procedures, i.e., enter the number of pages containing information.

7b. NUMBER OF REFERENCES: Enter the total number of references cited in the report.

8a. CONTRACT OR GRANT NUMBER: If appropriate, enter the applicable number of the contract or grant under which the report was written.

8b, 8c, & 8d. PROJECT NUMBER: Enter the appropriate military department identification, such as project number, subproject number, system numbers, task number, etc.

9a. ORIGINATOR'S REPORT NUMBER(S): Enter the official report number by which the document will be identified and controlled by the originating activity. This number must be unique to this report.

9b. OTHER REPORT NUMBER(S): If the report has been assigned any other report numbers *(either by the originator or by the sponsor)*, also enter this number(s).

10. AVAILABILITY/LIMITATION NOTICES: Enter any limitations on further dissemination of the report, other than those imposed by security classification, using standard statements such as:

(1) "Qualified requesters may obtain copies of this report from DDC."

(2) "Foreign announcement and dissemination of this report by DDC is not authorized."

(3) "U. S. Government agencies may obtain copies of this report directly from DDC. Other qualified DDC users shall request through _____."

(4) "U. S. military agencies may obtain copies of this report directly from DDC. Other qualified users shall request through _____."

(5) "All distribution of this report is controlled. Qualified DDC users shall request through _____."

If the report has been furnished to the Office of Technical Services, Department of Commerce, for sale to the public, indicate this fact and enter the price, if known.

11. SUPPLEMENTARY NOTES: Use for additional explanatory notes.

12. SPONSORING MILITARY ACTIVITY: Enter the name of the departmental project office or laboratory sponsoring *(paying for)* the research and development. Include address.

13. ABSTRACT: Enter an abstract giving a brief and factual summary of the document indicative of the report, even though it may also appear elsewhere in the body of the technical report. If additional space is required, a continuation sheet shall be attached.

It is highly desirable that the abstract of classified reports be unclassified. Each paragraph of the abstract shall end with an indication of the military security classification of the information in the paragraph, represented as *(TS), (S), (C), or (U).*

There is no limitation on the length of the abstract. However, the suggested length is from 150 to 225 words.

14. KEY WORDS: Key words are technically meaningful terms or short phrases that characterize a report and may be used as index entries for cataloging the report. Key words must be selected so that no security classification is required. Identifiers, such as equipment model designation, trade name, military project code name, geographic location, may be used as key words but will be followed by an indication of technical context. The assignment of links, rules, and weights is optional.

6509-65